SOLID DOSAGE FORM DESIGN AND EVALUATION

OF BERBERINE HCL FOR COLON DELIVERY

Thesis Submitted for the Award of the Degree of

DOCTOR OF PHILOSOPHY

in

Pharmaceutics

By

Gautam Kumar

Registration Number: 41800564

<table>
<tr><td>

Supervised By

Dr. Narendra Kumar Pandey (11355)

Department of Pharmaceutics
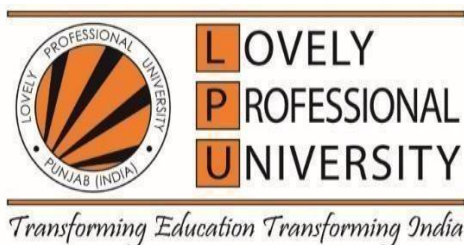(Professor)
Lovely Professional University
Punjab, India

</td><td>

Co-Supervised By

Dr. Jitender Singh

Department of Pharmaceutics
(Principal)
Lord Shiva College of
Pharmacy Haryana, India

</td></tr>
</table>

LOVELY PROFESSIONAL UNIVERSITY PUNJAB

2024

DECLARATION

I, hereby declared that the presented work in the thesis entitled "**Solid Dosage Form Design and Evaluation of Berberine HCl for Colon Delivery**" in fulfillment of degree of **Doctor of Philosophy (Ph.D.)** is outcome of research work carried out by me under the supervision of Dr. Narendra Kumar Pandey working as professor in the School of Pharmaceutical Sciences, Lovely Professional University, Punjab, India and co-supervision of Dr. Jitender Singh, Principal Lord Shiva College of Pharmacy, Sirsa (Haryana). In keeping with general practice of reporting scientific observations, due acknowledgements have been made whenever work described here has been based on findings of other investigator. This work has not been submitted in part or full to any other University or Institute for the award of any degree.

(Signature of Scholar)

Name of the scholar: Gautam Kumar

Registration No.:41800564

Department/School: School of Pharmaceutical Sciences

Lovely professional university,

Punjab, India

CERTIFICATE

This is to certify that the work reported in the Ph.D. thesis entitled, **"Solid Dosage Form Design and Evaluation of Berberine HCl for Colon Delivery"** submitted in fulfillment of the requirement for the award of the degree of **Doctor of Philosophy (Ph.D.)** in the school of pharmaceutical sciences, is a research work carried out by Gautam Kumar, 41800564, is bonafide record of his original work carried out under my supervision and that no part of thesis has been submitted for any other degree, diploma or equivalent course.

Place: Jalandhar

Gautam Kumar

Candidate

Date 19.03.2024

Prof. (Dr.) Jitender singh

Prof. (Dr.) Narendra K. Pandey

Co-supervisor

Supervisor

ABSTRACT

The research focuses on the development and evaluation of pH-triggered eudragit-coated microspheres of Berberine HCl (BBH) by using grafted copolymers for treating Irritable bowel disease (IBD). Polysaccharides from natural sources are frequently used as excipients in food and pharmaceutical sectors because they are biodegradable, biocompatible, readily accessible, and affordable. They do, however, have significant limitations that restrict their application, such as irregular hydration, viscosity variations during storage, solubility (based on their pH), and a shorter shelf life. These drawbacks can be addressed by chemically modifying natural polymers. Natural polymers can be chemically changed in a variety of ways, including etherification, graft copolymerization, and cross-linking. Natural polysaccharide modification has recently sparked a lot of curiosity. Grafting is one of the most promising polysaccharide modification techniques for imparting a range of functional groups to polysaccharides. Gum grafting with synthetic polymers can be used to develop novel compounds with improved releasing properties.

The microwave assisted approach was used to manufacture acrylamide grafted guar gum. A box behnken design was utilized to optimize acrylamide grafting on guar gum. Guar gum amount (g), monomer amount (g), and time (min) were taken as independent variables and three factors were considered as dependent variables: Percentage yield (%) (R1), Percent grafting (%) (R2), and Percent efficiency (%) (R3).To confirm the grafting, Fourier transform infrared spectroscopy (FTIR), X-Ray Diffraction (XRD), Differential scanning calorimetry (DSC), and Scanning electron microscopy (SEM) were employed to analyse the grafted copolymer.

W/O emulsion cross-linking approach was used to create BBH-loaded eudragit-coated microspheres. Software Design-Expert version 7 was selected. To optimise grafting, a 3-factor, 3-level Box-Behnken design (BBD) was employed. As the dependent variables varied greatly among the 17 batches (F1–F17), the BBD was used to evaluate the impact of independent variables during the formulation development process. The Guar gum ratio with polyvinyl alcohol (PVA) (A), revolutions per minute (RPM) (B), and Span 20 (%) (C) were independent variables.

Entrapment Efficiency (%) (R1) Drug Loading (%) (R2), and Particle Size (µm) (R3), were regarded as dependent variables.

The optimized formulation was coated with varied amounts of eudragit S-100 (ES) by employing an oil-in-oil (o/o) solvent evaporation approach. The C5 formulation was chosen for further study based on several evaluation characteristics, such as microscopic evaluation, micromeritic properties, percentage yield, percentage drug loading, and percentage entrapment efficiency. To ensure that the drug was entirely encapsulated inside the coated microsphere, FTIR, XRD and SEM were utilized. The microspheres created had a homogeneous spherical shape and high entrapment efficiency. The XRD demonstrated that ES-coated BBH microspheres had less intense peaks than free BBH, demonstrating the incorporation of drug within the microsphere. The coating and grafting effects on drug release from various formulations, *in vitro* release patterns were compared. Following zero-order kinetic models, uncoated BBH-microspheres displayed burst release within the first 4 hours.

A controlled release of the drug for up to 24 hours was demonstrated by ES-coated BBH microspheres, which prevented the drug's early release from the formulation in the upper gastrointestinal tract (GIT) and only allowed the drug to be released in the colonic region. According to an *in vitro* study, the suggested formulations are a potential choice for targeted medication administration in patients with IBD.

A stability analysis of the optimized formulation (C5) was carried out (by ICH guidelines) to assess storage conditions and expiration dates. During the stability evaluation, various parameters were monitored to assess any changes or degradation in the optimized formulation batch (C5). The data collected at each interval (30 days) provided valuable insights into the batch's stability and its potential shelf life under different storage conditions. The temperature and humidity selected for accelerated stability conditions (180 days) were 40 ± 2 C/$75 \pm 5\%$ RH (relative humidity), and for long-term stability conditions (360 days), they were 30 ± 2 C/$65\pm5\%$ RH. According to the findings, the coated microsphere from batch C5 is stable.

The *in vivo* study was carried out under the license (800/PO/Re/S/03/CPCSEA) and with the approval of Lord Shiva College of Pharmacy's Institutional Animal Ethics Committee (IAEC). 10-week-old Wister albino male rats (body weight 220 ± 20 g) were purchased from Small Animal House LUVAS, Hisar, Haryana (1669/GO/ReBiBt/S/12/CPCSEA).

The animals were housed in a variety of standard cages with unrestricted access to food and water in controlled environments. Before inducing colitis, rats were allowed unlimited access to water for 48 hours while starving. For the *in vivo* investigation, a colitis-induced model was used. Different formulations were administered to each group for 5 days and assessed. Nine groups of rats were selected at random. Each group had six rats. The polyurethane tube of medical grade with a 2 mm external diameter was carefully inserted up to 6–8 cm (proximal to the anus margin) to avoid any damage to the surrounding tissues.To induced colitis, 2 mL of 3% v/v acetic acid solution was filled into the colons of all the animal groups except the healthy one. To avoid the leakage of the solution, the rats were held in this position for a minimum of 2 minutes. The normal (healthy) group (Group I) was given 2 mL of a 0.5% carboxymethyl cellulose (CMC) solution despite the presence of an acetic acid solution. To develop an IBD model, all the animals were kept untreated for a time interval of 24 hours, during which food and water were provided with full access. Every group under treatment received a fixed volume of the suspension of different formulations, such as ES-coated BBH microsphere (ungrafted), uncoated BBH microsphere (grafted), placebo-control (blank microsphere), and ES-coated BBH microsphere (grafted). Each formulation was given one time per day for five consecutive days, these doses, which were equivalent to 20 mg/kg/day to 40 mg/kg/day, were administered orally via gavages. The administration of 1 mL of CMC was consistent across both the normal and colitis groups, regardless of the specific drug formulation used. In contrast, Group V was given a blank microsphere solution that did not contain any active drugs.

Each rat was anesthetized and sacrificed, and a 6 cm section of the colon was taken from each rat 24 hours after the last dose. Every colon sample was opened lengthwise, cleaned and dried. Colonic inflammation was assessed by using the disease activity

index scoring system. Indicators of colon inflammation were determined by measuring the weight and length of the colon and then converting those values into colon weight and length ratios and colon weight to body weight ratios, respectively. The microscopic evaluation was determined by the animals' histopathological score system. Scores were based on inflammatory criteria such as severity of inflammation, crypt damage, and inflammation extent. The finding that animal groups treated with optimized formulations (Groups 8 and 9) found reduced disease activity scores, improvements in their body weight, which is equivalent to that of normal rats, and also enhanced therapeutic activity of the drug, verified by histological investigation, indicating treated colons had reduced inflammation. The optimized formulation's effectiveness in animal tests supported the *in vitro* release studies. Human research is necessary to verify the findings of animal studies, to ensure the safety and efficacy of microspheres in the treatment of inflammatory bowel disease, and to confirm the results of animal studies.

Keywords: Colon specific delivery, Berberine HCl, EudragitS-100, microsphere.

ACKNOWLEDGEMENTS

TABLE OF CONTENTS

LIST OF TABLES

LIST OF FIGURES

LIST OF ABBREVIATIONS

Short Form	Full Form
BBH	Berberine HCl
IBD	Irritable bowel disease
FTIR	Fourier Transform Infrared Spectroscopy
XRD	X-Ray Diffraction
DSC	Differential Scanning Calorimetry
SEM	Scanning Electron Microscopy
PVA	Polyvinyl alcohol
RPM	Round per minute
ES	Eudragit S-100
GIT	Gastro intestinal tract
ICH	International council of harmony
mm	Micro Meter (unit of length)
mL	Milliliter (unit of volume)
Cm	Centimeter (unit of length)
Min	Minute (unit of time)
H	Hour (unit of time)
mg	Milligram
kg	Kilogram (unit of weight)
CD	Crohn's diseases
UC	Ulcerative colitis
CDDS	Controlled drug delivery system
°C	Degree Centigrade (unit of temperature)
CFU	Colony forming unit
%	Percent
P.o	Per. Os.
NMR	Nuclear magnetic resonance
UV	Ultraviolet Spectroscopy

Short Form	Full Form
w/v	Weight by Volume
w/w	Weight by Weight
μl	micro liter
μg	Microgram
MW	Microwave
% RSD	Percent Related Standard Deviation
CMC	Carboxyl methyl cellulose
ANOVA	Analysis of variance
^{0}	Degree (unit of angle)
et al.,	Latin term "et alia," meaning "and others."
BP	British Pharmacopoeia
HPLC	High Performance Liquid Chromatography
C_{max}	Maximum Concentration
g	Gram (unit of weight)
g/mol	Gram per moles
IP	Indian Pharmacopoeia
$K_{o/w}$	Oil/water Partition Coefficient
PKa	Dissociation Coefficient
RH	Relative Humidity
S	Second (unit of time)
SD	Standard Deviation
$_{max}$	Absorption Maxima
USP	United State Pharmacopoeia
% EE	Percent entrapment efficiency
% DL	Percent drug loading
% DR	Percent drug release
DAI	Disease activity index

Chapter 1: Introduction

1.1 INFLAMMATORY BOWEL DISEASE (IBD): Over the past 2–4 decades, inflammatory bowel disease (IBD) incidence and prevalence have increased globally, most likely as a result of people adopting more "Western" lifestyles. It is classified as a long-term gastrointestinal (GI) tract inflammatory condition that lowers quality of life. Although the exact causes of inflammation in IBD are unknown, it is believed that a hypersensitive immune response to the gut microbiota is involved. Although it is frequently linked to dysbiosis, it is unclear whether the latter is the source or result of inflammation [1]. It can be difficult to distinguish between the symptoms of irritable bowel syndrome (IBS) and inflammatory bowel disease (IBD) due to the pathological changes associated with IBD, such as inflammation or fibrosis [2]. The two primary intestinal diseases, ulcerative colitis (UC) and Crohn's disease (CD) that make up IBD can be separated by where they develop and how severely they impact the colon wall. In UC, the intestinal mucosa is sporadically inflamed; in most cases, UC affects the rectum, sigmoid, and beyond the sigmoid or the entire colon.The terminal ileum and colon are the two areas of the GI tract that are most frequently affected by CD. The severity and location of both disorders are categorized. Inflammatory, structuring, or penetrating phenotypes are additional classifications for CD [3].

1.1.1 Ulcerative colitis

It is a chronic inflammatory bowel illness that results in bleeding and diarrhoea because the colon's lining becomes inflamed and ulcers form. Inflammation can occur everywhere in the colon, not just the rectum or bottom portion of the colon. Instead of the usual 10 to 30 minutes each day, the inflamed colon's motility increased in such situations. Additionally, the colon's secretions increase, resulting in more often occurring bouts of bloody diarrhoea. It may just affect the distal rectum in rare circumstances, but it typically affects the entire

colon. However, only 20% of patients with this condition, which affects the rectum and splenic flexure, suffer pan colitis.

A. Causes of ulcerative colitis

The immune system of such a person is triggered by exposure to a disease or other environmental stimulus. Inflammation results from the immune system attacking the colon's lining after identifying it as alien. Later on, this inflammation turns into ulcers that bleed.

- **Genetics:** This disease's development has been significantly influenced by genetics. A sibling or parent with inflammatory bowel disease affects between 10 and 25 percent of persons who get ulcerative colitis.
- **Environment:** Numerous environmental factors are anticipated to cause ulcerative colitis in those who have a genetic predisposition to the condition.

B. Diagnosis

The typical methods for diagnosing ulcerative colitis include symptom observation, physical examination, and pathology investigations. IBS develops in people with a genetic predisposition to it as a result of an incorrect immune response in the colon to environmental triggers, including medications, poisons, infections, or intestinal microbes [4]. The majority of IBD cases affect adults between the ages of 15 and 30. A second surge of 10% to 15% of people who acquire IBD after the age of 60 tends to indicate a bimodal distribution [5]. Intracellular connections are damaged in IBD either as a result of fundamental barrier function impairment or because of acute inflammation. Excessive inflammatory responses cause the epithelium to continue to deteriorate and expose more of the body to intestinal bacteria, which exacerbates the inflammation [6]. Clinical symptoms, inflammatory laboratory markers, imaging results, and endoscopic biopsies must all be considered when diagnosing IBD [7].

1.2 TARGETED DRUG DELIVERY STRATEGY (TDDS) IN IBD

This method uses a variety of drug delivery systems, including nanoparticles, hydrogels, and microspheres, which ensure that the medication is released only into the inflamed area. Additionally, targeted drug delivery in IBD can help reduce systemic exposure to the medication, minimizing potential side effects on healthy tissues and organs. The targeted delivery method must fulfill requirements for full biodegradation and excellent biocompatibility while exhibiting no pro-inflammatory characteristics. To induce and sustain adherence, additionally, oral dosage forms must be prepared using TDDS.
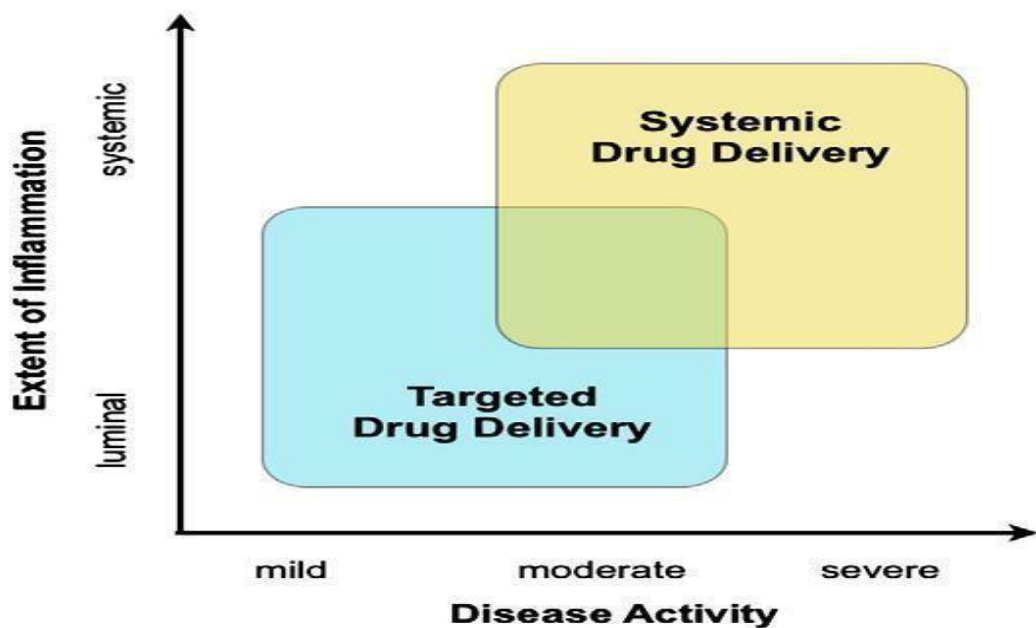
Figure: 1.1. Therapeutic advantages of targeted drug delivery strategy **[8]**

The therapeutic benefit of targeted drug delivery is primarily the topical treatment of inflammation of the lumen, as contrasted to systemic drug administration. Delivering drugs specifically to IBD patients is advantageous. A targeted drug delivery technique does not directly offer systemic treatment for severe IBD or extra-intestinal symptoms [8].

1.2.1 The CDDS or colon-specific drug delivery system

This is widely acknowledged for the treatment of several bowel illnesses, including colon cancer, local colonic pathologies, ulcerative colitis, and Crohn's disease. This technique can enable the overall distribution of some drugs [9]. Because the medicine does not reach the target site in an effective concentration, the standard formulation is less effective in treating IBD than it is in treating other GIT illnesses. Moreover, CDDS can shield medication delivery into the upper gastrointestinal system, which prevents drug degradation from occurring before it enters the colon [10]. For CDDS, the oral route is the most practical and preferable one. There are approximately 400 different types of colonic bacteria that break down glycosides through enzymatic cleavage and azoreduction. Numerous medications may be metabolised as a result of these metabolic mechanisms [11].

1.2.1.1 Advantages of CDDS [12-13]

- Reducing significant first-pass steroid metabolism.
- Avoiding stomach irritation caused by oral NSAID therapy.
- Delaying the administration of drugs for rheumatoid arthritis, angina, and asthma.
- Peptide and protein-containing drugs can be protected against stomach acid and digestive enzymes.
- Reducing the side effects of gastrointestinal diseases (such as Crohn's disease, colorectal cancer, and ulcerative colitis).
- The major objective of the targeting approach is to distribute the medicine in an effective concentration up to the inflamed intestinal tissues in order to decrease adverse effects and maximise treatment efficacy [13].

Table 1.1: List of drugs prescribed in conditions associated with colonic disorders [14-15]

Targeted Sites for drugs	Disease related to colon	Signs and symptoms of disease	Drugs used for the treatment
Topical Action	Ulcerativ ecolitis	Rectal bleeding and inflammation with pain	Sulfasalazine, mercaptopurine Mesalamineand Balsalazide,
	Crohn's Disease (CD)	Abdominal crampingand pain with diarhoea, blood in the stools, ulcers, loss of appetite, and loss in body weight.	Prednisolone, Sulfasalazine, Hydrocortisone and Budenoside
	Irritable bowel syndrome (IBS)	Abdomen blotting, gas, diarrhea or constipation (alteration episodes), mucus in stools.	Cimetropium, Alosetron, Tegaserod, Dicyclomine, Hyoscine and Propantheline
	Colorecta lcancer	Alteration in bowel habits, thin stool with rectal bleeding, persistent abdominal cramps, gas or pain, bowel movement associated with abdominal pain and unexplained weight loss.	Leucovorin, 5 Flourouracil and Cetuximab
Systemic action	Ulcerativ ecolitis (UC)	Ulcerative proctitis, fulminantcolitis, and pancolitis	Fluticasone propionate, Beclomethasone, Prednisolone metasulfobenzoate and Tixocortol pivalate

1.2.1.2 Selection criteria of drug for CDDS

Drug, especially peptides with minimal intestinal or stomach absorption, is the best candidate for CDDS. The best choices for local colon delivery include medications used to treat IBD, ulcerative colitis, diarrhoea, and colon cancer.

Table 1.2: Selection criteria of drug for CDDS [15]

Criteria	Pharmacological class	Peptide drugs	Non-peptide drugs
Locally acting drugs for colonicdisorders	Anti-inflammatory drugs	Amylin, Antisense Oligonucleotide	Oxyprenolol, Metoprolol, Nifedipine
Weakly absorbed drug from GIT's upper part	Anti-hypertensive Anti-anginal drugs	Cyclosporine, Desmopressin	Theophylline Ibuprofen, Isosorbides
Drugs used in cancer of colon	Antineoplasticdrugs	Epoetin, Glucagon	Pseudoephedrine
Drugs, degradablein the stomach and small intestine	Peptides andproteins	Gonadoreline, Insulin, Interferons	Bromophenaramine, 5-Flourouracil, Doxorubicin
Drugs that are extensively metabolised in the first pass	Nitroglycerin and corticosteroids	Protirelin, sermorelin, Saloatonin	Bleomycin, Nicotine
Targeting drugs	Anti-arthritic andAnti-asthamatic drugs	Somatropin, Urotoilitin	5-Aminosalicylic acid ,Prednisolone, Hydrocortisone

1.2.1.3 Approaches utilized for site-specific drug delivery

Various methods are employed for site-specific medication delivery. These proceduresare listed in the flow chart below as some of the main methods for CDDS.
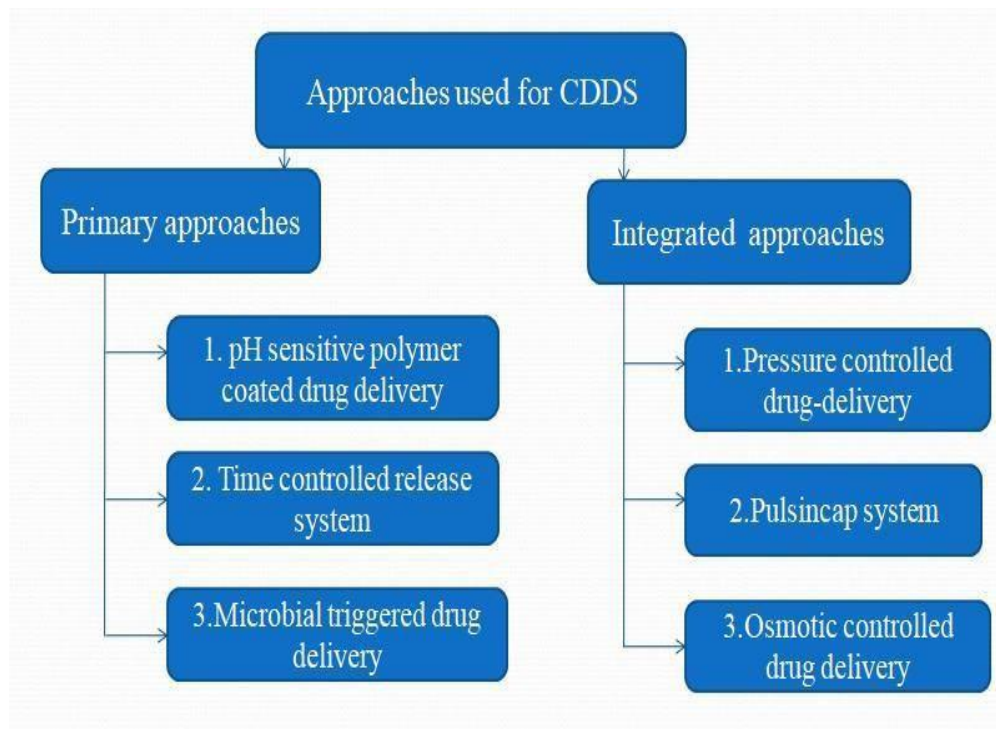
Figure 1.2: Flow chart of different approaches for CDDS

A. PH-controlled release: By using multiple films with distinct qualities, the formulations can effectively target specific pH levels in different parts of the gastrointestinal tract. This approach ensures that the film coatings dissolve precisely in the colon, allowing for controlled drug release at the desired location. Time dependence and pH dependence can sometimes coexist. The considerable person to person pH variability throughout the GI-tract is the main drawback of these systems, especially for individuals with GI-tract problems [16].

B. Time-controlled release system (TCRS)

These techniques ensure that the drug is guaranteed to be released slowly and steadily over a predetermined amount of time, allowing for better control of drug concentration in the body.This not only improves the efficacy of the drug but also minimises potential side effects. Because of variations in human gastric emptying times, these techniques cannot estimate the colon arrival time of dosage forms, which has a negative impact on clinical availability. By extending the lag time by approximately 5 to 6 hours, the

dosage forms were modulated into colon-specific.The three parts of (TCRS) tablet are as follows: an acid resistance layer (enteric coating), a layer of hydrophobic polymer that has been press coated and a core tablet having drug (for quick release). Limitations of this system include the following:

i. The rate at which the stomach empties varies greatly between individuals or isinfluenced by the kind and quantity of food consumed.

ii. The drug's gastrointestinal transit would alter in response to gastrointestinalmotion (peristalsis or contraction) in the stomach.

iii. Patients with IBD, carcinoid syndrome, diarrhoea, and ulcerative colitis haveshown accelerated transit across various parts of the colon.

Because of this, time-dependent systems are not the most effective for administering drugs to the colon specifically for the management of colon illnesses. It may enhance the site-specific delivery of the medication to the colonby successfully fusing the pH and time-related approaches into a single dosage form [14].

C. Microbe Induced colon specific Delivery

i) Prodrug Approach

Prodrugs are inactive variants of drug molecules that degrade into their active form when attacked by digestive enzymes, such as those found in the colon. The colonic area should undergo the greatest amount of hydrolysis relative to the upper section of the GIT for the best medication distribution in the colon. Azo conjugates are the chemical classes for this category that have been investigated the most. This method is not very versatile since it is dependent on the functionalgroups of the medication. Another method to keep it intact while it moves along the stomach and small intestine is by covalently connecting the drug carrier system. A drug may bind to cyclodextrin, glucuronide, dextran, and amino acids as carriers for the drug. An azo bond may also be used to connect it to a carrier. Colonic bacteria or enzymes break down each of these bonds [14].

(ii) Polysaccharide-Based Delivery Systems

Due to a number of benefits such accessibility, simplicity in modification, stability, safety, and biodegradability, polysaccharide-based delivery systems arebecoming a favoured choice for colon-specific medication administration. In CDDS, using many polysaccharides is more efficient than using only one. These polymers are unsoluble in highly acidic mediums, but they dissolve as pH rises above a specific range. Different levels of pH are necessary for the polymer to dissolve depending on the degree of esterification**.** Pectin, chitosan, chondroitin sulphate, galactomannan, and amylose are examples of polysaccharides that are excellent candidates for colon-specific administration since they may be broken down by colonic enzymes and are non-toxic to organisms [17].

D. Intigrated Approaches for CDDS

(i) Pressure Controlled Drug Delivery Systems:

The digestion process needs the contraction of the stomach and peristaltic motions for the propulsion of intestinal contents. The crushing and transportation of the intestinal contents as well as variations in the intensity and duration of pressure throughout the GIT are caused by the contraction of muscles in the gut wall, with the colon being thought to have higher luminal pressure as a result of the processes that take place during stool formation.

(ii) Pulsincap system

Due to variations in gastrointestinal transit brought on by peristalsis or conditions like IBS, as well as variations in the time it takes for the stomach to empty, time-dependent systems are not always the best for administering medication to the colon. Therefore, colon-targeted distribution may be achieved by integrating a timed release system with pH-sensitive features.A formulation that makes use of both of these methods is the pulsincap system.

(iii) Osmotic controlled drug delivery

This system can consist of a single osmotic unit or up to 5 or 6 push-pull units, each measuring 4 mm in diameter and enclosed inside a hard gelatin capsule. Each push-pull unit is a bilayered laminated structure that is encircled by a semi-permeable membrane and has an osmotic push layer and a drug layer [18].

1.3 THE COLON'S PHYSIOLOGY AND ANATOMY

The colon is split into various parts, as shown in Figure 1.3 and asdescribed in Table 1.3.
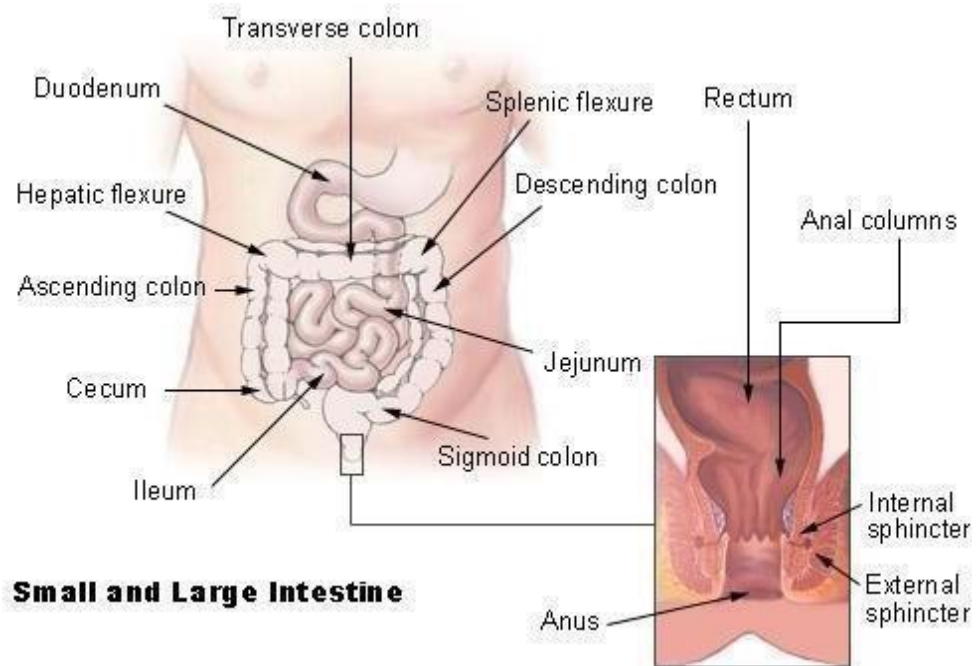
Figure1.3: Anatomy of GIT [19]

Table 1.3: Anatomy of large intestine [19-20]

Name of the part	Location
The ascending colon	It continues into the dilated section of the cecum, which is internally bound
The transverse colon	It crosses the abdominal cavity in front of the duodenum and the stomach to the area of the spleen

The descending colon	It exits the abdominal cavity on the left side before bending towards the midline
The sigmoid colon	It is an S-shaped part that continues downward to turn into the rectum
The superior and inferior mesenteric arteries	It supply the colon with arterial blood
The superior and mesenteric veins	It drain the colon's blood

A. The human colon primarily serves three purposes:

1. Because of motor patterns in the proximal colon, the transverse colon can either hold the material or move it distally.

2. The proximal colon, which serves as a storage area for faeces and enables defecation to be postponed until an opportune time.

3. The proximal colon and cecum function as a chamber for fermentation.

B. Colonic pH: As shown in table no.1.4, the pH of the gastrointestinal tract has been seen to significantly vary from the stomach to the small as well as the large intestine. Dietary habits, dietary consumption and disease status all has an impact on the GIT's pH. Utilizing a pH-sensitive enteric coating polymer, researchers are taking advantage of these pH fluctuations to deliver drugs to the colon and produce both local and systemic effects [21].

Table 1.4: Region of Gastrointestinal tract and pH

Region of GIT	Stomach	Small intestine			Large intestine	Rectum
		Duodenum	Jejunum	ilium		
pH	Fasting- 1.5 During fed -2 to 5	Fasting- 6.1 During fed- 5.4	5.4	7.8	5.5-7.0	7-8

Orally delivered medications are subjected to a dynamic environment. A medication will be exposing both the colon and the upper GIT if it is intended to target the colon. Table shows the various situations encountered while travelling through the GIT. The alteration of the intestines tract's pH is one of the main applications. The pH of the stomach typically lies between 1 to 3.5 [22]. Higher stomach pH is to be expected for that taking acid blocker medication, which has been shown to increase gastric pH in healthy human beings as high as 4.6. It can also increase in elderly people due to a pH > 5 [23]. The small intestine has a pH of 5.5 to 7.5 [24-25]. Additionally; the intestinal lumen includes a large number of enzymes (amylases and lipases as well as hydrolases and proteases like trypsin, chymotrypsin, and carboxypeptidases) and salts of bile. About 95% of the bile salts are reabsorbed in the ileum and circulated again [26]. Between the fasting and fed states, Bile and enzyme concentrations vary significantly between individuals.The upper GI-tract has a much lower concentration of bacteria than the colon, at 103–104 CFU/mL and as a result, bacterial enzymes have a much smaller impact than indigenous enzymes in the small intestine [27-29].

Table 1.5: GIT transit times of small oral dosage forms

GIT region	Stomach /Condtion		Intestine	
	Fasting	**Fed**	**Small**	**Large**
Transit time (In hours)	Less than 1	More than 3	3 to 4	20 to 30

1.4 POLYSACCHARIDES

Polysaccharides are found in most of the living things. They can be found in the tissues of various seeds, crab shells, leaves, stems, animal body fluids and insect wings. They are also present in the extracellular fluids, cell walls, and yeast, fungi, and bacteria [30-31].They represent a renewable source of high-yielding materials. As coagulants and flocculants, polysaccharides such guar gum, starch, sodium alginate, xanthan gum, and chitosan are used in their natural

forms [32-33]. They can be used as a super sorbent for water in a modified form, such as guar-graft-poly (sodium acrylate) [34-36]. Derivatization of functional groups, polymeric chain grafting, oxidative [37-39] or hydrolytic degradation, and polymeric chain grafting are popular techniques for altering polysaccharide materials [40]. Polysaccharides are formed by combining the monosaccharides. Because of their wide variety of forms and affordability, polysaccharides are plentiful in nature and less expensive [41]. The polysaccharides are employed in targeted drug delivery systems because they are simple to alter. They are also biodegradable, stable, safe, and non-toxic. Most polysaccharides, including guar gum, amylose, pectin, chitosan, and inulin, have already been employed as colon-specific drug delivery vehicles [42]. The food and pharmaceutical industries have long used natural sources of polysaccharides as excipients because they are inexpensive, readily accessible, biodegradable, and biocompatible.The natural polysaccharides do, however, have several drawbacks such as viscosity changes during storage, a shorter shelf life, uncontrolled hydration, and variations in solubility with pH changes. The foregoing disadvantages are diminished by the chemical alteration. There are numerous chemical processes that can be used to modify natural polymers, such as graft copolymerization, etherification, and cross-linking [43-44].
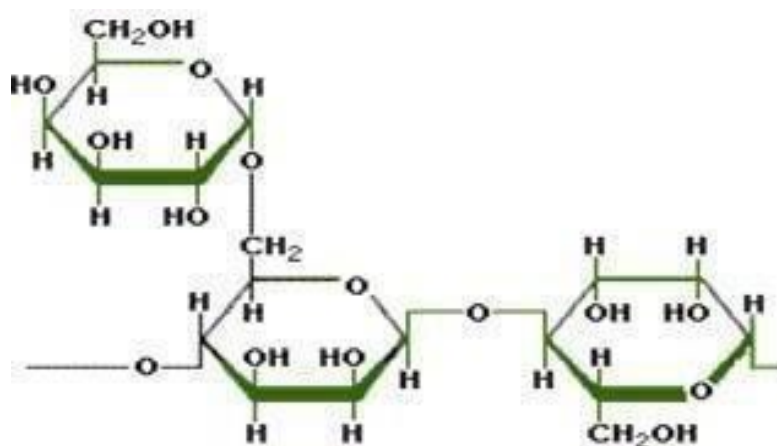
Figure 1.4: Structure of Polysaccharide [42]

1.5 GRAFT COPOLYMERIZATION

When a lengthy sequence of one polymer is mixed with another, such as polysaccharides, to generate a graft polymer [45-46]. With the help of an agent, free radical sites will develop on the surface of a pre-made polymer. The agent must be powerful enough to generate the required free radical sites while being gentle enough not to compromise with the structure's integrity of the produced chain of polymers. The chain propagation mechanism allows the addition of monomers to produce grafted chains. The benefit of grafting is that it allows a natural polymer to gain new properties without losing its original ones. For the graft polymers, natural polysaccharides are used as a base. Graft polymerisation is achieved by attaching vinyl and acryl monomers to the backbone of the biopolymer [47].

1.5.1 Types of Polysaccharides Grafting

Grafting can be mainly done by two methods are shown in Figure: 1.5.
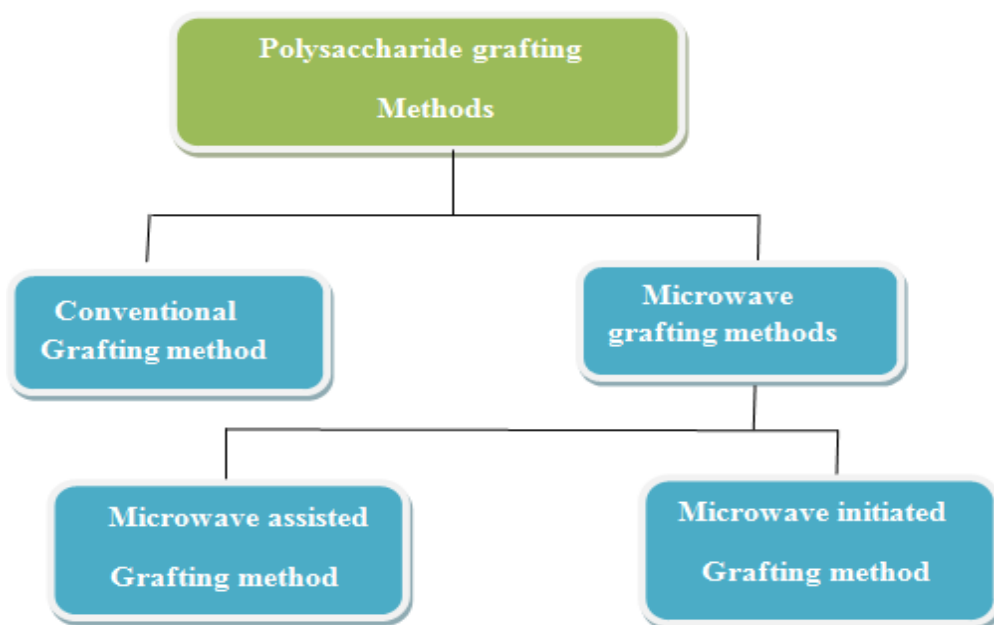
Figure 1.5: Methods of polysaccharides grafting

1.5.1.1 Conventional Grafting

There are three approaches to grafting monomers onto the surfaces of carbohydrates in the conventional grafting procedure and they are as follows:

A. Grafting through

When using the grafting via process, pre-synthesised vinyl functionalized polysaccharides are copolymerized with co-monomer components [48].

B. Grafting from

With this method, grafts are directly formed from the polysaccharide components that serve as their backbones. The most popular method is this one.

C. Grafting to

With this technique, free radicals are created along the polysaccharide backbone using chemical initiators [49]. Tetra acetic acid and ceric ammonium nitrates are two often used initiators [50].

The polysaccharide backbone may deteriorate when using conventional grafting methods.Only a few applications can make use of the traditional grafting method since it has little to no control over the weight distribution of the graft molecule. These issues have been resolved by creating macromolecular materials based on graft-functionalized polysaccharides by controlled/living radical polymerizations [51]. Sterculia gum [52], cashew gum [53], okra mucilage [54] and xylo glucan [55] were all grafted using the conventional method.
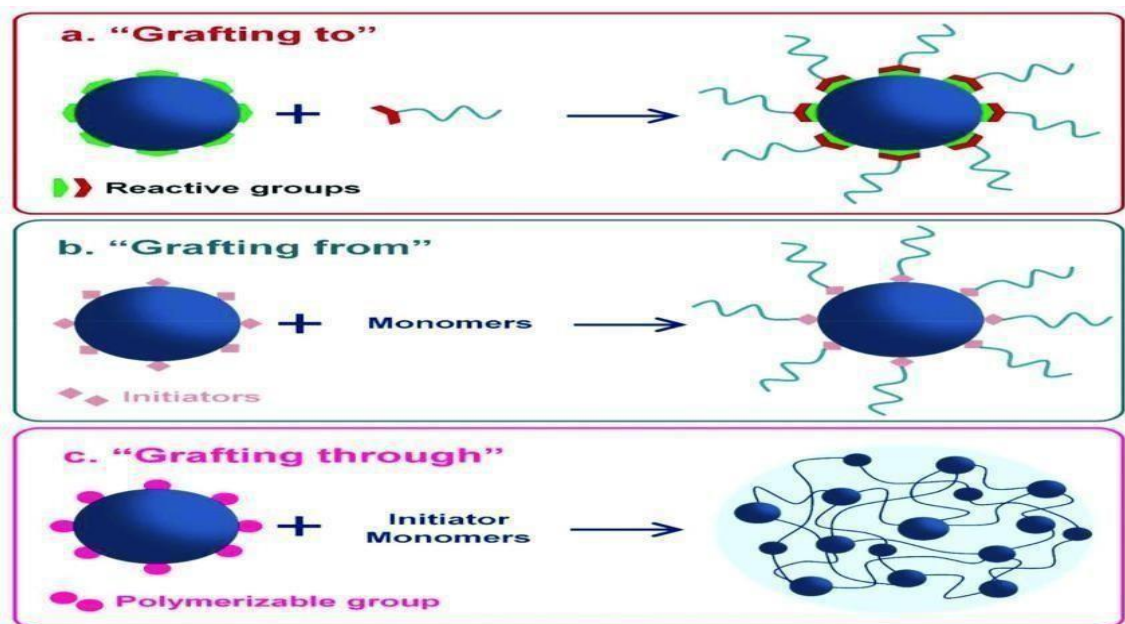
Figure 1.6: Conventional grafting techniques [49]

1.5.1.2 Microwaves

The academic and pharmaceutical communities have seen an increase in interest in microwave irradiation for chemical synthesis [56]. Microwave frequency (300 MHz to 300 GHz) generates electromagnetic radiation. When exposed to microwaves, charged particles align with the microwave's electric field, flipping their orientation and heating the medium [57]. Both a solution and a dry media can be used for microwave reactions. Preadsorption of the reagents onto an inorganic substrate occurs. Due to safety concerns, the use of microwave ovens was discouraged despite their popularity and inexpensive cost due to their ease of use and insufficient ability to control the temperature and pressure of the reaction. Domestic microwave ovens have undergone a number of modifications over the past ten years to solve these problems. The power of the microwave oven can be changed to obtain different percentages of grafting. The proportion of grafting is impacted by the irradiation's duration [58-59]. A microwave oven appeared in Figure 1.7.

Figure 1.7: Microwave Oven

A. **Microwave assisted grafting**

This method involves the use of an aqueous reaction mixture along with exogenous redox initiators. The redox initiator will produce the ions.The presence of these ions will enhance the reaction mixture's capacity to convert microwave energy into heat [60–63]. This accelerated reaction is due to the ability of microwave dielectric heating to rapidly generate heat within the

initiator, causing free radicals to form more effectively. As a result, grafting can go much more quickly than it could with conventional heating techniques. [64]. Microwave-assisted acrylamide graftingis an illustration of this technique on locust bean gum [65]. Utilising KPS (potassium per sulphate) as an initiator, microwave-aided grafting was used in an aqueous environment to crosslink and graft PVP on kcarrageenan backbone and agar [66].
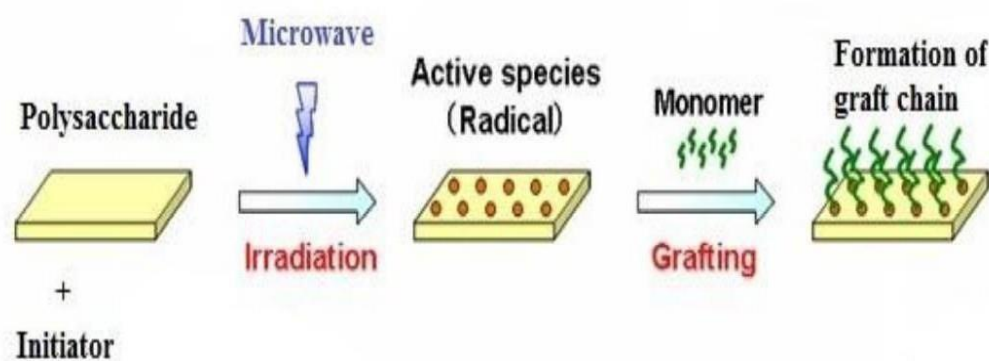
Figure 1.8: Mechanism for grafting of monomer on polysaccharide [66]

B. Microwave initiated grafting

For the goal of grafting, this technique does not require an initiator. The started grafting strategy is beneficial when high repeatability and exact control of percentage grafting are needed. Free radical formation is prevented by hydroquinone. Grafting of acrylamide on sodium alginate and carboxymethyl starch was done in microwaves and revealed the feasibility of grafting polysaccharides without the need of a redox initiator or catalyst [67-69].

1.5.1.3 Microwave technology has a number of advantages over traditional methods

- Increased in process speed.
- High reproducibility.
- Unlike traditional grafting techniques, uniform heating occurs throughout the material rather than surface heating.
- High is heating efficiency.

- Better and greater rapid process control is achieved.

- Unwanted side effects are decreased.

- Purity in final product.

- Floor space requirements are less.

- In certain cases, selective heating occurs, which may result in increased efficiency and lower running costs.

- Attractive physical and chemical effects are produced.

- Minimize the wastage of heating reaction vessel.

- Super heating: In traditional heating, where the heat originates from the outside, the solvent's core may be 5°C colder than the edge, whereas in the microwave, where the heat is employed from the inside, the core is 50°C hotter than the outside, we can raise the boiling point by 5°C, a phenomenon known as super heating [70–72].

1.5.2 Grafting on solid support

In recent years, microwave-assisted polymer grafting has grown rapidly, especially when coupled with solvent-free methods, which produce clean, simple-to-perform, affordable, secure, and environmentally friendly conditions [73]. On a microwave-transparent support, like silica or alumina, polymers are adsorbed [74–76].

1.5.3. Solvents used in microwave grafting procedures

Solvents are one of the most crucial elements of the microwave grafting process. They cannot affect the polymeric system in any way. The solvent used in the microwave grafting procedure must also produce acceptable yields and grafting. Without causing any negative side effects, the following solvents can be employed in the microwave grafting technique [77].

Table 1.6: Solvents used in microwave grafting process [77]

S. No.	Name of the Solvent	Boiling Point (^{o}C)
1	Acetone	56
2	Acetonitrile	86
3	Diethyl ether	35
4	Dimethyl sulfoxide (DMSO)	189
5	Ethanol	78
6	Methanol	65
7	N,N Dimethyl formamide (DMF)	153
8	Pyridine	115
9	Toluene	110
10	Water	100
11	Xylene	137

1.5.4 Microwave grafting techniques application

Recent years have already seen the use of polysaccharides and their grafted copolymers in a number of drug delivery techniques.They have been used in transdermal systems, controlled systems, buccal systems, and colon targeted systems.

A. Colon drug delivery systems

Graft copolymers are employed in systems connected to the colon because they provide advantages include a pH near to neutral, a longer transit time, and reduced enzymatic activity.Grafted katira gum was used to create colon-targeted formulation of Ibuprofen [78].

B. Controlled drug delivery systems

The application of grafted soy protein isolate (SPI) in pharmaceuticals was studied by Rattan S. and her associates. The grafted hydrogel of SPI was researched as a sustained and controlled release of ciprofloxacin drug. In situations of oral cavity bacterial infections, the hydrogel may be employed as a controlled medication delivery mechanism [79].

C. Buccal drug delivery systems

Shailaja T and her coworker have isolated tamarind seed polysaccharide from seeds of Tamarindus indica linn. It was attempted to graft methyl methacrylate with the polysaccharide found in tamarind seed. The chemical method of potassium per sulphate was utilised as an initiator for grafting. Metoprolol succinate, a drug having a limited bioavailability (40–50%), was used to make buccal patches. The grafted tamarind seed polysaccharide and 2% tamarind seed polysaccharide buccal patches demonstrated sustained drug release for 12 hours [80].

D. Modified binder properties

Tablets containing diclofenac sodium were made by Huanbutta and associates using tamarind seed gum as a binder. Physicochemical characterization information indicates that the carboxymethylation procedure added a carboxymethyl group to the chemical composition of crude gum. Results from Fourier transformed infrared (FTIR) analysis demonstrated that chemical modification was successful. An X-ray diffractogram of powder revealed that the gum was amorphous in both the unmodified and modified forms. By boosting the amount of gum in the formulation, disintegration time and drug dissolution were both slowed [81].

E. Super viscosifier

Polymethyl methacrylate grafted sodium alginate was created by Rani and her colleagues with the aid of a microwave. Examination of the intrinsic viscosity supported the grafting of polymethyl methacrylate chains onto the backbone of polysaccharide. After polymethyl methacrylate chains were grafted on top of sodium alginate; its inherent viscosity was greatly increased, creating a grafted product that may be employed as a better viscosifier [82].

F. Transdermal drug delivery approach

In vitro skin penetration tests were used to evaluate the efficacy of D, L-tetrahydropalmatine graft copolymer nanoparticles. *In vitro* studies on transdermal permeability were carried out using Franz diffusion cells. Drugs could be administered via the rats'skin with the help of this nanotechnology [83].

1.6 ORAL DOSAGE FORMS

The best way for delivering different drug delivery systems is the oral route. The best way when creating different dosage forms is the oral route. Oral drug delivery systems mostly use diffusion, dissolution, or both as their mechanism. Because they produce greater treatment efficacy, targeted oral delivery systems are superior to standard dose forms. Both traditional and cutting-edge drug delivery systems can be prepared for oral administration [84-85].

1.6.1 Downsides of conventional drug delivery systems

- Poor patient assent
- Variations in concentration of drug
- Peak-valley plasma concentration time formation makes it harder to maintain steadystate concentration.
- Variations in drug concentrations can result in a variety of undesirable side effects, especially when the agent has a therapeutic index that is small [86].

1.7 SUSTAINED RELEASE

A drug substance is slowly released from a dosage form in sustained release formulations (SRFs) in order to maintain therapeutic response for an extended length of time. Depending on the dosage type, time. The dosage is given orally in hours, and parenterally in days and months [87].

The primary purpose of developing SRFs was to extend the drug's duration of action, reduce dosing frequency, minimise adverse effects, and lower the amount of drug needed while still delivering uniform drug delivery [88].The interest in continuous release drug delivery systems has risen majorly during the last two to three decades.
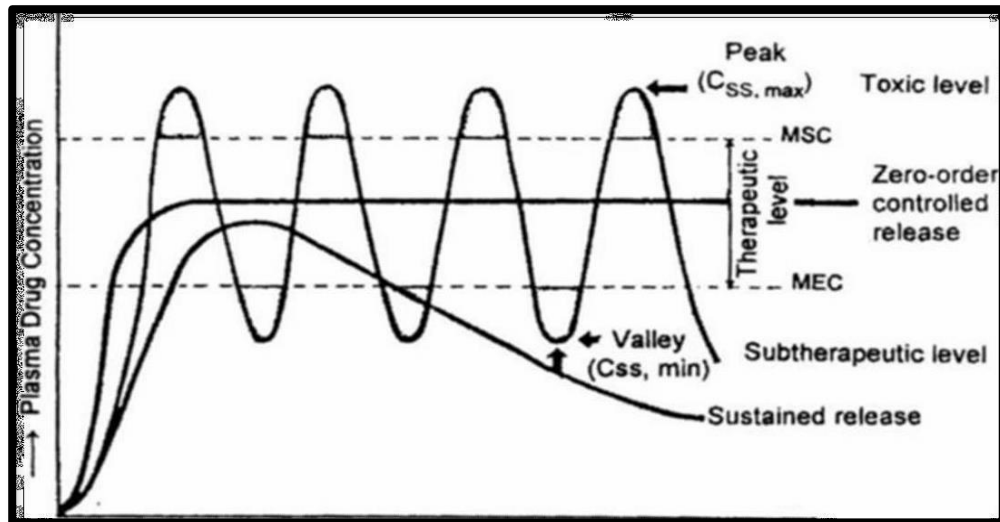
Figure 1.9: Plasma drug concentraion-time curves showing different release pattern of sustained and conventional dosage forms [89]

1.7.1 Advantages of sustained release

- Improved patient compliance due to reduced frequency of drug administration.
- Maximum utilization of the drug.
- Higher drug safety margins for highly potent substances.
- Total amount of dose is decreased.
- Improved efficiency in treatment.
- Less fluctuation during steady state level.
- Minimize local as well as systemic side effects.
- Decreased healthcare costs by improved treatment.
- Improved bioavailability of some drugs [90-91]

1.7.2 Designing of sustained release drug delivery systems [90]

The Sustained release system for oral use is generally made of solids and is on the basis of dissolution, diffusion, or a combined mechanism to control the drug's release rate.

A.Dffusion controlled release system

In these systems, one of the rate-limiting steps is the diffusion of the dissolved medication through a polymeric barrier. Rather, as a result of the matrix's and

the surrounding medium's reducing concentration gradient, the drug release rate gradually decreases over time. This phenomenon highlights the importance of considering both diffusion and matrix erosion in predicting drug release kinetics. It is classified into two types:

1. **Systems with matrix diffusion control**

Matrix diffusion control refers to systems where the drug is dispersed within a solid matrix, such as a polymer, and the release rate is dependent on the diffusion of the drug through this matrix.

2. **Reservoir systems**

On the other hand, reservoir systems involve a separate compartment or reservoir where the drug is stored, and release occurs through a membrane or barrier. Both types of diffusion-controlled release offer advantages in terms of controlling drug release kinetics and achieving desired therapeutic outcomes.

B. Dissolution-controlled release systems

Systems are made to release a drug's active ingredient at a predetermined rate. These systems typically involve the drug being dispersed or dissolved in a matrix or reservoir, which then gradually releases the drug as it dissolves. The drug release rate is determined by the matrix or reservoir's rate of dissolution, allowing for precise control over its delivery. In these systems, drugs with a very slow dissolving rate or great water solubility and dissolution are utilised. Controlling the rate of release of medicines with high solubility is difficult. These systems were created by polymer-coating drug candidates and integrating the drug into an insoluble polymer.

1. Dissolution-controlled matrix (monolithic) systems

This system is also characterised due to the uniform distribution of drugs throughout the medium. In this procedure, waxes such as bees wax and carnauba wax are used to limit the dissolving rate by reducing the wettability of the tablets. The release rate in these systems is first order.

2. Dissolution-controlled reservoir (encapsulation) systems

This approach used cellulose and polyethylene glycol encapsulation techniques to encapsulate the medication candidate. These chemicals will slow down the dissolving rate depending on the thickness of the coating.

C. Systems for controlled release through diffusion and dissolution: In such systems; a membrane that is only partially soluble covers the drug core. As a result of the membrane's parts dissolving, pores are formed, allowing aqueous medium to enter the core and, in turn, allowing drugs to diffuse out of the system.

1.8 MICROSPHERE

Mirosphere is another type of multi-particulate carrier that is commonly used to enhance drug absorption and targeting in the colon. These homogeneous, monolithic particles, which can be anywhere between 1 and 1000 μm in size, are widely used as drug carriers for controlled release. For injection mode of distribution, microspheres smaller than 125 μm are used [94]. These solid, almost spherical particles of the drug are released either as a solution or in microcrystalline form. Utilizing microspheres enables controlled drug release in the colon, enabling targeted treatment for conditions like colorectal cancer or inflammatory bowel disease.

These carriers offer:

- Controlled drug release, extending the duration of the drugs' stay in the colon.
- Improving therapeutic effectiveness.
- They can also prevent drugs from degrading in the challenging gastrointestinal environment, ensuring the best possible drug delivery to the site of action.

- Because of their tiny particle size, these carriers can pass through the GIT more readily than single-unit dosage forms, resulting in less variance within and among people.

- Additionally, scattering multi-particulate systems in the GIT can result in more consistent medication absorption [93].

Drug entrapment during manufacturing can be achieved through coacervation, phase separation, polymerization, gelation, or encapsulation techniques, as well as covalent and ionic attachment. Either the medication is uniformly dispersed throughout the microsphere or it is totally encapsulated inside a special capsule wall. Polymer breakdown, drug solubility, and diffusion through the microsphere matrix, the wall of the microcapsule, or both, and control drug release. Microspheres have been extensively researched as prospective drug delivery systems.

1.8.1 Methods of preparation [95-96]

Different techniques have been used to create microspheres, including:

A. Emulsification and solvent evaporation method
B. Ion gelation method
C. Spray drying method
D. Spray hardening method

The chitosan polymer is essentially rigidized by every approach, which is also referred to as crosslinking or denaturing in the literature. Different rigidization methods used for different preparation methods.

A. Emulsification and solvent evaporation method

The method involves forming an inner aqueous phase chitosan-containing w/o emulsion. To allow the solvent in the inner layer to evaporate, the emulsion is agitated for generally three hours. Chitosan is additionally crosslinked when a suitable chemical (like glutaraldehyde) or physical agent (like heat) is added.

B. Ion gelation technique

This process, which is similar to the emulsion and solvent evaporation method, involves preparation of emulsion and then crosslinking the chitosan present in

inner aqueous phase of emulsion. The only difference is that crosslinking compounds used in the ion gelation process, like sodium dioctyl sulphosuccinate, a crosslinking agent with a negative charge, interact ionically with the chitosan polymer.

C. Spray drying method

The aqueous chitosan polymer solution is sprayed into tiny droplets, which are then exposed to hot air to cause the solvent inside to evaporate. As a result, chitosan microspheres are produced.

D. Spray hardening method

The technique includes spray drying, solvent evaporation, and emulsification. The droplets are produced by spraying as instead of emulsification. However, the droplets are subjected to a crosslinking agent, such as acetic anhydride, to achieve the crosslinking.

1.9 PH-DEPENDENT COATING OF MICROSPHERES

The pH fluctuations occurring throughout the GI tract are used in the drug delivery strategy. Because the pH of the terminal ileum and colon is found to be higher generally than in the rest of the GIT, the use of pH-sensitive biocompatible polymers in the coating of the formulation makes it a pH-dependent drug release formulation, which releases the drug at colonic pH [97]. The enteric coating additionally shields the integrated active compound from degradation in the GIT environment. By providing a slow release, the enteric coating enhances the bioavailability and efficacy of the drug [98]. In addition to triggering release at a particular pH range. Methacrylic acid copolymers (Eudragit®) are the most widely utilised pH-dependent coating polymers for oral administration. Rohm GmbH & Co. KG in Darmstadt, Germany, initially began marketing Eudragit in the 1950. Eudragit is created by polymerizing acrylic and methacrylic acids, or their esters, such as dimethylaminoethyl ester or butyl ester. By modifying the side-group composition of the chemical, Eudragits® may be change the solubility at different pH [99]. Eudragit L100 and

Eudragit S100 are excellent choices for pH-responsive targeted drug delivery systems. These polymers increase therapeutic efficacy while reducing the risk of side effects by only releasing the drug when the pH is between 6-7. The desired release profiles can be achieved by combining them in various ratios, providing flexibility in drug delivery systems. Methacrylic acid, methyl acrylate, and methyl methacrylate mix to form an ionic copolymer that is increasingly being employed for colon specific delivery [100].

1.10. LIMITATIONS OF REPORTED FORMULATIONS TO TARGET THE DRUG TO THE COLON

Sustained release, delayed release oral delivery devices, and intravenous injection are the main treatment options for colonic illnesses like UC, CD and colon cancer. As they fail to successfully reach the colon's target area, these techniques have one or more drawbacks. The larger, healthy area of the intestine is frequently exposed during the oral administration of medications for the treatment of colonic diseases using sustained or delayed release systems, which can result in negative side effects and inadequate treatment because the active ingredient is less readily available where the disease is present. When a result, when treatment duration increases, so do the problems connected to illness management, which lower patient compliance. Contrarily, intravenous injections cause the drug to be systemically transported throughout the body via blood, increasing the risk of harm to non-target areas. The last option in these circumstances is surgical excision of the malignant tissue. The removed portion of the colon is the principal component of a surgical excision of the colon. This is expensive, necessitates anextensive hospital stay, and most critically, there is a risk of metastasis.

1.11 BENEFITS OFFERED BY HERBAL BASED TREATMENT

There is currently no medication that can cure inflammatory bowel disease (IBD). All anti-IBD medications have unfavorable side effects and low efficacy, and one of the biggest disadvantages of the newer biological agent-based therapies is their high cost. Therefore, it is crucial to use natural products as a safer and more effective IBD treatment alternative. In addition to the many

pharmacological effects of berberine that have been documented recently, there may be particular therapeutic potential for IBD.

1.12 WHY CDDS NEED TO BE DEVELOPED?

Polysaccharide based CDDS have received a lot of attention, the method was unable to be implemented in commercial formulations due to systemic limitations. The native microbiota in the colonic environment is typically killed by the some medications, which are typically cytotoxic in nature. The release of pharmaceuticals from future dosages is compromised because the process by which drugs are released from polysaccharide- based delivery systems is entirely dependent on the activity of microbiota. The therapeutic technique becomes unsuccessful as a result. It is needed to design a novel delivery mechanism that can deliver the medication to the colonic site in order to get over these difficulties. By increasing the drug's availability at the local colon location, targeted drug delivery will not only increase the effectiveness of the treatment but also lessen any side effects by reducing the drug's availability throughout the body. In addition to the previously mentioned method, the formulation will be co-administered with probiotics in order to receive the triple benefits of probiotics, which include improving the drug's availability at the colonic site by utilising the polysaccharide coat and making it necessary to maintain the gut microbiota. This, in turn improves the therapy by reducing the side effects associated with drug such as diarrhoea.

Due to this, attempts have been made in the current study to create eudragit coated microspheres containing BBH using grafted copolymers to give site-specific release at the colonic region. The invention of microspheres was primarily motivated by the need for easier medication delivery to experimental animals to produce pre-clinical data and a reduction in the amount of excipients required for coating because polysaccharides swell when exposed to water. The effectiveness of the generated formulation was proven by *in vitro* and *in vivo* study by using Wister albino rats.

CHAPTER 2: REVIEW OF LITERATURE

2.1 DRUG REVIEW

Berberine Hydrochloride (Model drug)

Berberine hydrochloride (BBH) is an isoquinoline alkaloid found in many clinically significant medicinal plants, including *Berberis aristata* (tree turmeric), *Berberis aquifolium* (Oregone grape), *Berberis vulgaris* (barbery), *Hydrastis canadensis* (goldenseal), and several others [101]. It is a common component of Chinese medicine [102–103]. *Hydrastis canadensis*, *Berberis aquifolium*, and *Berberis vulgaris* are the sources of the isoquinoline alkaloid, berberine [104]. It is used for its anti-inflammatory property [105]. Previous research has demonstrated that BBH can reduce experimental colitis by increasing tight junction protein levels, decreasing lipid peroxidation, boosting epithelial barrier function, and balancing the gut microbiota [106].

IUPAC Name: 1, 3-Benzodioxolo [5, 6-a] benzo[g]quinolizinium, 5, 6-dihydro-9, 10-dimethoxy-, hydrochloride

Proprietary names: Berbamax.

Molecular formula: $C_{20}H_{17}NO_4 \cdot HCl$

Molecular weight: 371.81 g mol^{-1}

Structural formula:
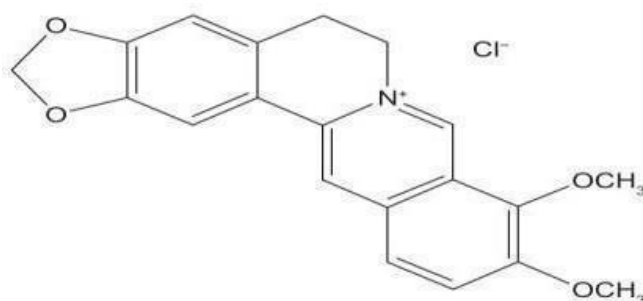
Figure 2.1: Chemical Structure of BBH [107]

Solubility:	Its aqueous solubility is very low. It is slightly soluble in ethanol but it is sparingly soluble in methanol. Additionally, phosphate buffer pH 7.0 was found to have the highest solubility of the drug out of all the tested pH values [102].
Category:	Anti-inflammatory
Description:	It appears as a yellow, crystalline powder that is either odourless or has a mild, distinguishing (faint characteristic) odour with a bitter taste.
Storage:	It must be stored in an air-tight container away from sunlight.

Mechanism of action of BBH

Previous research has demonstrated that BBH can reduce experimental colitis by increasing tight junction protein levels, decreasing lipid peroxidation, boosting epithelial barrier function, and balancing the gut microbiota [108]. Surprisingly, BBH has been shown to improve insulin resistance related to obesity through modifying the gut microbiota [109]. Many scientists who have studied how BBH affects anticolitis are still curious about how BBH works in UC [110]. Furthermore, Yan et al.'s study [111] discovered that in addition to BBH's capacity to boost the Nrf2/HO-1 pathway and repress the MAPK/PGE2 signalling pathway. The activation of the Nrf2/HO-1 pathway by BBH suggests its potential as a therapeutic agent for colitis, as this pathway is known to regulate oxidative stress and inflammation. Additionally, the involvement of the MAPK/PGE2 signalling pathway highlights the multifaceted nature of BBH's anti- inflammatory effects, providing valuable insights for future research on novel treatments for colitis.

Additionally, the role of BBH in oxidative stress and apoptosis, as well as its underlying mechanisms of action, were studied.

Uses-BBH is frequently used for its anti-inflammatory properties.

Dosage forms:

The following strengths and formulations are available for this medicine:

Table 2.1: Marketed strengths and form of BBH

S. No.	Brand Name	Company	Dose	Form
1.	Berber care	AdvaCare pharma	50 mg	Tablet
2	Solaray Berberine	Shasva Health	500 mg	Capsule
3	HealthyHey Nutrition Berberis	Hyuga life	750 mg	Capsule

2.2 EXCIPIENTS REVIEW

2.2.1 Guar gum [112-114]

Chemical Constituents in Guar gum

Cyamposis tetragonolobus, a member of the legume family, produces the crushed endosperms used to make guar gum. The gum primarily consists of hydrocolloidal, high molecular weight polysaccharide, which is composed of mannan and galactan units that have been joined together by glycosidic connections. A single-membered -D- galactopyranosyl unit appears as a side branch and is connected to the linear chain of - D-mannopyranosyl units by the bonds (1–4). Guar gum is widely used in the food, pharmaceutical and cosmetics industries as a thickening and stabilizing agent. Its ability to form a viscous gel when mixed with water makes it an ideal ingredient for creating hydrophilic matrix tablets. Moreover, guar gum's viscosity can act as a barrier of defence in the digestive system, delaying the medication's quick dissolution and absorption

and making the drug more susceptible to colonic environmental degradation. Guar gum has been employed as a controlled-release carrier by a variety of workers.
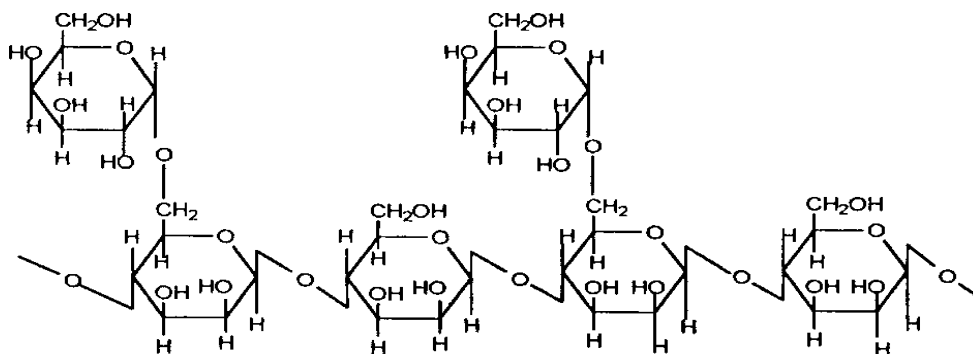
Figure 2.2: Chemical Structure of Guar gum [112]

Pharmaceutical applications

Galactomannan, known as guar gum, is frequently utilised in medicinal, culinary, and cosmetic compositions. It has also been researched as a potential replacement forcellulose derivatives like methylcellulose in the manufacture of matrix tablets with extended release as well as a controlled-release carrier, a suspending, thickening, and stabilising ingredient in oral and topical preparations, and as a disintegrant and binder in solid-dosage formulations (see Table 2.2). Additionally, the use of guar gum in colonic medication administration has been investigated. Oral controlled-release formulations have been tested using three-layer matrix tablets made of guar gum. Guar gum has been included in diabetic patients' diets for therapeutic purposes.

Table 2.2: Varieties of applications depending on Guar Gum's concentration

S. No		Concentration (%) Used as
1	1	Stabilizer (Emulsion)
2	Up to 10	Binder (Tablets)
3	Up to 2.5	Thickener (for lotions and creams)

Storage Conditions

Dispersions of guar gum in water act as buffers and remain stable at pH values between 4.0 and 10.5, although heating for a long time decreases their viscosity. A preservative containing 0.15% methylparaben and 0.02% propylparaben may improve its stability against bacteria. The powdered guar gum should be kept in a firmly sealed container. It isimportant to note that guar gum dispersions should not be exposed to extreme temperatures or humidity, as this can affect their stability and quality.

2.2.2. Acrylamide [115-119]

Hydration of acrylonitrile results in the formation of acrylamide, a crystalline solid that is biodegradable, highly mobile in soil and groundwater, and soluble in water, acetone, and ethanol. Polyacrylamide gels are preferred for electrophoresis due to their high resolving power and compatibility with various protein samples. These gels create a porous matrix that allows proteins to migrate based on their size and charge, enabling researchers to analyse and compare protein samples effectively. Additionally, the use of acrylamide as a quencher and modifier in protein investigations highlights its versatility and importance in studying protein structure and function**.** According to reports, due to their pH- responsive nature, polyelectrolytes that are frequently used for drug administration to particular parts of the gastrointestinal tract.

Chemical structure:
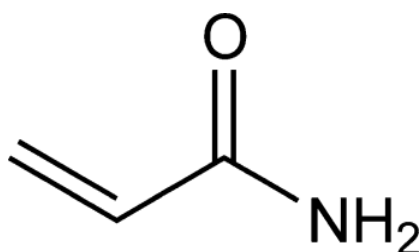
Figure 2.3*:* Chemical structure of Acrylamide [117]

Table 2.3: Physicochemical Properties of Acrylamide

S. No.	Property	Inference
1	Chemical name	2-propenamide
2	Molecular formula	C_3H_5NO
3	Molecular weight	71.08 g mol^{-1}
4	Appearance	Flakes that are colourless or white, or crystalline flakes that are practically white
5	Solubility	Water and methanol soluble and in ethanol, freely Soluble.
6	Odour	Odourless
7	Density	1.122g/cm^3

Uses:

- Acrylamide is utilised in several industrial processes, including colour manufacturing.

- Usually, acrylamide serves as a precursor in the production of polyacrylamide. As flocculants, poly acrylamide has been used to cleanse municipal and industrial effluents and purify drinking water. Additionally, poly acrylamide is found in hygiene and cosmetics.

- It is used to make polyacrylamide gels in biotechnology labs.

- Additionally, acrylamide is utilised as a soil stabiliser in tunnels, sewage systems, wells, and reservoirs as well as the production of pigments and organic chemicals like N-methylacrylamide**.**

  Storage: Store at a cold, dry, ventilated area. As it is stable at room temperature, it should be kept away from the sources of heat.

2.3 REVIEW LITERATURE RELATED GRAFT–COPOLYMER

Gouranga et al 2019

In the current work, ceric ammonium nitrate (CAN) was used as a free radical initiator to create a polyacrylamide(PAAM)-grafted copolymer of tamarind seed gum (PAAM-g-TSG) through microwave-assisted synthesis.The characterization of grafted gum was done by elemental analysis, FTIR, solid state 13C NMR, DSC, TGA, XRD, viscosity, and SEM. The grafted gum was found to be nontoxic and biodegradable. Finally, the grafted gum was tested for its flocculating properties in paracetamol suspension. According to the flocculation investigation, all grafted copolymer batches showed increased efficiency of flocculation ( ) in paracetamol suspension, and the efficiency also rose with increasing concentration and grafting. Among the other batches, the S_{11} batch (highest % G = 89±0.3) had the highest (= 5.14± 0.26) [120].

Shubhasis et al 2018

The current work uses the grafting strategy to utilize natural polysaccharides with the unique controlled characteristics of the grafted polymer under microwave irradiation in an effort to establish the grafting approach as a powerful tool for the synthesis of valuable derivatives with specialized properties. Acrylamide was grafted onto Cassia tora (CT) using microwave-assisted graft copolymerization, and the procedure was described. The grafted Cassia tora was found to be non-toxic. The established bioanalytical technique using LC-MS/MS to detect both medications in rat plasma was shown to be simple, accurate, and reproducible.The procedure was also validated in accordance with the legal requirements. Rats were used in the pharmacokinetic profiling study of the created tablet formulation, which contained sitagliptin, metformin, and the grafted CT as a polymer [121].

Singh et al 2018

The author studied the development of a colon specific formulation by using grafted gum, which was prepared by using polyacrylamide and natural gum (locust bean) with the helpof microwave-initiated graft copolymerization. The grafting of gum was established byXRD, DSC, FT-IR, SEM, swelling studies, and elemental analysis. The unbalanced swelling patterns of polyacrylamide grafted gum have been observed in comparison topure gum. The grafter gum was found to be non-toxic in acute oral toxicity studies [122].

Eswaramma et al 2017

The main purpose of the work was to synthesise sodium alginate hydrogel microbeads whose polymer network was functionally modified. The graft copolymerization technique used to modify guar gum was the use of N-vinyl caprolactam. Glutaraldehyde was used as a crosslinker, and the technique used for crosslinking was the emulsion crosslinking method. The copolymer graft was formulated using sodium alginate to produce hydrogel microbeads of Zidovudine (test drug). The graft characters, structural studies, morphology, and polymer-drug interactions were analysed by FTIR, NMR, SEM, DSC, and XRD studies. The microbead's potential sensitivity to pH and temperature was verified by the swelling sample [123].

Bardajee et al 2017

The microwave irradiation technique employed a synthesised silver nanocomposite hydrogel. The silver nanocomposite hydrogel (SNH) was synthesised and characterised by thermogravimetric (TC), FTIR, TEM, and SEM. The hydrogel is used to evaluate variables such as centrifugation time (min), methyl red solution pH, absorbent quantity (g), volume of acetone (mL), and chloroform volume (mL) [124].

Shruthi et al 2016

The acrylic acid-grafted guar gum nanocomposites were made by microwave irradiating Silane-modified nanoclay. While XRD diffractograms showed that the modified nanoclay in the guar gum-grafted acrylic acid had exfoliated, infrared spectroscopy validated the grafting. The optimised kinetic parameters of the reaction were determined through a series of experiments, allowing for the

efficient synthesis of the acrylic acid-grafted guar gum nano-composites. The findings demonstrated that adding nanoclay to the acrylic acidgrafted with guar gum greatly enhanced the nano-composite's swelling characteristics. Furthermore, the nanoclay also played a crucial role in enhancing the mechanical properties of the nanocomposites, as confirmed by tensile testing. Additionally, the pH sensitivity of the highly absorbent nanocomposite loaded with 1.75% modified nanoclay has been found to further improve its ability to remove crystal violet dye efficiently [125].

Badwaik et al 2016

The graft copolymer of carboxymethyl xanthan gum and acrylamide was synthesised by free radical polymerization using the initiator ammonium persulfate. The ideal grafting efficiency percentage was attained by altering the concentration of carboxymethyl xanthum gum, acrylamide, ammonium per-sulphate, reaction temperature, and time of reaction. The grafted copolymer was characterised by $_1$H, NMR, FTIR, XRD, thermal analysis, viscosity measurement, and SEM. Acrylamide was grafted onto carboxymethyl xanthan gum to increase the copolymer's thermal stability [126].

Giri et al 2015

In aqueous medium, Locust bean gum grafting was performed with microwave-assisted techniques and potassium per sulphate (KPS) as initiator. Several reaction parameters, including concentrations (monomer, initiator and polymer), time and microwave power, were investigated. The graft copolymer's behavior in terms of swelling was significantly impacted by the pH of the surrounding medium.FT-IR, DSC, XRD, and DSC studies were used for the characterization of the grafted copolymer. When compared to the native polymer, the graft copolymers performed better in terms of flocculation. Acute toxicity testing revealed the graft copolymer to be safe, and there was no mortality throughout the14-day period following graft copolymer therapy [127].

Setia et al 2014

The copolymer of natural gum (Aegle marmelos) was grafted by acrylamide using a microwave assisted technique. The combination of microwave radiation and the radical initiator ammonium per-sulphate (chemical free) was used. The

factorial experimental design using 3-level, 3-factor, microwave-assisted acrylamide gum was created and optimised. The microwave power effect, exposure time of the microwave, and gum concentration were studied for graft efficacy. The characterization of grafted copolymer and gum was performed by XRD, DSC, SEM, and FT-IR. The test drug Diclofenac was used to formulate controlled-release tablets. The controlled release assessment of tablets was studied *in vitro*, which showed promising results in comparison to ungrafted gum Aegle marmelos. Therefore, grafted copolymers might be used for CDDS [128].

Kaity et al 2013

The microwave irradiation technique allowed for a rapid and efficient grafting process, reducing the overall reaction time. The optimal conditions for grafting were determined by varying the irradiation time, acrylamide concentration, and redox initiator amount while keeping the locust bean gum concentration constant. Additionally, ceric ammonium nitrate was selected as the redox initiator due to its effectiveness in initiating the grafting reaction. The grafting gum was characterized by SEM, FT-IR, XRD, NMR, and DSC, contact angle, elemental analysis, viscosity, and swelling studies. The results of the characterization studies demonstrated the successful grafting of acrylamide onto locust bean gum. The controlled release matrix tablet of buflomedil HCl was prepared using the optimised grafted gum. The release profile of was evaluated using dissolution studies, and it was found that the grafted gum matrix provided a prolonged release of the drug over a desired period of time. The in-vitro release profiles of the controlled release matrix tablet further confirmed that the grafted gum exhibited rate controlling properties [129].

Concheiro et al 2013

They are evaluated Ionic polysaccharides that have been cross-linked for drug delivery to stimuli. The current state of cross-linked ionic polysaccharides as delivery system components that can control drug release in response to changes in ion nature and concentration, electric and magnetic field intensity, pH, temperature, redox potential, light wavelength, and specific molecules was examined in the study (enzymes, illness markers, and so on) [130].

2.4 REVIEW LITERATURE RELATED COLON TARGETING FORMULATION

Usama et al 2018

Nanoparticles of budesonide were created and studied. Budesonide pre-formulation studies were found, including information on the drug's solubility in aqueous form in deionized water, different buffer solutions, and solutions containing surfactants.Calculations of the partition coefficient were made using a water/octanol system at various pH levels. Studies on forced deterioration calculations of the partition coefficient were made using a water/octanol system at various pH levels. A LC-MS-MS spectrophotometer was used to investigate forced degradation experiments under a range of stress conditions, such as those that are neutral, oxidative, light, acidic, or alkaline. Budesonide has an aqueous solubility of 0.02566 mg/mL and a modest improvement in solubility when tween 80 is added. With the exception of greater alkali settings, where the drug entirely deteriorates into another product, budesonide has a 2.14 partition coefficient and exhibits good stability. Studies on the physically and chemically insoluble budesonide provided useful information for making nanoparticles [131].

Arigela et al 2018

Budesonide controlled-release ileal pellets with identical *in-vitro* release characteristics but a different manufacturing process were developed. Different coating methods (Matrix, barrier and enteric) were employed to create budesonide controlled release ileal pellets. The drug was not transported to the colonic region due to its rapidly absorbable nature. In order to make its use and availability at the ileum effective, a few strategies, such as controlled release systems and palletization procedures, are included. In this investigation, the pH solubility of drugs in solvents of different pH, postparameters, and dissolution profiles of the optimised-designed product of the innovator were compared. Given that the innovator's product's release was found to be comparable to that of the manufactured product, Entocort was considered to be the same as its counterpart [132].

Sirisa et al 2017

Sirisa et al. formulated karaya gum-based site-specific medication delivery of Cromolyn sodium. Both the ionic gelation method and the emulsion-ionic gelation approach were used to create the microspheres. FT-IR spectroscopy, DSC, and SEM were employed to confirm the grafting. Particle size analysis, percent entrapment efficiency (% EE), and *in vitro* drug release investigations were used to characterise and assess microspheres in various simulated stomach fluids. Studies on stability were conducted for a month at 40°C and 75 % RH. According to the SEM pictures, the surface morphology of the coated and core microspheres was, respectively, rough and smooth. IK1 and EK8 coated microspheres (15% w/v) from the optimised batch released drugs at rates of 95.24 and 99.74 percent over the course of 24 hours, respectively. The inclusion of enjzyme, which affects the polymer matrix as well as rat cecal components, boosted the drug's release rate. Higuchi kinetics was used to predict the drug release from each formulation of karaya gum microspheres. Additionally, the Korsmeyer-Peppas equation with a Fickian kinetic mechanism was followed by the optimized formulation. Finally, stability analyses showed that there was little change in the Microsphere's *in vitro* drug release and trapping efficiency, indicating well formulation stability [133].

Andremont et al 2008

Anderemont and coworker formulated Systems for delivering drugs to the colon that are intended for medicinal or diagnostic purposes are disclosed. The systems consist of zinc- or any other divalent cation-crosslinked pectin beads covered with Eudragit®-type polymers. The active agents of the drug delivery systems can be administered orally, and in certain cases, they can reach other parts of the gastrointestinal tract, including the colon. A wide range of ailments, such as malignancies, inflammatory illnesses, infectious diseases, and the like, can be identified, treated, prevented, or studied using the agents. Some agents can decrease the amount of leftover antibiotics that reach the colon after antibiotic therapy. Examples of these agents include metallo-dependent enzymes, such as -lactamase Ll from Stenotrophomonas maltophilia, and agents that inactivate macrolide, quinolone, fluoroquinolone, or glycopeptide antibiotics [134].

Fang et al 2016

Because polymeric core-shell microspheres are so convenient for treating a wide range of disorders with different treatments, they have been employed extensively in dual-drug release systems. In this study, acrylamide-modified chitin and chitosan core-shell microspheres were produced using coaxial electrospray. By adjusting the spray solution feed rate and the applied voltage, the thickness of the layer and the size of the microspheres may be delicately regulated. Scanning electron microscopy (SEM), Fourier transform infrared spectra (FT-IR), and stereo fluorescence microscopy were used to identify the core-shell structure of the microspheres. Small molecule FITC-dextran and macromolecular dextran blue 2000 were used as model medicines to study the dual-drug release behaviour of the core-shell microspheres. Regardless of where the FITC-dextran was located within the microspheres, the release rate of tiny molecular FITC-dextran was higher than that of macromolecular dextran blue 2000. The core-shell microspheres' biocompatibility, biodegradability and dual-drug release characteristics give them the potential to be used in combination therapies [135].

Liu and Zhou 2015

Using a natural polysaccharide, guar gum, a novel budesonide (BUD) colon delivery release method was developed. A chemical process used glutaraldehyde as the cross-linker, which was responsible for microspheres becoming stiff. These results indicate that the formulation successfully achieved a uniform particle size distribution, with an average size of 15.21 ± 1.32 μm.Additionally; the formulation demonstrated a high drug loading capacity, with $17.78 \pm2.31\%$ of the microspheres being composed of the desired drug compound, resulting in an impressive entrapment efficiency of $81.6 \pm5.42\%$. The microspheres were uniform in size, spherically shaped, and had a smooth surface. BUD was released in sustained way from the microspheres, per *in vitro* release profiles. $R^2= 0.9993$, the correlation coefficient, the Higuchi kinetic model had the best fit for BUD released from the microspheresin studies evaluating the safety of BUD guar gum microspheres. This suggests that the formulation is well-tolerated and

does not cause significant damage to the epithelial cells. Overall, BUD guar gum microspheres show promise as a potential treatment option for improving patient outcomes in respiratory conditions [136].

Sandborn et al 1998

Sandborn and coworkers were invented a therapeutic approach for treating inflammatory bowel disease (IBD), which involves locally providing an effective dose of nicotine to a patient's colon, rectum, and/or terminal ileum as necessary. One version of the current technique involves giving the patient oral nicotine in the form of a unit dose form that delivers the drug selectively into their colon, terminal ileum, or both. In a different variation of the technique, rectal administration of an enema formulation or rectal foam containing nicotine is an efficient way to deliver nicotine to the colon. An enterically coated unit dosage form can also be used to administer nicotine to an IBD patient's colon or ileum. Additionally, the current invention offers a unique composition that is especially well-suited for the colonic delivery of nicotine and is composed of polyacrylic acid polymers that have been crosslinked and complexed with nicotine. [137].

2.5 REVIEW LITERATURE RELATED TO EUDRAGIT COATING

Jeganath and senthilkumaran 2014

Budesonide colon-targeted medication delivery was created by Jeganath and Senthilkumaran (2014) to treat ulcerative colitis (UC). In order to treat UC, budesonide was chosen as a standard medication. The strong, synthetic, non-halogenated corticosteroid budesonide has a strong local anti-inflammatory action with few systemic side effects. Using HPMC K4M and Eudragit L30D coatings, tablets were created for sustained release in the colon. All the physical characteristics were assessed as part of quality control tests for the formulations and were within the pharmacopoeial acceptable bounds. In comparison to the other formulations, Formulation S15 showed appreciable dimensional stability, drug content, drug release, and lag time in the colon.

The optimised formulation S15 was the subject of stability tests over a three-month period at 40^0C/75% RH. Finally, it was shown that even after three months of storage at 40°C/75% RH, no change was observed in the physiochemical properties or the drug release profile [138].

Pandey et al 2016

In order to manage type-2 diabetes mellitus, they created and characterised floating microspheres using nateglinide as a model medication. Ethyl cellulose and eudragit S-100 were used as release retarding polymers in the oil-in-water emulsion solvent evaporation process to create floating microspheres. Assessments of the floating microspheres included *in vitro* drug release studies, percentage yield (%), drug content, drug entrapment efficiency, and particle size. Scanning electron microscopy was used to describe the surface morphology of the produced microspheres. The microspheres were discovered to have a spherical form and to be permeable. By using FTIR technology, compatibility studies were carried out. The produced microspheres demonstrated a sustained 12-hour drug release and continued to float for longer than 12-hours. Different release kinetics models, such as zero order, first order, Higuchi, and Korsmeyer-Peppas models, were studied for *in vitro* release kinetics, and the Higuchi plot with a release exponent n value smaller than 0.89 was shown to be the best match model. The floating nateglinide microspheres were discovered to be a practical and effective technique for extended drug release over an extended period of time, improved efficacy, oral bioavailability, and patient compliance [139].

2.6 REVIEW LITERATURE RELATED TO *IN VIVO* STUDY

Owusu et al 2020

Due to the recurrent inflammation in the bowel region, innermost lining of the colon and rectum becomes inflamed for a long period of time causing ulcerative colitis (UC). Traditional medicine has employed Cordia vignei leaf decoctions to treat the condition, either on their own or in conjunction with other plant treatments. In this study, we looked at how Cordia vignei leaf hydroethanolic extract (CVE) affected rat models of UC brought on by acetic acid. For seven days, CVE (30-300 mg/kg) were given orally to male Sprague Dawley rats and comared with other group whom 500 mg/kg of sulfasalazine and 10 ml/kg of saline were administered. On day, acetic acid (4% v/v) was administered intrarectally just once to cause colitis. On day 8, rats were slaughtered, and the colons were harvested for histological analysis. Additionally, blood was taken for a haematological evaluation. Colonic ulceration was considerably avoided by CVE (P <0.05), and the inflammatory score was decreased. TNF- and IL-6 serum levels were markedly decreased. Acetic acid effectively suppressed the reduction of catalase (CAT) and superoxide dismutase (SOD) activity while lowering the level of malondialdehyde (MDA), a marker of lipid peroxidation, in the colon. However, treatment with CVE had no discernible impact on weight loss. These findings imply that CVE may have an antiulcerative effect [140].

Shalkami et al 2018

The current study assesses the effects of diosmin (DIO) in ulcerative colitis (UC). Acetic acid (AA) was rectalally administered to rats to cause UC. This study's findings show thatAA increased the DAI and colon damage index scores. Additionally, a significant increase was seen in oxidative stress as well as inflammation markers. The expression of colon caspase-3 increased along with these alterations. DAI and colon damage index scores also reduced (as per the dose) in rats given two doses of DIO. Additionally, DIO led to a significant decrease in oxidative and inflammatory stressindicators as well as a decrease in caspase-3 expression. DIO therapy prevented the development of UC in rats by reducing apoptosis, oxidative stress, and inflammation [141].

Adakudugu et al 2020

A furanocoumarin called bergapten (5-methoxysporalen) decreases oxidative stress by inhibiting reactive oxygen species and improving neutrophil and macrophage clearance from the site of inflammation. In colitis caused by acetic acid, bergapten's anti-inflammatory abilities were evaluated.After acclimatization; the animals were obtained and split into six groups at random. Rats that were Sprague-Dawley were given 4% v/v acetic acid intraperitoneally for five days prior to the onset of colitis.The oral dosages of bergapten were 3, 10 and 30 mg/kg, while saline was administered orally in the control group at a dose of 5 mL/kg and sulphasalazine at a dose of 500 mg/kg as the standard medication. Colonic damage, the ratio of the colon's weight by length, and mucosal mast cell degranulation were all evaluated. In comparison to the disease control group, animals given bergapten in doses of 10 and 30 mg/kg had significantly lower colon-weight-to-length ratios ($p<0.05$). Additionally, there was less microscopic and macroscopic damage, and there were fewer mast cells that had degranulated.These findings suggest that higher doses of bergapten (30 mg/ kg) are more effective in reducing macroscopic damage. Further studies should be conducted to determine the optimal dosage for therapeutic use and to investigate potential side effects. Bergapten significantly decreased degranulation, with a p-value of <0.001 being significant. As a result, there was less damage and inflammatory cell infiltration at inflamed locations. Bergapten generally lessens inflammation in colitis brought on by acetic acid [142].

Thippeswamy 2011

The current study's objective is to assess how embelin extracted from Embelia ribes affects rat colitis brought on by acetic acid (3% v/v). Experimental animals received embelin and sulfasalazine at doses of 25, 50, and 100 mg/kg (p.o.) before colitis was induced.The therapy continued for up to seven days. Clinical, macroscopic, biochemical, and histological tests were used to gauge the severityof the intestinal mucosal injury. Embelin therapy significantly reduced the weight, gross lesion scores, clinical activity, percent affected area, and percent affected area of the wet colon when compared to acetic acid-induced

controls. Additionally, the drug markedly reduced serum lactate dehydrogenase, lipid peroxides, and colonic myeloperoxidase activity while markedly enhancing reduced glutathione. The aforementioned findings and protective impact were also supported by the histological examinations [143].

Rahman 2008

Performing pharmacokinetic and pharmacodynamic tests, as well as determining the distribution of colon-specific sodium alginate microspheres encapsulated in Eudragit S- 100 in rat's GI tracts, were the objectives of this work. Comparisons were made against a 5-flurouracil (5-FU) immediate-release (IR) formulation used as a control. The distribution of 5-FU from the IR formulation was mostly in the upper GI tract, whereas the distribution of 5-FU from the microsphere formulation was found primarily in the colonic region. Rats were given subcutaneous injections of 1, 2-dimethyl hydrazine (40 mg/ kg) for ten weeks in order to cause colon cancer. After the tumour was induced, the 5-FU formulations were administered for a period of four weeks. Colon-specific microspheres fed to animals resulted in a negligible reduction in tumour volume and multiplicity. The liver enzymes SGOT, SGPT, and alkaline phosphatase were elevated in animals given the IR formulation of 5-FU. It was discovered that these values were significantly different (P 0.001) from those of animals given colon-specific microsphere treatment. According to this study, delivering 5-FU to colonic tissues using alginate microspheres coated with Eudragit S-100 may be a more targeted method with fewer systemic side effects. However, additional research is necessary to examine the long-term dosage effects and identify all of this delivery method's therapeutic benefits [144].

CHAPTER-3

3.1 HYPOTHESIS OF THE STUDY

Because of their biodegradability, biocompatibility, accessibility and low cost, natural polysaccharides have historically been used as excipients in food and medications. They do, however, have a number of drawbacks that limit their applicability, such as unpredictable hydration, solubility based on pH, variations in viscosity with time, and a brief lifespan. These issues can be fixed by chemically altering natural polymers. Ethylation, graft copolymerization, and cross-linking are just a few of the chemical modifications that can be made to natural polymers. Recently, natural polysaccharide modification has attracted a lot of attention. There are other ways to modify polysaccharides, but grafting is the most effective approach. With this technique, novel copolymers with improved release properties can be made using a variety of polymers with synthetic origins. Natural polysaccharides are modified using a variety of synthetic monomers, including acrylic acid, acrylamide, and acrylonitrile. The polysaccharide's flocculating and releasing characteristics are both improved by vinyl treatment. Initiator-driven reactions, which were traditionally used in grafting copolymerization processes, take a lengthy time to create the graft copolymers and have a lower grafting effectiveness. An efficient method for swiftly distributing energy throughout the reaction mixture is microwave irradiation for grafting. Chronic inflammatory bowel disease, called ulcerative colitis, mainly affects the colon. Using the emulsion cross linking method, Eudragit- coated BBH microspheres were created for this study. Eudragit S-100 is a perfect polymer for targeted delivery to the colon because it can release the drug only in the inflamed areas associated with ulcerative colitis due to its pH-sensitive nature, which has a threshold pH above 7. This makes localised treatment possible and may lessen systemic side effects. The grafted copolymer is exposed when the Eudragit covering dissolves above pH 7.0, and this causes swelling. This swelling creates a porous network that facilitates the diffusion of BBH, resulting in its gradual release from the gel. Additionally, the higher concentration of the grafted copolymer may create a denser network within the

microspheres, impeding the diffusion of drug molecules. This could explain the slower release rate observed with increasing concentration.This controlled release system enhances the therapeutic efficacy of BBH. A literature review revealed that eudragit coated formulation by using grafted copolymer are preferable dosage form for encounter the disease where conventional dosage form are not effective.Therefore we can formulate eudragit coated microspheres of BBH by using grafted gum which deliver the drug only to the colon and rectify the disease.
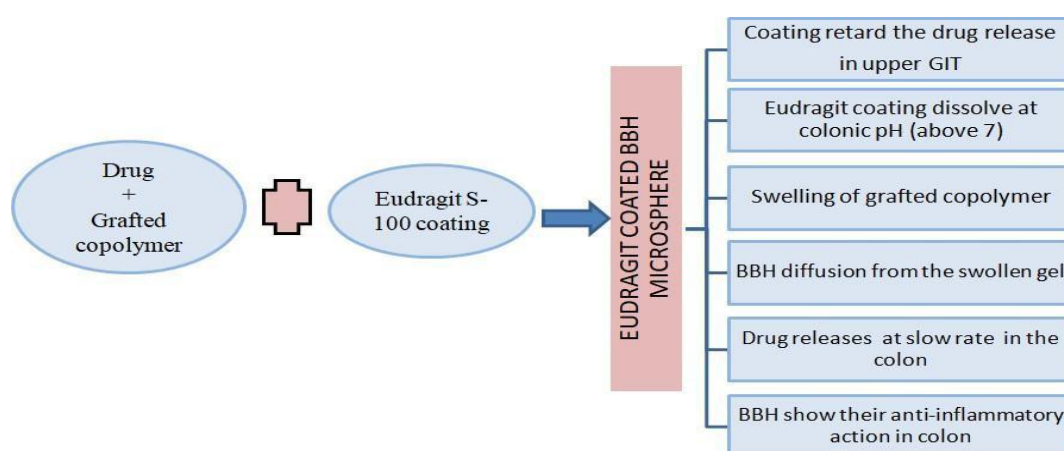
Figure 3.1: Mechanism of eudragit coated BBH grafted microsphere

3.1 AIM OF THE RESEARCH

The goal of the present investigation was to formulate and evaluate the eudragit coated solid dosage form of Berberine hydrochloride (BBH) containing grafted guar gum for Irritable bowel disease therapy.

3.2 OBJECTIVES

- To synthesize, optimize & characterize grafted copolymer using polyacrylamideand natural guar gum.

- To formulate, optimize & characterize solid dosage form of Berberine HCl by using grafted copolymer and eudragit coating of optimized formulation.

- To conduct *in vitro* and *in vivo* studies of optimized formulations.

- To perform the stability study.

CHAPETER -4: EXPERIMENTAL WORK

4.1 MATRIALS USED

Table 4.1: Research-related materials

S. No.	Name	Company/Model
1	Berberine HCl	PRS infotech and engineers, Faridabad
2	Guar gum	India scientific corporation, Sirsa
3	Acrylamide	India scientific corporation, Sirsa
4	Potassium di-hydrogen-O-Phosphate (KH_2PO_4)	Thermofisher scientific india pvt.Ltd, Powai,Mumbai
5	Di-Sodium hydrogen phosphate	Qualikems fine chem. Pvt Ltd.Vadodra
6	Gluataraldehyde (GA)	Loba chemical Pvt Ltd, Mumbai
7	Methanol	Fihar Chemical Ltd., Ahmedabad
8	Hydrochloric Acid	Thermofisher scientific india pvt.Ltd Mumbai
9	Acetone	Thermofisher scientific india pvt.Ltd Mumbai
10	Potassium persulfate	CDH Fine chemicals(P) Ltd, New Delhi
11	Span 20	Qualikems fine chem. Pvt Ltd.Vadodra
12	Polyvinyl alcohol(PVA)	CDH Fine chemicals (P) Ltd, New Delhi
13	Eudragit S-100	India scientific corporation, Sirsa
14	Light liquid paraffin	Fisher scientific
15	Carboxy Methyl Cellulose	Nice chemical pvt.Ltd. Kerala

4.2 EQUIPMENT'S USED

Table 4.2: Research-related equipments

S. No.	Name	Company
1	UV Spectrophotometer	Shimadzu, Japan
2	RT-HPLC	Shimadzu, Japan
3	Dissolution Test Apparatus	Lab india
4	Hot air oven	Narang Scientific Works, New Delhi, India
5	Bath Sonicator	Mesonix, New York, USA
6	Mechanical Stirrer	REMI Equipment
7	Magnetic Stirrer	REMI Equipment
8	pH meter	Shimadzu,Japan
9	Digital Balance	Cipzen CET-600
10	Test tube rack	Tarsons Products Pvt. Ltd., Kolkata, India
11	Melting Point equipment	Remi Equipment, Mumbai
12	Vortex mixer	Genei (SLM-VM-3000), Bangalore
13	FTIR	Perkin-Elmer
14	DSC instrument	Perkin-Elmer DSC 6000
15	FE-SEM	Jeol, JSM- 6510, Tokyo, Japan
16	Humidity chamber	REMI Equipment, Mumbai
17	XRD instrument	Malvern, UK

4.3 PREFORMULATION STUDIES

Before designing any kind of dosage form, a drug candidate is subjected to the preformulation research phase. Processing variables, including the technique of preparation and the pharmacokinetic response of the formulation, are greatly affected by the nature of the drug being used. In the simplest case, these preformulation experiments may only serve to validate that there are no significant hurdles impeding the compound's development. Basic information on candidate polymers and drugs is provided during the preformulation step. The decision taken based on the data produced during this step can have a significant impact on the compounds that are developed. FT-IR, UV spectroscopy, solubility, partition coefficient, and melting point were used to determine the BBH's chemical and physical characteristics.

4.3.1 Physical appearance

The drug's organoleptic properties were observed. The substance was characterised by its surface morphology, colour, odour and taste.

4.3.2 Determination of Melting Point [145-146]

The temperature at which a material transition from its solid state to liquid state under a single atmosphere of pressure is known as the substance's melting point. The purity of the drug compound was implied by the melting point determination. The melting point of BBH was ascertained using the following techniques.

A. Capillary tube method

A little quantity of BBH was introduced to a capillary tube with a thin wall, a length of 10-15 mm, an inner diameter of 1 mm, and one end closed.To gently andevenly heat the samples, the capillary carrying the sample was mounted and a thermometer was placed to measure the temperature. Berberine hydrochloride's stated melting point and measured melting point were discovered to be remarkably identical [147].

B. Differential scanning calorimetry

Perkin-Elmer DSC 6000 differential scanning calorimetry was used to examine the thermal characteristics of BBH. Sample powder was placed in an aluminium pan and sealed there, with an empty pan used as a reference. Scanning was carried out at 30–250°C per minute at a 10°C per minute heating rate. Additionally, the dry nitrogen purge pressure of 20 mL/min at 2.8 bar helps maintain a stable and inert environment within the system. The sample was cooled from 250°C to 30°C at arate of 20°C per minute after being maintained at 250°C for one minute [148-149].

4.3.3 FTIR Spectroscopy

The characterization of drug by FTIR (Perkin -Elmer) is to detect the any impurity in drug was ascertained by FTIR. The potassium bromide dispersion method was used to determine the infrared spectra of BBH. The functional groups found in drug candidates are shown by the spectrum. The drug's infrared spectrum was obtained, and the peaks were then determined by comparing it to reference spectra. Scanning was done between 400 and 4000 cm^{-1} [150].

4.3.4 Determination of drug's solubility in various solvents

The ability of a solid to dissolve in a liquid solvent and create a homogeneous solution is known as solubility. According to the IUPAC, solubility is defined as the analytical composition of a saturated solution expressed as a percentage of a particular solute in a particular solvent [151–152].

A. Qualiitative Solubility of BBH

Numerous solvents, such as methanol, ethanol, water, phosphate buffer of different pH (6.8 and 7.4), HCl of pH 1.2, chloroform and acetone, were used to assess the solubility of BBH. BBH was added in separate glass tubes with 10 mL of solvent. BBH solubility was then visually assessed.

B. Quantitative Solubility of BBH

Solubility of drug BBH was determined by dissolving its excess amount in 3 mL of selected solvents separately in tightly-capped glass vials. The vials were stirred with the help of vortex mixer for 10 minutes. The vials were then placed in a shaker bath at 25±1.0°C for 24 hours to achieve equilibrium.The equilibrated samples were taken out of the shaker and centrifuged for 30 minutes at 15000 rpm. A 0.45 μm membrane filter was used to filter the supernatant. The UV spectrophotometer (Shimadzu, UV-1800, Japan) was used to measure the concentration of BBH in each solution by scanning from 200 to 400 nm [153-154].

4.3.5 Method

Absorption Maxima (λmax) determination by UV Spectroscopy

Depending on the kind of electronic transition taking place, drug molecules in a solution absorb light of a specific wavelength when exposed to the UV-region of the spectrum.The determination of absorption maxima in methanol, The chromophoric portion of drug molecules in solution is frequently studied using a UV-visible spectrophotometer to obtain structural data.The absorbance versus wavelength plot of the UV spectrum is typically used to represent it. The absorption maxima were determined using a double beam UV-visible spectrophotometer.Using methanol as the solvent, a 14 μg/mL solution of BBH was scanned between 200 and 400 nm [155].

4.3.6 Preparation of standard curve of BBH in methanol

10 mL of methanol are added to a volumetric flask, which is then gently swirled to dissolve the 10 mg of BBH that was precisely weighed. 10 mL volumetric flasks containing 1 mL of the previously described stock solution were filled to the appropriate level with methanol, and the mixture was sonicated for a period of five minutes. Methanol was used to further dilute this solution, yielding varied concentrations ranging from 2 to14μg/mL. Using a UV-visible spectrophotometer, the absorbance of these solutions was measured at 350 nm with methanol serving as the blank, and a standard curve was constructed in opposition to concentration. The calibration curve was used to compute the intercept, slope, straight line equation, and correlation coefficient.

4.3.7 Analytical method development of BBH by using RP-HPLC

A.Instruments and apparatus [153]

To characterize the drug, an RP-HPLC device (Shimadzu, Japan) was employed, which was furnished with an auto-sampler, Nucleodur, C18 (4.6 ×250 mm i.d., 5 μm particle size), an SPD-10AVP UV-vis detector (Shimadzu, Japan), and LC-solution software. Following equipments were used

- Digital pH meter
- Bath Sonicator
- Analytical balance
- Pre-validated pipettes, volumetric flasks etc.
- Nylon membrane (0.22　m) filter

A.Reagents and materials

Following reagents were used

- Potassium di-hydrogen phosphate (KH_2PO_4)
- Acetronitrile
- O- phosphoric acid
- Double distilled water of HPLC grade

B. RP-HPLC Method

Chromatographic conditions were optimised and mobile phase was selected for above method.

- Stationary Phase: C_{18}, 250 × 4.6 mm, 5μm particle size, Nucleodur
- Elution mode: Isocratic elution mode (50:50 v/v)
- Mobile phase used:

  Solvent A: pH 3.0 buffer containing 50 mM potassium dihydrogen phosphate and o-phosphoric acid, Solvent B: pure Acetonitrile.

- Detector:UV-visible detector

- Absorption maxima: 346 nm

- Temperature of the Column:30 C

- Flow rate: 1.0 mL/min.

- Volume of Injection used:20 µL

- Diluent used :Methanol

- Run Time: 7 minutes

C. **Standard Stock Solution Preparation**

Blank: A 0.22 µ millipore membrane filter was used to filter the diluent and injected in HPLC system.

D. **Preparation of standard stock solution:** 10 mg of drug were accurately measured and put in a volumetric flask of 10 mL. After that, 5 mL of diluent was added and ultrasonically diluting the mixture for 10 minutes, then the volume was adjusted with diluents up to the mark to get the strength of 1000 µg/mL.To get the strength 100 µg/mL, 1mL further dilueted up to10 mL.

E. **Sample solution preparation:** From the stock solution, a sample solution of several concentrations ranging from 1 to 10 µg/mL was made by further dilutions. The sample solution was filtered with the help of membrane filters (0.22µ Millipore) and fed into the HPLC apparatus.

F. **Chromatogram of standard by HPLC:** Analysis of the standard was carried out by using HPLC and the chromategram was optimised, and the drug retention time was reported.

4.3.8 Berberine Hydrochloride calibration curve preparation utilising RP-HPLC

10 mg of BBH were precisely weighed and then added to a standard 10 mL volumetric flask along with 5 mL of the diluent.Using the ultrasonication bath, the solution was sonicated for a period of 10 minutes.To get the strength of 1000 µg/mL, the final volume of the solution was produced up to 10 mL using the diluent (solution A).The sample was further diluted to obtained solution B of strength of 10 µg/mL.

A. Development of calibration curve

BBH calibration curve was prepared by using aliquots (1 to 10 mL) of solution B and diluted up to 10 mL with diluent to reach a concentration of 1 to 10µg/mL. The method's linearity was evaluated by analysing the previously generated standard dilutions of BBH. The RP-HPLC received approximately 20 µL injected volume of each of the five standard solutions (working). The BBH calibration curve was generated by plotting the mean peak areas against standard solution concentration. The experiment was repeated five times, and the mean data was obtained at a wavelength of 346 nm.

B. Validation of analytical method

The analytical technique developed has been validated in accordance with the International Council for Harmonisation (ICH) Q2 (R1) guidline (169). The system's performance was validated by measuring system suitability characteristics. System's relevancy was assessed on the basis of the values of the theoretical plate, theoretical plate/metre, tailing factor, and peak purity index across all five replicate injections of BBH (5µg/mL) solution.

C. Linearity and Range

Plotting the mean peak areas of five replicate samples yielded the calibration curve with analogous BBH concentrations, and the regression equation was reported.

D. Accuracy

The accuracy of the newly developed method was assessed by computing the drug's absolute recovery from the mobile phase. Lower quantified concentration [LQC (80%)], medium quantified concentration [MQC (100%)], and high quantized concentration [HQC (120%)] were the three different technique concentration levels (i.e., 5 µg/mL) at which the dilutions were made. This was accomplished by taking individual aliquots of 4, 5, and 6 mL from a 10 µg/mL standard stock solution and adding them to a 10 mL standard volumetric flask.

They were further diluted with diluent to accomplish the LQC, MQC, and HQC. To calculate the percentage absolute recovery, divide the actual drug recovery by the theoretical concentration and multiply by 100 (Eq. 1). The investigation was repeated three times, and the mean data were assessed.

$$Absolute\ \%\ recover = \frac{Actual\ concentration\ recovered}{Theoritical\ concentration} X\ 100 \qquad Eq.No \qquad (1)$$

E. Precision

The repeatability and intermediate precision of the LQC, MQC, and HQC samples were evaluated to assess the consistency and reliability of the experimental measurements. By injecting the samples multiple times during the same day and measuring them on different days and by different analysts, any potential sources of variability were accounted for. The calculated percentage Relative Standard Deviation (% RSD) provided a quantitative measure of the precision and reproducibility of the analytical method.

F. Robustness

Robustness is generally carried out to check the effect of small changes on the precision of the mobile phase. Change in flow rate (0.80 and 1.2 mL/min) and absorbance maxima (344nm and 348 nm) were carried out. 5μg/mL sample concentration was injected three times to examine their influence on the acquired peak area, percent recovery (% R), and retention time (RT). The mean value and % RSD were calculated.

G. LOD and LOQ estimation

The calibration curve's slope (S) was used to calculate the LOD, which was 3.3 times the Y intercepts' standard deviation ( ), and the LOQ, which was 10 times that of the Y intercepts' standard deviation ( ) divided by the slope (S). These calculations provide a reliable measure of the limit of detection and limit of quantification for the analytical method. Eqs. 2 and 3 are as follows:

LOD= 3.3× standard deviation ( ) of the Y intercepts /Slope (S) Eq.No... (2)

LOQ= 10× standard deviation ( ) of the Y intercepts / Slope (S) Eq.No .... (3)

4.3.9. Determination of Partition Coefficient [156]

The BBH partition coefficient (oil/water) is used to evaluate a drug's capacity to pass cell membranes as well as its hydrophilic and lipophilic properties. At equilibrium, the amount of unionised drug (C) is equally distributed throughout both phases (organic and aqueous). Lipophilic drugs have partition coefficient (P) values more than one, whereas hydrophilic drugs have P values less than one. An n-octanol and water oil phase is commonly used to compute the partition coefficient.

Partition coefficient (P) = $C_{n\text{-octanol}}/C_{water}$ Eq.No   (4)

Where:

$C_{n\text{-octanol}}$: Fraction of drug in n-octanol

C_{water}: Fraction of drug in water

Consequently, the logarithm to base 10 (log P) of the partition coefficient (P) is acommon way to express it.

Procedure- Using the shaking flask method, the log P was measured experimentally at 25 °C. The octanol and water mixture (solvent) were taken in a flask and pre-saturated for 24 hours prior to the experiment in order to achieve equilibrium. For 24 hours, the equilibrated solvent mixture was shaken with measured quantity of drug. After the solvent mixture had settled following the shaking phase, samples of the octanol and water phases were taken. Analytical methods (UV- Visible spectrophotometer) were used to measure the drug concentrations in each phase [157].

4.4 DRUG EXCIPIENT COMPATIBILITY STUDIES

To check for incompatibility and physical alterations, the drug spectra with various excipients were investigated. In a ratio of 1:1, the drug was thoroughly mixed with the other excipients. By using FTIR, the drug's compatibility with the excipients was evaluated by scanning the samples in the range of 400-4000 cm^{-1}[158-159].

4.5 SYNTHESIS, OPTIMIZATION AND CHARACTERIZATION OF GRAFTED GUAR GUM

Acrylamide grafted guar gum was synthesised using the microwave assisted grafting method.

4.5.1 Microwave assisted Guar Gum Grafting trials using Acrylamide [160-161]

The gum solution was made by combining 50 mL of water with the desired amount of Guar gum (between 0.5-2 g). For each trial, the monomer was dissolved in 50 mL of distilled water to create the acrylamide solution at various concentrations ranging from 5 to 15 g. Following the addition of various concentrations (0.1-0.4 g), of the initiator (Potassium persulphate) the solution of monomer was poured dropwise into the solution of gum and continuously stirred this for two hours. The mixture was mixed with the initiator, which started the polymerization process. This mixture was heated in a microwave oven (Panasonic) at 50 to 100 MW for 2 to 4 minutes, or until it began to boil. Ice-cold water was used to quickly cool this hot solution. When acetone was added, a precipitate formed which was then filtered and washed with excess of acetone, then dried to obtain the final product.

The percentage and efficiency of grafting were calculated as:

Percentage yield (% Y)= $\dfrac{\text{Practical yield}}{\text{Theoritical yield}}$ X 100   Eq. No   (5)

Percent Grafting (% G) = W_1-W_0/W_0×100   Eq. No   . (6)

Percent Efficiency (% E) = W_1-W_0/W_2×100   Eq.N ....(7)

The weights of the grafted guar gum, the original guar gum, and the monomer used are indicated by the symbols W1, W0, and W2, respectively.

Initiation

$$R \longrightarrow R^*$$

$$MA\text{-}OH + M \xrightarrow{\text{Microwave-Irradiation}} MA\text{-}O^* + M^*$$
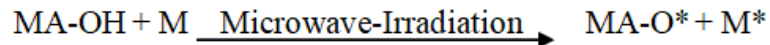
Where,

- R is initiator
- MA-OH is Guar gum
- M is monomer (Acrylamide)

Propagation

$$MA\text{-}O^* + M \longrightarrow MA\text{-}OM^*$$

$$MA\text{-}OM^* + M \longrightarrow MA\text{-}OMM^*$$

$$MA\text{-}OMM^*n\text{-}1 + M \longrightarrow MA\text{-}OM^*n$$

Termination

$$MA\text{-}OM^*_n + MA\text{-}OM^*_n \longrightarrow \text{Grafted Copolymer}$$

Formation of Homopolymer

$$M^* + M \longrightarrow MM^*$$

$$M^*_{n\text{-}1} + M \longrightarrow M^*_n \text{ (Homopolymer)}$$

$$M_n + MA\text{-}OM_n \longrightarrow MA\text{-}O^* + M_nH$$
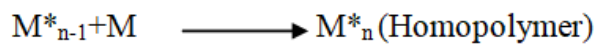
4.5.2 Box-Behnken design for guar gum grafting optimization and preparation

Software Design-Expert version 7 was selected. A 3-factor, 3- level Box-Behnken design was employed for a comprehensive analysis of the variables, considering three factors at three different levels. This approach provided valuable insights into the relationship between the independent and dependent variables, highlighting the significant variations observed among the 17 batches (G1-G17). The detailed information regarding these variables can be found in Table 4.3.

Table 4.3: Box Behnken Design (levels of independent variables) for Guar gum grafting

Variables	Unit	Level	
		-1 Level	**+1 Level**
Independent variables (factors)			
A= Amount of Guar Gum	G	0.5	1
B= Amount of monomer	G	5	15
C= Time	Min	2	3
Dependent variables (respons)			
R1= Percentage yield	%		
R2 =Percentage grafting	%		
R3 =Percentage Efficiency	%		

Table 4.4: Design Matrix of Box Behnken Design for Guar gum grafting

Experimental trial no.	Factor		
	A: Amount of Guar gum(g)	**B: Amount of Monomer(g)**	**C: Time (min)**
G 1	0.50	10	3.0
G 2	0.75	05	3.0
G 3	0.75	10	2.5
G 4	1.00	10	3.0
G 5	0.5	15	2.5
G 6	0.75	10	2.5
G 7	0.50	05	2.5
G 8	1.00	05	2.5
G 9	0.75	15	3.0
G 10	0.50	10	2.0
G 11	0.75	10	2.5
G 12	1.00	15	2.5
G 13	0.75	10	2.5
G 14	1.00	10	2.0
G 15	0.75	05	2.0
G 16	0.75	10	2.5
G 17	0.75	15	2.0

4.5.3 Characterization of ungrafted Guar gum and optimized grafted gum

The ungrafted gum and optimized grafted gum were further characterized by using different techniques of analysis (FTIR, DSC, XRD and SEM) [162].

A. FTIR Analysis

Powerful analytical methods like infrared spectroscopy can reveal important details about the chemical composition of the guar gum grafting procedure. It was possible to determine whether gum was successfully grafted onto the polymer backbone by comparing the IR spectra of the natural and grafted gum in the range of 4000 to 400 cm^{-1} [163].

B. DSC Analysis

The DSC analysis found distinct endothermic peaks that suggested the gum samples and grafted gum sample had gone through various phases or transitions. To ascertain the sample's thermal behavior samples were heated in a nitrogen atmosphere (at a rate of 20 mL/min) while being hermetically sealed in a flat-bottomed pan made of aluminium. 30℃ to 250℃ was selected as the temperature range, and 10°C per minute was the heating rate [164–165].

C. SEM

Both-sided adhesive tape was utilised to apply guar gum and grafted gum to the stubs, and fine coat ion sputtering was employed to coat them in gold palladium alloy (150- 200A^0). SEM was used to examine the materials' external surface structure [166-167].

D. XRD Analysis

The X-ray diffractometer was used to get the XRD pattern of the drug, excipients, and optimised grafted gum. The scan range employed was 0-50^0 of diffraction angle 2 . A voltage of 40 kV and a current of 30 mA were employed to measure the XRD pattern. In the XRD research, equivalent quantities of sample were provided.

4.6 PREPARATION AND CHARACTERIZATION OF BBH-LOADED MICROSPHERES USING GRAFTEDAND UNGRAFTED GUAR GUM

4.6.1 Preparation of microspheres (water in oil w/o emulsion method) [169]

BBH-microspheres were created using w/o emulsion cross-linking process. 20 mL solution of 2% (w/v) polymer was made by mixing different ratio of polyvinyl alcohol (PVA) and grafted gum (AA-g-GG) in deionized water (double-distilled). BBH (100 mg) was dissolved in the polymer mix solution described above, which was gradually emulsified with light liquid paraffin (100 g, w/w) and varied concentrations of different surfactants (Tween 80 and span 20). A magnetic stirrer was used to mix the emulsion at varied speeds for 15 minutes. Varied concentration (2.5-7mL) of glutaraldehyde (crosslinking agent) and HCl (0.5mL) were added to this w/o emulsion, which was then agitated for three hours. To eliminate the unreacted GA, the filterd solid microsphere waswashed with benzene and water.
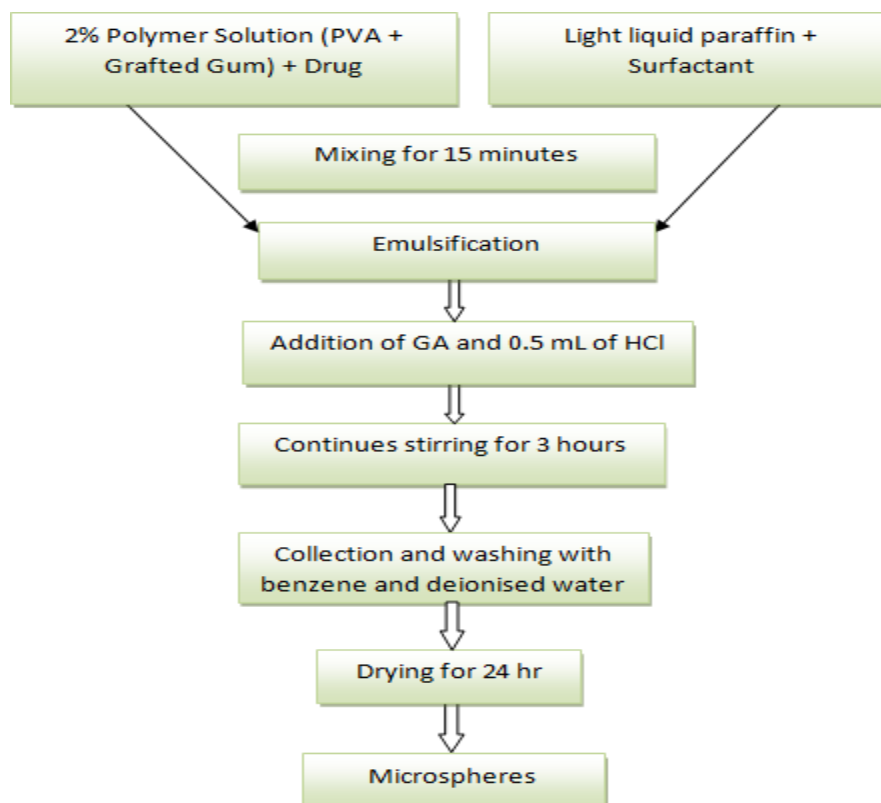
Figure 4.1: Preparation of microspheres by the w/o emulsion technique

4.6.2 Evaluation of Microsphere

A. Microscopic examination and Surface appearance

Process: Dried microspheres were studied using an optical microscope to measure the particle size and surface characteristics. The particle size was measured by taking 10–20 particles on a glass slide under regular polarized light. Prepared microspheres were examined under optical microscope at 10 X.

B. % Entrapment Efficiency (%EE)

Microspheres (50 mg) were dissolved in 10 mL methanol and the resulting solution was filtered through 0.45 m membrane filter paper (MDI Ambala). The filtrate was diluted and analyzed for drug content using ultraviolet spectrophotometer (Shimadzu 1800, Kyoto, Japan) at 350 nm. The entrapment efficiency was calculated using following equations the following equations:

$$\% \ EE = \frac{\text{Added drug} - \text{Free drug}}{\text{Added drug}} \times 100 \ \text{Eq.No}..............(8)$$

C. Drug Loading Capacity

Microspheres (50mg) were crushed in pestle and motor, dissolved in 10 mL methanol and the resulting solution was filtered through 0.45 m membrane filter paper (MDI Ambala). The filtrate was diluted and analyzed for drug loading using ultraviolet spectrophotometer (Shimadzu 1800, Kyoto, Japan) at 350 nm. Drug loading Capacity was calculated using following equations the following equations:

$$\% \ DL = \frac{\text{Drug loaded in microspheres}}{\text{Total Weight of Microspheres}} \times 100 \ \text{Eq.No} \qquad (9)$$

4.6.3 Box-Behnken design for preparation and optimization of microsphere formulation

4.6.3.1 Experimental design

Software Design-Expert version 7 was selected. To optimize formulation, a 3-factor, 3- level Box-Behnken design was employed. As the dependent variables varied greatly among the 17 batches (FM1–FM17), the Box-Behnken design was used to evaluate the impact of independent variables during the formulation development process. The guar gum: PVA ratio (A), RPM (B), and Span 20(%) (C) were independent variables. Percentage Entrapment Efficiency (%) (R1) Percentage Drug Loading (%) (R2) and Particle Size (µm) (R3), were regarded as dependent variables.

Table 4.5: Independentand dependent variables used in Box-Behnken design

Variables	Unit	Level	
Independent variables (factors)		**-1 Level**	**+1 Level**
A= Grafted Gum ratio with PVA	Ratio	30	40
B= RPM	--	600	1400
C= Span 20	%	0.5	1
Dependent variables (response)			
R1= % Entrapment Efficiency	%		
R2 = % Drug Loading	%		
R3 = Particle Size	µm		

Table 4.6: Box-Behnken design of experiment for microspheres

Experimental trial no.	Factor		
	Polymer 2% (w/v) A: Grafted Gum: PVA (w/w)	B: RPM	C: Span 20 (%)
FM 1	35:65	1000	0.75
FM 2	30:70	1000	0.50
FM 3	35:65	600	1.00
FM 4	35:65	1400	0.50
FM 5	35:65	1400	1.00
FM 6	35:65	600	0.50
FM 7	35:65	1000	0.75
FM 8	35:65	1000	0.75
FM 9	30:70	600	0.75
FM 10	35:65	1000	0.75
FM 11	30:70	1400	0.75
FM 12	35:65	1000	0.75
FM 13	40:60	1000	0.50
FM 14	40:60	600	0.75
FM 15	30:70	1000	1.00
FM 16	40:60	1000	1.00
FM 17	40:60	1400	0.75

4.7 EUDRAGIT COATING OF PREPARED MICROSPHERES AND CHARACTERIZATION

4.7.1 Coating procedure: Using the oil-in-oil (O/O) solvent evaporation technique, BBH-loaded microspheres (FMS6) were coated with Eudragit S-100 (ES). The BBH-loaded microspheres (equal to dosage weight) were dispersed in 10 mL of coating solution containing various concentrations of Eudragit S-100 (ES) in an ethanol: acetone solvent mixer with a ratio of 2:1. Then, 70 mL of light liquid paraffin containing 1% w/v span 80 was added to this organic phase. After three hours of continuous stirring at 1000 RPM, the solvent was completely evaporated at room temperature. To get the dried product, the coated microspheres were filtered, washed with n-hexane, and dried in a dessicator [170].

Figure 4.2: Sequential representation of steps involved in preparation of Eudrgit coated microspheres

Table 4.7: Composition of different formulations

S.No.	Formulation code	Microspheres (FMS6) (mg) Equivalent to 100mg of BBH	Eudragit-S 100(mg)	Ratio (w:w)	RPM
1	C1	500	100	1:0.2	1000
2	C2	500	250	1:0.5	1000
3	C3	500	500	1:1.0	1000
4	C4	500	1250	1:2.5	1000
5	C5	500	2500	1:5.0	1000
6	C6	500	3750	1:7.5	1000

4.7.2 Evaluation of coated microsphere

A. Microscopic examination and Surface appearance [171]

Process: The size and surface properties of coated microspheres were determined under light, the size was determined. A 10X optical microscope was used to examine the prepared microspheres. The microscopic pictures are shown shown in result section.

B. Percentage yield

The percent yield was determined using the following calculation based on the mass of BBH and polymer added:

$$Percentage\ Yield = \frac{Practical\ amount}{Theortical\ amount} \times 100 \quad \text{Eq.No} \dots\dots\dots\dots (10)$$

C. Percentage Entrapment Efficiency (%EE)

50 mg of microspheres were dissolved in 10 mL of methanol and than the solution was filtered by using membrane filter paper (0.45μm). The filtrate was then diluted and analysed for drug concentration using a UV spectrophotometer set to 350 nm. To calculate the entrapment efficiency, the formula given below was used:

$$\% \text{ EE} = \frac{Added\ drug - Free\ drug}{Added\ drug} \times 100 \quad \text{Eq.No} \dots\dots\dots\dots (11)$$

D. Drug Loading Capacity (%DL)

50 mg of microspheres were crushed in a mortar and pestle, and than the solution was filtered by using membrane filter paper (0.45μm). The filtrate was then diluted with10 mL of methanol and analysed by employing UV spectrophotometer at 350 nm. % DL was determined by using the following formula:

$$\% \text{DL} = \frac{Drug\ loaded\ in\ microspheres}{Total\ Weight\ of\ Microspheres} \times 100 \quad \text{Eq.No} \dots\dots\dots\dots (12)$$

E. Micromeritic study

Angle of repose ( ) [172-174]

The angle of repose ( ) of different formulations was measured using the fixed funnel standing method.

$$= \tan^{-1} hight\ (h)\ /radius\ (r) \quad \text{Eq.No} \dots\dots\dots\dots (13)$$

The angle of repose, which is used to describe how powder flows, better flow characteristics and angles of repose result from smaller particle sizes.

Table 4.8: Flow characteristics and Angles of repose according to USP

Flow property	Angle of repose (degrees)
Excellent	25-30
Good	31-35
Fair	36-40
Passable	41-45
Poor	46-55
Very poor	56-65
Very very poor	>66

Bulk and Tapped density

Pre-weighed microspheres were inserted into a graduated cylinder of 5mL capacity and the final volume was measured to calculate bulk density (BD). The cylinder was then tapped mechanically 100 times to get the tapped volume required to determine the tapped density (TD).

$$\text{Bulk Density (BD)} = \frac{\text{Mass of microspheres}}{\text{Untapped volume}} \quad \text{Eq.No} \quad (14)$$

$$\text{Tapped Density (TD)} = \frac{\text{Mass of microspheres}}{\text{Tapped volume}} \quad \text{Eq.No} \quad (15)$$

Carr's index (Ci) and Hausner's ratio (H.Ratio):

The following equations were used to calculate the microspheres compressibility index (Ci), also known as Carr's index value as well as H.Ratio:

$$\text{Carr's Index} = \frac{\text{(Tapped density} - \text{Bulk dendity)}}{\text{Tapped density}} \times 100 \quad \text{Eq.No} \quad (16)$$

:

$$\text{Hausner's ratio} = \frac{\text{Tapped Density}}{\text{Bulk Density}} \quad \text{Eq.No} \quad (17)$$

The value of both the parameters and their effect on flow characterstics of product are given in table 4.9.

Table 4.9: Scale of Flow ability as per USP

Carr's Index(Ci)	Nature of Flow	H. Ratio
<10	Excellent	1.00-1.11
11-15	Good	1.12-1.18
16-20	Fair	1.19-1.25
21-25	Passable	1.26-1.34
26-31	Poor	1.35-1.45
32-37	Very poor	1.46-1.59
>38	Very very poor	>1.60

4.7.3 Characterization of optimized formulation C5 (Eudragit coated)

A. FTIR Spectroscopy

The spectra of optimized formulation C5 were obtained using a Perkin-Almer IR spectrophotometer with a wavelength range of 400–4000 cm^{-1}. The spectra of the final formulation were investigated and compared to reference spectra.

B. XRD

X-ray diffractometer was used to get the optimised formulation's XRD pattern. The diffraction angle 2 was scanned in the range of 0-50^0. The XRD pattern was obtained using a high-voltage power supply to generate a 40 kV voltage. Additionally, 30 mA current was applied during the measurement to ensure accurate data collection. In the XRD study, equivalent amounts of samples were employed.

C. SEM

The shape and surface morphology of the produced microspheres (C5) were evaluated using a scanning electron microscope (SEM). A high vacuum evaporator's gold sputter module was used to coat the microspheres in gold after being mounted on a carbon-glued aluminium stub.The images were captured at a 10 kV excitation voltage. The chosen magnifications were adequate to show the detailed morphology of the study materials [175].

4.8 *IN VITRO* DRUG RELEASE STUDIES

The *in vitro* drug release profiles of pure BBH , uncoated microsphere of BBH, Eudragit coated BBH microspheres (grafted), and Eudragit coated microsphere of BBH (ungrafted) were determined by using a USP dissolution apparatus I basket type (Model DS-8000 Lab India). Separate capsules were filled with pure drug and microspheres of different formulations containing 100 mg of BBH, which were then added to the basket of the dissolution device. By modifying the dissolving medium's pH at various time intervals, the fluctuation in gastro-intestinal pH was simulated**.** The dissolution study was carried out at pH 1.2 for 2 hours, and this pH was adjusted with 0.1N HCl, pH 6.4 with phosphate buffer for the next 2 hours, and pH 7.4 up to the next 20 hours with phosphate buffer. 1.7 g of Potassium di- hydrogen phosphate (KH_2PO_4) and 2.225 g of di-sodium hydrogen phosphate ($Na_2HPO_4.2H_2O$) were added to the dissolving media to raise the pH from 1.2 to 6.4, which was thereafter adjusted using 1.0 M NaOH. After 4 hours, 1.0M NaOH was added to the dissolving media to bring its pH to 7.4.A buffer medium volume of 900 mL, a rotational speed of 100, and a temperature of 37± 0.5 °C were maintained. To keep the sink condition consistent, 5 mL of samples were taken out and replaced with an equal volume of fresh medium at regular intervals. Following filtration through a 0.45 µm membrane filter, the samples were subjected to HPLC (Shimadzu, Japan) analysis. HPLC analysis was used to determine the filtrate's area. The amount of drug found in the filtrate and the percentage of drug release (% DR) were both determined using the calibration curve [176–177].

4.8.1 Calculation of Similarity factor (f2) and Dissimilarity factor (f1)

The similarity (f2) and dissimilarity (f1) factors were calculated by using to compare two drug release profiles. Mathematical approach used to compare the dissolution profile using two factors, f1 and f2 were:

$$f_1 = \{[\textstyle\sum_{t=1}^{n} |R_t - T_t|]/[\sum_{t=1}^{n} R_t]\} \cdot 100$$

$$f_2 = 50 \cdot \log \{[1+(1/n)\textstyle\sum_{t=1}^{n} (R_t - T_t)^2]^{-0.5} \cdot 100\}$$

Where Rt and Tt are the cumulative percentage dissolved at each of the selected n time points of the reference and test product respectively.

Many regulatory rules state that when the f1 value is less than 15 and the f2 value is more than 50, the two product profiles are deemed to be similar or equal, and when the f1 value is more than 15 and the f2 value is less than 50, the two drug release profiles are deemed to be dissimilar.

Figure 4.3: Sequential steps of dissolution study

4.9 DRUG RELEASE AND KINETICS [178-180]

These model parameters aid in calculating the drug release kinetics and forecasting the drug's behaviour under various circumstances. The following data treatment models were used to visualise the findings of *in vitro* release studies:

- Percent drug released vs. time (Zero order rate kinetics)
- Log percent drug retained vs. time (First order rate kinetics)
- Log percent drug released vs. Square root of time (Higuchi's classical diffusion equation)
- Log of percent released vs. Log time (Peppas exponential equation)

A. Zero Order Kinetics

The equation given below makes the assumption that, regardless of the drug's concentration, the drug release rate stays constant over time. In systems

where drug release is regulated by mechanisms other than concentration, such as diffusion through a matrix or polymer erosion, zero-order release is frequently seen.

$$At = A_0 - K_0t \quad \text{Eq.No} \qquad (18)$$

Where

- At - The drug's amount released in time, t
- A_0 -The initial drug concentration (mostly it is, $A_0 = 0$)
- K_0- The zero order release rate constant expressed in concentration/time units would predict a zero-order release.

To analyse the release kinetics, data from *in vitro* studies were plotted as the amount of drug released (At) vs. time (t). If the plot is found to be linear with a slope of K_0, the data is consistent with zero-order release kinetics.

B. First Order Kinetics model

This model describes a system in which the release rate of drug from the formulation is concentration-dependent. The equation below would predict a first-order release.

Where $\qquad \text{Log } C = \text{Log } Co - Kt/2.303 \quad \text{Eq.No} \qquad (19)$

- C_0 - Initial drug concentration
- C - Quantity of drug released over time t
- K- First order rate constant

A straight line is obtained when the data are plotted as log percent drug remaining vs. time, showing that the release fits first-order kinetics. By multiplying 2.303 by slope values, the constant 'K' can be obtained.

C. Higuchi's Design

Huguchi developed the first mathematical model to describe drug release from a matrix system in 1961. It was first designed for planar systems, but it was later expanded to include porous systems and various geometrical types. The following hypotheses underpin the given model:

- The initial drug's solubility is significantly outweighed by its matrix concentration.

- Drug diffusion only takes place in one dimension

- System thickness is much greater than drug particle size.

- The matrix doesn't swell or dissolve very much.

- The diffusion of drugs is constant.

- The release environment always results in ideal sink conditions.

Higuchi was developed an equation first time which express the square root of a time-dependent process based on Fickian diffusion as the release of a drug from an insoluble matrix. Here is the Higuchi equation in its simplest form:

$$Q_t = K_H \, (t)^{0.5} \quad \text{Eq.No} \qquad (20)$$

Where:

K_H is the release rate constant.

Q_t is the drug's amount which is released during the time (t).

A straight line results from plotting the data as drug release versus square root of time, indicating that the drug was released via a diffusion process. The slope is denoted by "K_H."

D. Peppas and Korsmeyer Model

Korsmeyer et al.'s equation may be used to describe release rates from controlled release polymeric matrices.

$$Q = Kt_n \quad \text{Eq.No} \qquad (21)$$

Where Q represents the drug's proportion released at time (t)

K is a kinetic constant.

'n' is the diffusional exponent

For Fickian release, n equals 0.45, 0.45 to 0.89 for anomalous (non-Fickian) transport, and 0.89 for zero order release. Table shows the R_2 values for several release kinetic models.

4.10 STABILITY STUDIES [181-183]

For pharmaceutical products, stability studies are conducted to evaluate storage conditions and expiration dates. According to ICH guidelines, a stability analysis of the eudragit-coated BBH microsphere was conducted. Then the optimised batch (C5) was stored in a humidity chamber maintained at 40 ± 2 C/$75 \pm 5\%$ RH for 180 days (accelerated stability conditions) and 30 ± 2 C/$65 \pm 5\%$ RH for 360 days (long term stability conditions) and evaluated at 30-day intervals The physical appearance, flow characteristics, % EE, and % DL of the samples were assessed after each month. HPLC was used to determine how storage affected products.

4.11 *IN VIVO* EVALUATION OF OPTIMIZED FORMULATION

The *in vivo* study was carried out under the licence (800/PO/Re/S/03/CPCSEA) and with the approval of Lord Shiva College of Pharmacy's Institutional Animal Ethics Committee (IAEC). 10 week old male Wister albino rats (220± 20 g) were purchased from Small Animal House LUVAS, Hisar (1669/GO/ReBiBt/S/12 /CPCSEA).The animals (Rats) were kept in controlled environments with unrestricted access to food and water in various standard cages. Prior to inducing colitis, rats were starvingfor 48 hours while having free access to water [184-185].

4.11.1 Induction of colitis [186-187]

Nine groups of rats were selected at random. Each group had six rats (Table 4.10). An enteral feeding tube (medical grade) with an external diameter of 2 mm that was inserted 6–8 cm deep into the anus of the animals was used to induce colitis in them. Induction of Colitis in Animal Model werer performed under light and ether anesthesia. .Except for the healthy group, the colon was filled with approximately 2 mL of a 3% v/v acetic acid solution. The rats were kept inverted for at least two minutes in order to prevent solution leakage.The Normal (healthy) group (Group 1) was given 2 mL of a 0.5% Carboxy Methyl Cellulose (CMC) solution despite of acetic acid solution. To develop an IBD model, all the animals were kept untreated for a time interval of 24 hours during which food and water was provided in full access. Every group under treatment received a fixed volume of suspension of different formulations such as Eudragit coated BBH microsphere (ungrafted), uncoated BBH microsphere (grafted), placebo control (blank microspheres), and Eudragit coated BBH microsphere (grafted). Each formulation was given one time per day for five continues days; these doses, which were equivalent to 20 mg/kg/day to 40 mg/kg/day [178], were administered orally via gavages. Both the normal and colitis groups got 1 ml of 0.5% of CMC inspite of the drug formulation, whereas group 5 received a blank microsphere solution. The rats were sacrificed under anaesthesia after 24 hours from the last dose of administration. And a 6 cm portion of the colon was removed.

Table-4.10: Pharmacodynamic study

Group No.	Name of the group	Route and dose of drug (p.o.)	No. of animal
1	Normal (No colitis induced)	CMC (0.5%)	6
2	Experimental control (Acetic acid induced colitis)	CMC (0.5%)	6
3	Eudragit Coated BBH microsphere (ungrafted) Low dose(CMUGLD)	20 mg/kg/day	6
4	Eudragit Coated BBH microsphere (ungrafted) High dose (CMUGHD)	40 mg/kg/day	6
5	Placebo control (blank microsphere)	40mg/kg/day	6
6	Uncoated BBH microsphere (grafted) Low dose (UCMGLD)	20 mg/kg/day	6
7	Uncoated BBH microsphere (grafted) High dose (UCMGHD)	40 mg/kg/day	6
8	Eudragit coated BBH microsphere (grafted)Low dose (CMGLD)	20 mg/kg/day	6
9	Eudragit coated BBH microsphere (grafted) Highdose (CMGHD)	40 mg/kg/day	6

BBH-Berberine hydrochloride**, CMC-** Carboxy methyl cellulose
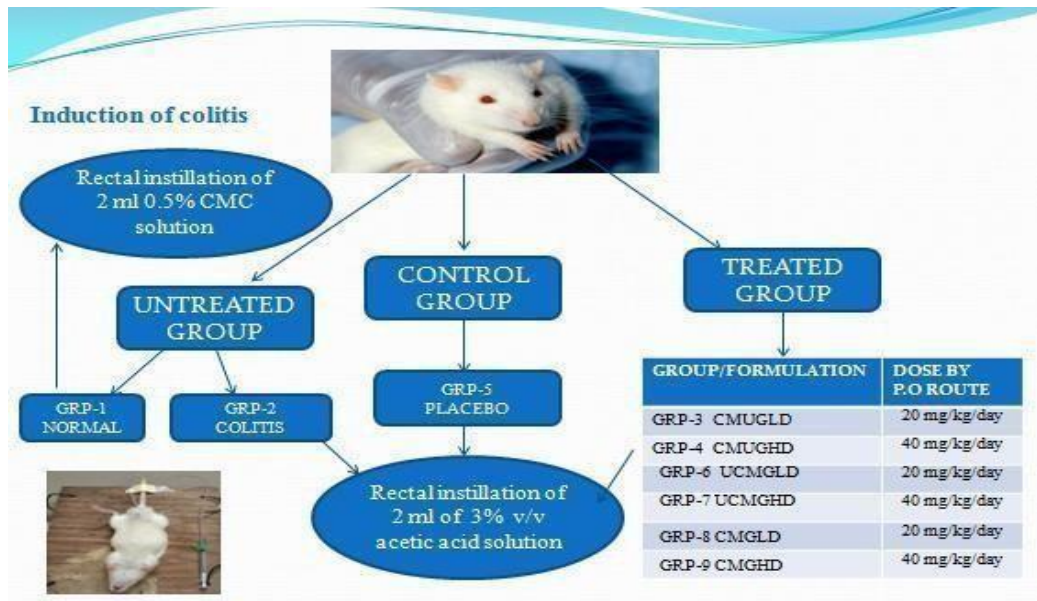
Figure 4.4: Schematic diagram of *in vivo* study

Figure-4.5: Sequential steps of *in vivo* study

4.11.2 Colonic Inflammation Evaluation

The rats were sacrificed under anesthesia after 24 hours from the last dose of administration, and a 6 cm portion of the colon was removed. All colon samples were opened lengthwise, washed, and dried. Colonic inflammation was assessed by using disease activity index scoring system. As indicators of colon inflammation, Colon's weight and length ratios and colon and body weight ratios were calculated based on the colon's weight and length, respectively.

A. Disease Activity Index

Every day, the colitis model's clinical activity was evaluated. We assessed three crucial clinical indicators, including anal haemorrhage, weight loss, and stool consistency (Table-4.11) [188-189].

Table 4.11: Disease Activity Index (DAI) Scoring System

Scoring parameter	Score's definition	Score
1. Body weight of Rat	No weight loss	0
	1-5%	1
	5-10%	2
	10-20%	3
	20%	4
2. Consistency of stool	Well formed	0
	Pasty and semiformed	2
	Sticky (liquid type) stool to anus	4
3. Bleeding in stool	No blood in stool	0
	Positive finding	2
	Gross anal bleeding	4
Total score		12

B. Colitis Macroscopic Examination

The rats were sacrificed under anesthesia after 24 hours from the last dose of administration, and a 6 cm portion of the colon was removed. All colon samples were opened lengthwise, washed, and dried. Colonic inflammation was assessed by using disease activity index scoring system. As indicators of colon inflammation, Colon's weight and length ratios and colon and body weight ratios were calculated based on the colon's weight and length, respectively [190-191].

C. Histopathological Assessment

Tissue samples from all groups were taken for microscopic examination of colon tissues. To fix the tissue, colon specimens were submerged in a formalin solution (10%) for 24 hours. The tissues were put onto paraffin-containing holders and dried in an oven after being rinsed with phosphate buffered saline solution to eliminate any remaining formalin solution. Using a microtome (outsourced), sections with a 20 µm thickness were cut. Hematoxylin and eosin (HE) stain was then applied to the sections. The produced slides were analysed using light microscopy and imaging. By using the score systems, pathological assessment of Colitis, morphological alterations were evaluated. The four main factors used in scoring systems are percentage of involvement, severity, extent, and degree of inflammation inflicted upon the tissue. The total of the results for crypt damage, inflammation severity, and inflammation extent represents the overall histopathology score. Table 4.12 displays the grading scheme for the pathological evaluation of colitis [192-197].

Table-4.12: Scoring System for Histopathological Examination

Scoring parameter	Score	Scoring definition
Inflammation severity	0	None
	1	Mild
	2	Moderate
	3	Severe
Inflammation extent	0	None
	1	Mucosa
	2	Mucosa and submucosa
	3	Transmural
Crypt damage	0	None
	1	Basal 1/3 damage
	2	Basal 2/3 damage
	3	Crypt lost, Surface epithelium present
	4	Crypt lost Surface epithelium lost
Percent of involvement	0	0%
	1	1-25%
	2	26-50%
	3	51-75%
	4	76-100%
Total score	10	

A. Statistical Evaluation

All trials were carried out on several formulations, and the mean of the obtained valuewas computed. GraphPad inStat software was used for statistical analysis. P values of 0.05 were deemed statistically significant (0.05).

CHAPTER 5: RESULT AND DISCUSSION

5.1 PREFORMULATION STUDIES

5.1.1 Organoleptic properties

Table 5.1 displays the organoleptic qualities of drug BBH discovered to be in accordance with the reference.

Table 5.1: Organoleptic Properties of BBH

Sr. No.	Properties	Inferences
1	Colour	Yellowish brown
2	Odour	Slightly characteristic odour

5.1.2 Determination of melting point

The capillary fusion method was used to determine the drug's melting point, and the findings indicated that the temperature was 196°C, which is compatible with the official measurements. DSC also measured the melting point of the BBH. The thermograph has shown that BBH has a melting point approximately 196°C.

Table 5.2: Melting Point of pure drug (BBH)

Sample	Melting point (°C)		
	Reference	Observed(Cappilary fusion method)	DSC
BBH	196	196.6 ±0.78	196
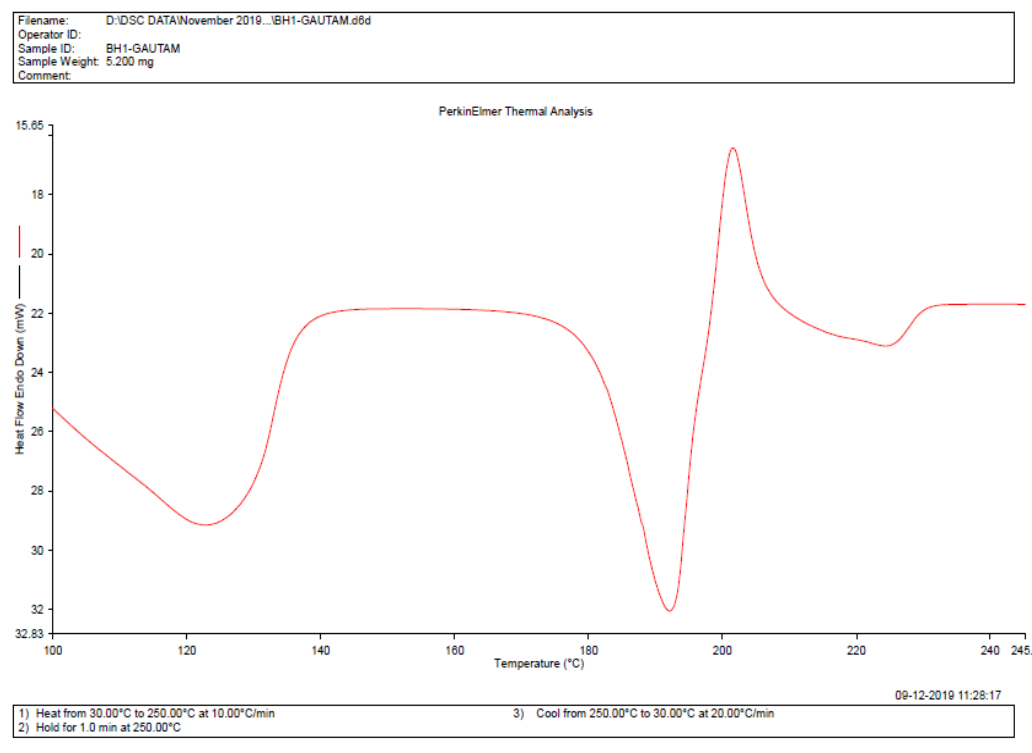
Figure 5.1: DSC thermograph of BBH

Discussion: The pure drug's melting point of berberine hydrochloride has been found to be in the range of 196°C. Consequently, the drug sample was free of all contamination.

5.1.3 Fourier-Transform Infrared Spectral Assignment

The FTIR spectrum reveals the functional groups contained in BBH, and these functional groups act as the main criterion in the identification and purity of the drug candidate. The drug's infrared spectrum was compared to reference spectra in order to identify the peaks. The sample was scanned between 400-4000cm^{-1} with an FTIR scanner.
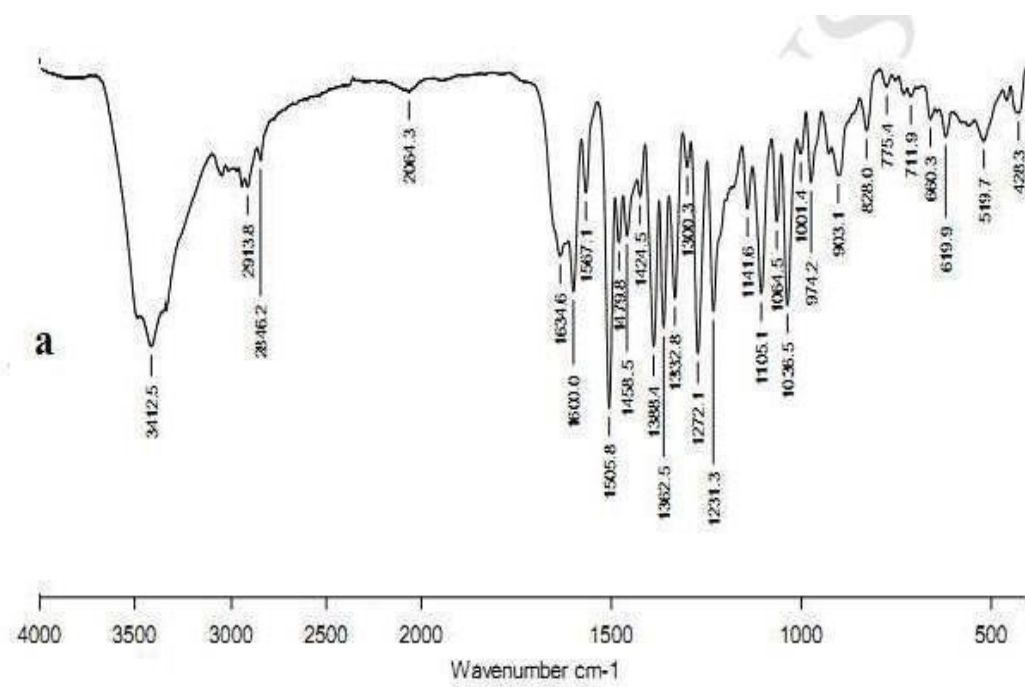
Figure 5.2: FTIR spectrum of BBH (Reference)
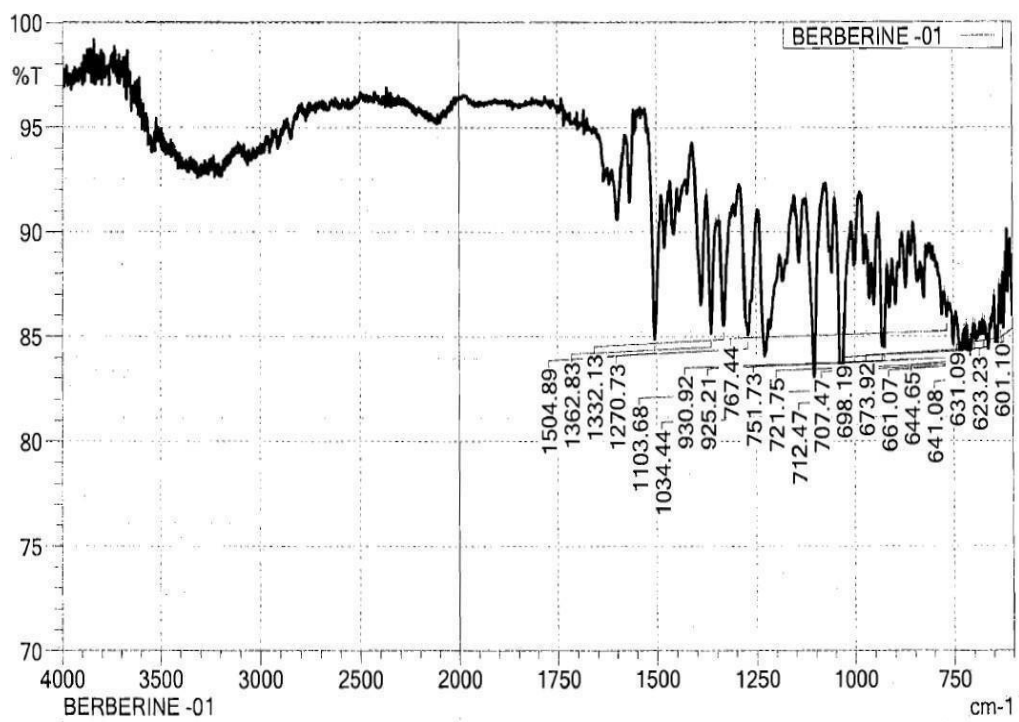
Figure 5.3: FT-IR spectra of BBH

Table 5.3: FTIR Interpretation of BBH

S. No.	Functional Group	Observed (cm^{-1})	Reported (cm^{-1})
1.	C-H stretch	2834	2820
2.	C=C stretch, C=Nstretch	1504.89 1610	1597
3.	C–H deformation	1362.13	1354-1383
4.	C-O stretch	1034.44	1060

The aforementioned spectra contain all of the distinctive peaks of BBH, including those at 2834 cm^{-1} (showing C-H stretch structure), 1504.8 cm^{-1} (showing C=C stretch),1610 cm^{-1} (C=N stretch), 1362.13 cm^{-1} (indicating C-H deformation), and 1034.44 cm^{-1} (C-Ostretch). As a result, the drug is pure and devoid of contaminants.

Note: Peaks showed in FTIR spectra as per IP are ranges from 400-2000 cm^{-1}, where as pure drug spectra range from 400-4000cm^{-1}.

5.1.4 XRD of pure drug BBH
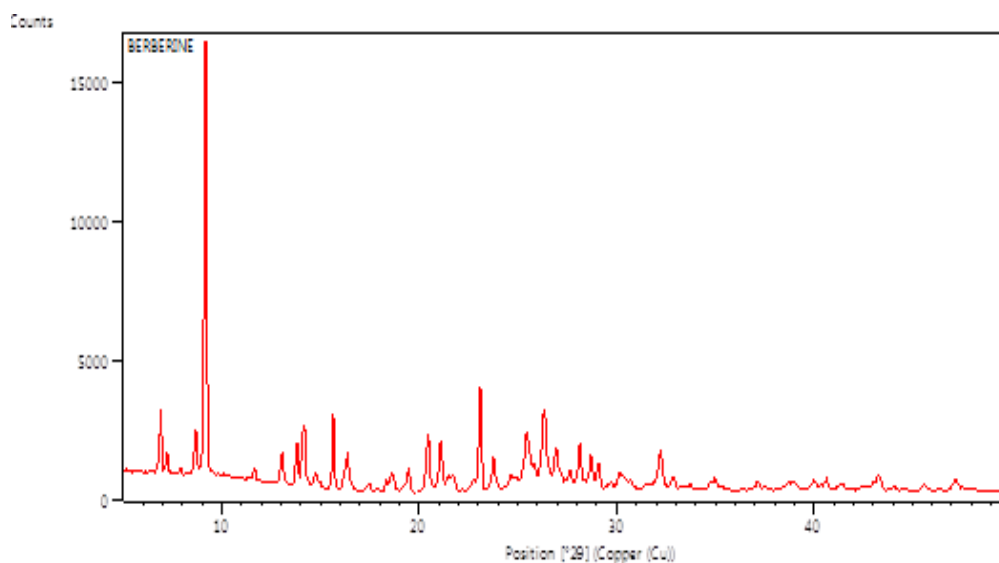
Figure 5.4: XRD of BBH

Discussion: According to the XRD pattern of BBH, which reveals sharp and intense diffraction peaks at 2 of 8.66°, 9.15°, 13.01°, 16.33°, 20.4°, 25.4°, and 30.19°, BBH is crystalline in nature.

5.1.5 Solubility studies

A. **Qualitative Solubility of BBH**

A variety of solvents were used in the solubility tests of BBH. By visually examining the solutions, the results were found (Table 5.4).

Table 5.4: Qualitative solubility data of BBH

S. No.	Name of Solvent	Solubility
1	Methanol	+++
2	Ethanol	+++
3	PB 7.4	++
4	Water	++
5	PB 6.8	++
6	HCL 1.2	+
7	Chloroform	+
8	Acetone	+

(+)Very slight soluble (++)- Slightly Soluble, (+++)- Soluble

B. **Quantitative Solubility of BBH**

Spectrophotometric measurements were made at the absorption maxima to determine the solubility of BBH in various solvents.

Table 5.5: Solubility detrmination of BBH for different solvents

S. No.	Name of the Solvent	Solubility of drug in mg/mL (mean±SD) *	Solubility results
1	Methanol	58.971±0.147	Soluble
2	Ethanol	37.490±0.034	Soluble
3	PB 7.4	3.304±0.031	Slightly soluble
4	Water	3.127±0.052	Slightly soluble
5	PB 6.8	2.230±0.034	Slightly soluble
6	HCL 1.2	0.339±0.002	Very slightly soluble
7	Chloroform	0.244±0.011	Very slightly soluble
8	Acetone	0.227±0.004	Very slightly soluble

n=3, *SD=Standard deviation
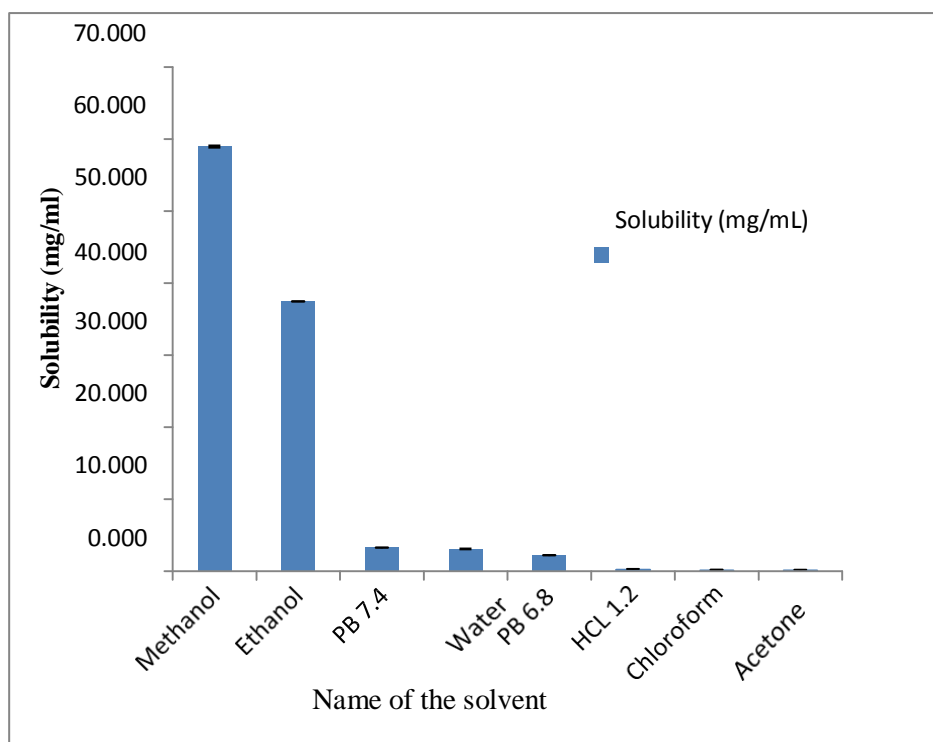
Figure 5.5: Solubility determination of BBH in various solvents

Discussion: It is abundantly clear from Figure 5.5 and Table 5.5 that methanol and ethanol are the two solvents in which BBH is most soluble. 3.127 mg/mL was found to be the drug's water solubility, which means it is only slightly soluble. Out of all the pH tested, phosphate buffer pH 7.4 demonstrated the highest drug solubility (3.304 mg/mL). BBH was less soluble at pH 1.2 (0.1N HCl) and pH 6.8 (phosphate buffer) than it was at pH 7.0 (phosphate buffer).

5.1.6 Absorption Maxima (λmax) determination by UV Spectroscopy

The max of BBH of found to be 350 nm which were concordant with the Official monographs.
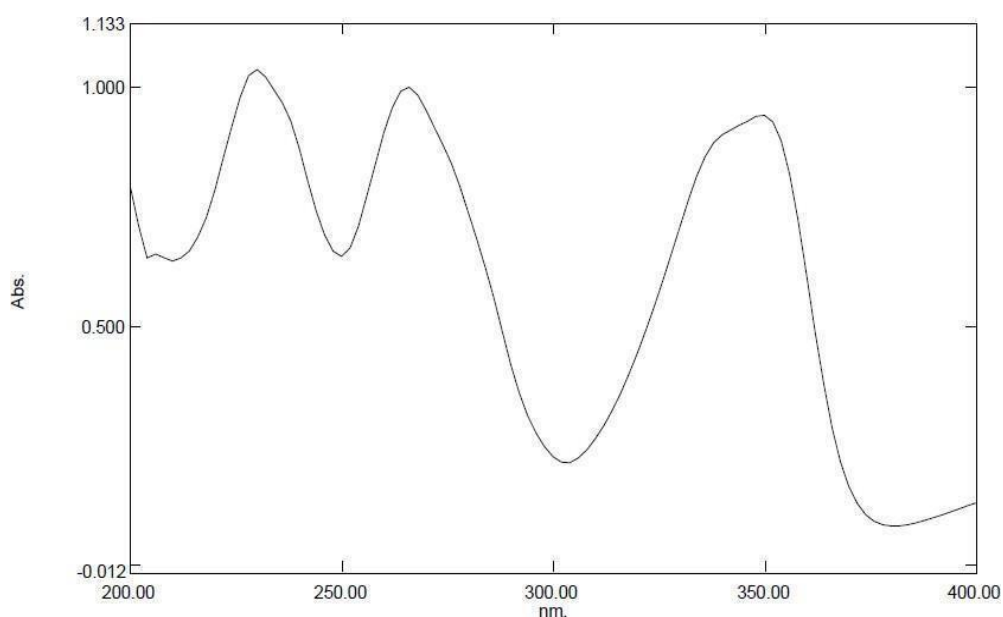
Figure 5.6: Absorption maxima of BBH

5.1.7 Calibration curve of BBH in methanol

The absorbance of BBH at different concentrations in methanol is presented in Table 5.6 at a maximum of 350 nm (Figure 5.6).

Table 5.6: Calibration curve of BBH in methanol

S.No	Concentration (μg/mL)	Absorbance (mean±SD)*
1	2	0.128±0.002
2	4	0.262±0.001
3	6	0.403±0.002
4	8	0.536±0.002
5	10	0.696±0.001
6	12	0.811±0.002
7	14	0.942±0.001

*SD=Standard deviation
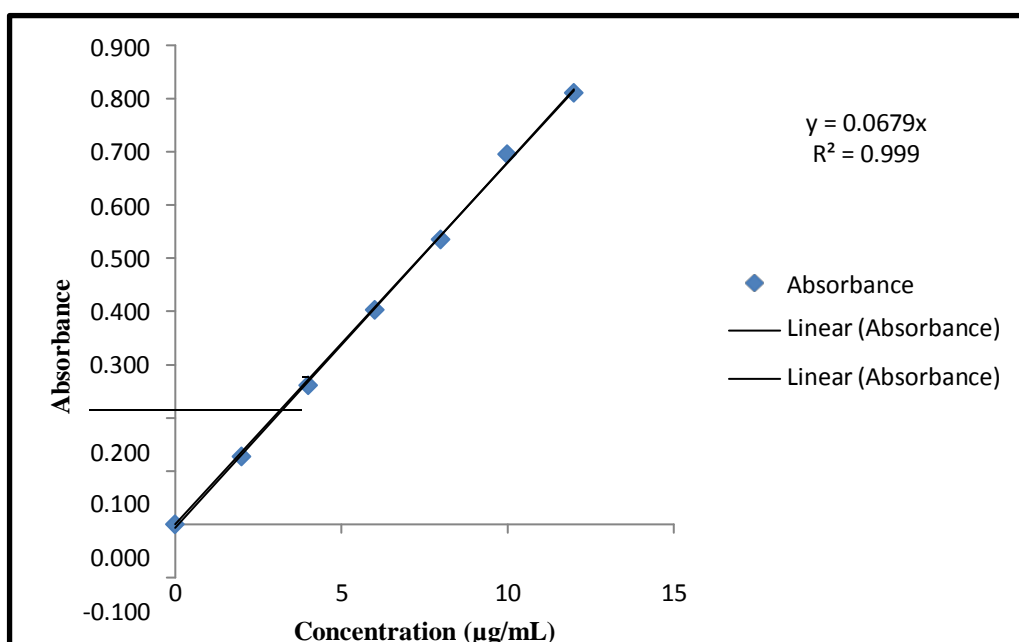
Figure 5.7: Standard calibration curve of BBH in methanol at $_{max}$350 nm

Table 5.7: The outcome of a regression study of the UV method for estimating BBH

Statistical parameters	Results
λ_{max}	350 nm
Regression equation Y=mx+C	Y=0.067x
Slope (b)	0.067
Intercept (c)	0.00
Correlation coefficient(r^2)	0.999

Discussion: - BBH concentration in methanol ranged from 2 to 14 µg/mL was utilized to develop the calibration curve. At $_{max}$ 350 nm, the absorbance was determined. The regression equation Y=0.067x was shown in the calibration curve of BBH and as shown in Table 5.7 and Figure 5.7 ,the R^2 value was found to be 0.999, which indicates high linearity.

5.1.8 Analytical method development of BBH by using RP-HPLC

5.1.8.1 HPLC Chromatogram of BBH

As a result of standard HPLC analysis, the chromatogram was optimised, and Table 5.8 and Figure 5.8 (Chromatogram) illustrate the drug retention times.Figure 5.8 displays the final chromatograms of berberine HCl. It was discovered that the retention period for berberine HCl was 2.978 min (Figure 5.8). Additional validation of this method was performed for a number of the parameters covered in section 5.1.3.

Table 5.8: Retention time of drug (BBH)

S.No.	Name of drug	Retention time (min.)
1	BBH	2.978
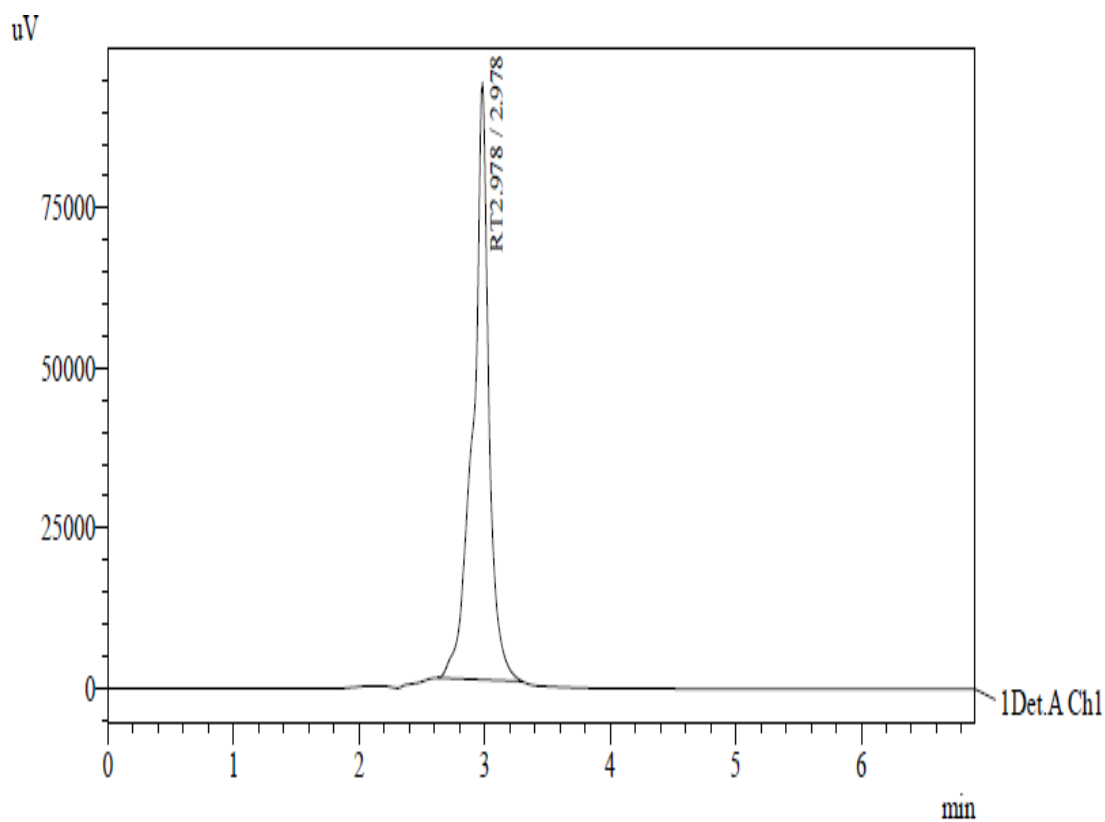
Figure 5.8: Chromatogram of BBH in potassium dihyrogen orthophosphate buffer (50Mm) with, flow rate 1.0 mL/min

5.1.8.2 Validation of RP-HPLC method

A. Linearity and Range

By drawing a graph between concentration and mean peak area, the calibration curve was created. With a determination co-efficient (r^2) of 0.998, the obtained curve was linear in the 1–10µ g/mL range (Figure 5.9).

Table 5.9: Linearity table of BBH

Concentration (μg/mL)	Mean Area	±SD[*]
1	68153.333	348.764
2	122523.000	1745.816
3	191547.333	649.751
4	278681.666	1668.954
5	329372.666	2173.506
6	398304.666	4232.561
7	462209.000	3128.870
8	545923.666	4909.451
10	688034.333	3166.513

[*]SD=Standard deviation
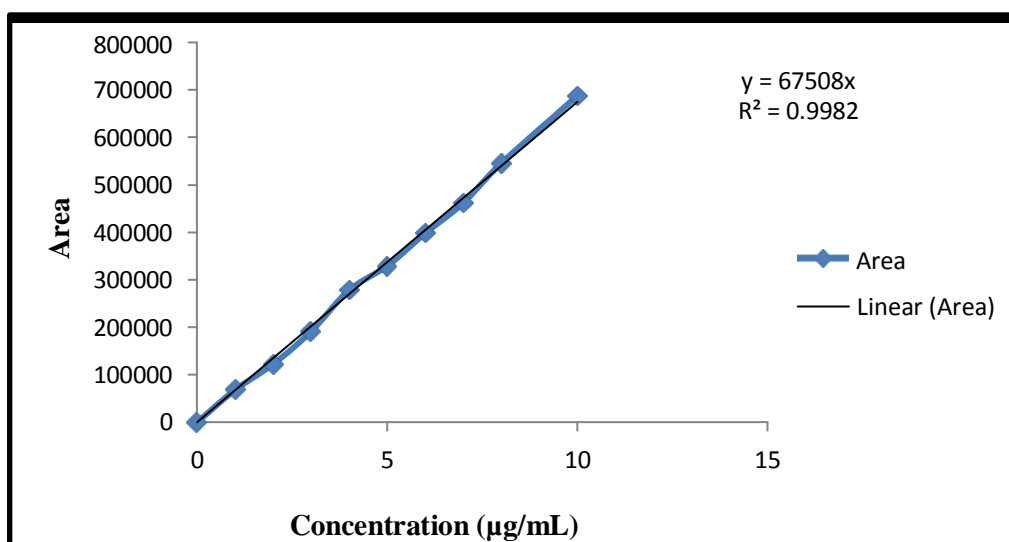
Figure 5.9: Calibration curve of BBH

B. Accuracy

The mean % recovery of the LOQ, MQC, and HQC solutions in the mobile phase was calculated in order to evaluate the developed method's accuracy. The results revealed that the mean percentage recovery in the mobile phase for each of the three levels was within predefined limits. A percentage relative standard deviation of less than 2% supported the established method's correctness. The results of the precision investigation are summarised in Table 5.10.

LIMIT OF DETECTION (LOD)

LOD= (3.3*SD of intercepts)/Mean of slope

LOD= (3.3*391.855)/68834.333= 0.0187 µg/mL

LIMIT OF QUANTITATION (LOQ)

LOQ= (10*SD of intercepts)/Mean of slope

LOQ= (10*391.855)/68834.333=0.0569 µg/mL

C. Precision

Table 5.10: Precision results showing for repeatability, Intraday, Interday

Concentration(µg/mL)	Repeatability	Intraday	Interday
	Area	Area	Area
5	343557	333890	334408
5	350057	337496	337643
5	345291	330110	331582
5	345384	334350	334408
5	341025	337407	336859
5	342315	333883	331313
Mean	344604.833	334522.666	334368.833
SD	3161.029	2737.552	2608.782
%RSD	0.917	0.818	0.780

*SD=Standard deviation

D. Accuracy

Table 5.11: Accuracy readings of BBH

Level of addition	Area	Statistical Analysis		
		Mean	±SD	% RSD
80%	578524 580261 578986	579257.0	899.651	0.155
100%	731834 732307 734648	732929.6	1506.796	0.205
120%	762801 765384 765997	764727.3	1696.175	0.221

*SD=Standard deviation

E. Robustness

Table 5.12: Change in wavelength

Concentration (µg/mL)	344 nm		348 nm	
	Area	Statistical analysis	Area	Statistical analysis
5	375420	Mean = 376125	337133	Mean =333752
5	377535	SD = 1221.095	328228	SD = 4823.804
5	375420	% RSD = 0.324	335895	% RSD = 1.445

*SD=Standard deviation

Table 5.13: Result showing Robustness (change in flow rate)

Concentration (µg/mL)	0.80 mL/min.		1.2 mL/min	
	Absorbance	Statistical analysis	Absorbance	Statistical analysis
5	430469	Mean =426906	331196	Mean=329090.666
5	420973	SD =5172.637	327492	SD =1903.270
5	429276	% RSD=1.211	328584	% RSD=0.578

F. Ruggedness

Table 5.14: Results showing Ruggedness (change in analyst)

Concentration (µg/mL)	Analyst -1		Analyst -2	
	Area	Statistical analysis	Area	Statistical analysis
5	344179	Mean = 343920.670	345326	Mean =342787
5	342288	SD – 1520.034 % RSD =0.441	340854	SD = 2296.763 % RSD = 0.670
5	345295		342181	

*SD=Standard deviation

Table 5.15: Summary of the method developed

Parameter	Result
Mobile phase	50mM Potassium dihydrogen phosphate buffer pH 3.0 and Acetonitrile (50:50 v/v).
Injection volume	20 µL
Flow rate	1.0 mL/min.
Absorption maxima	346 nm
Conc. Range	1-10 µg/mL
Correlation coefficient	0.998
Regression equation	y = 67508x
Slope	67508
Intercept	-
Accuracy (%RSD)	80% (0.155), 100% (0.205), 120% (0.221)
Precision (%RSD)	Repeatability (0.917), Intraday (0.818), Interday (0.780)
LOD	0.0187 (g /mL)
LOQ	0.0569 (g /mL)
Robustness (%RSD)	Change in absorption maxima, 344nm (0.324), 348nm(1.44) Change in flow rate, 0.80 mL/min (1.211), and 1.2 mL/min. (0.578),
Ruggedness (%RSD)	Analyst 1 (0.441), Analyst 2 (0.670)

*SD=Standard deviation

5.1.9 Partition Coefficient of Drug

Using the shake flask method and two solvents (n-octanol and water with a pH of 6.8), the partition coefficient of BBH was determined. The findings from the comparison of the estimated partition coefficient value with the literature value are shownin Table 5.16.

Table 5.16: Partition coefficient (log P) of BBH

Drug used	Solvent system used	Values of log P ±SD
BBH	n-octanol:water	-1.967±0.001

n=3, *SD=Standard deviation

Discussion: Partition coefficient of BBH was determined to be -1.967,indicating that the drug has a hydrophilic character.

5.2 SYNTHESIS AND OPTIMIZATION AND CHARACTERIZATION OF GRAFTED GUAR GUM

The microwave assisted grafting method was used for the purpose of grafting.

5.2.1 Optimization of Grafting process using box behnken design (BBD)

Grafting was optimized with Design-Expert version 7 software applying a 3- factor, 3- level BBD. Because the dependent variables varied greatly among the 17 batches, in the formulation development process, the influence of independent variables on dependent variables was determined with the help BBD software. Amount of guar gum (g) (A), Amount of monomer (g) (B), and Time (min.) (C) were independent variables. Three factors are considered as dependent variables: percentage yield (R1), percentage grafting (%) (R2), and percentage efficiency (%) (R3). Tables 5.17, 5.18 and 5.19 show the experimental setup for several grafting batches and the results that were achieved.

A. Optimization of grafted Gum

Table 5.17: Box Behnken design of experiment

Experimental trial no.	Factor			Yield (%)	Grafting (%)	Efficiency (%)
	A: Amount of Guar gum (g)	B: Amount of Monomer (g)	C: Time (min)			
G 1	0.50	10	3.0	92.99	1890.00	94.50
G 2	0.75	5	3.0	95.79	660.00	99.01
G 3	0.75	10	2.5	105.02	1433.33	107.50
G 4	1.00	10	3.0	99.64	1016.00	101.60
G 5	0.50	15	2.5	97.19	2952.00	98.40
G 6	0.75	10	2.5	101.82	1386.66	104.01
G 7	0.50	5	2.5	95.78	992.00	99.20
G 8	1.00	5	2.5	106.45	560.00	112.00
G 9	0.75	15	3.0	92.91	1876.00	93.80
G 10	0.50	10	2.0	90.65	1840.00	92.00
G 11	0.75	10	2.5	99.17	1348.00	101.10
G 12	1.00	15	2.5	105.49	1609.00	107.20
G 13	0.75	10	2.5	97.35	1321.33	99.10
G 14	1.00	10	2.0	99.64	1016.00	101.60
G 15	0.75	5	2.0	89.07	606.33	91.00
G 16	0.75	10	2.5	100.18	1362.66	102.20
G 17	0.75	15	2.0	96.62	1922.66	96.10

Table 5.18: Design Matrix of BBD taking in account three responses

Number of Solutions	Guar Gum amount (g)	Monomer amount (g)	Time (min)	Yield (%)	Grafting (%)	Efficiency (%)
1	**0.59**	**10.74**	**2.4**	**98.210**	**1861.245**	**101.234**
2	0.51	12.33	2.63	97.830	3142.291	100.579
3	0.56	05.59	2.65	97.080	1456.030	102.952
4	0.54	08.08	2.15	92.749	1961.601	96.2153
5	0.71	12.08	2.47	100.248	2327.458	103.172
6	0.96	06.91	2.43	104.645	1185.097	112.387
7	0.64	09.31	2.16	95.065	1930.192	98.201
8	0.59	12.62	2.70	71.299	2846.808	100.287
9	0.70	11.40	2.63	99.675	2225.916	102.832
10	0.92	08.12	2.07	98.508	1228.016	103.903

B. Evaluation of Optimized Numerical Solutions

Table 5.19: Evaluation of Optimized Numerical Solutions GS-1 to GS -10

formulation	Guar Gum amount (g)	Monomer amount (g)	Time (min)	Yield (%)	Grafting (%)	Efficiency (%)
GS-1	**0.59**	**10.74**	**2.4**	**97.311**	**1801.695**	**98.975**
GS-2	0.51	12.33	2.63	92.599	2267.647	93.795
GS-3	0.56	05.59	2.65	99.086	1023.571	102.540
GS-4	0.54	08.08	2.15	100.000	1496.296	100.000
GS-5	0.71	12.08	2.47	92.956	1600.704	94.081
GS-6	0.96	06.91	2.43	106.071	791.666	109.985
GS-7	0.64	09.31	2.16	99.212	1473.438	101.288
GS-8	0.59	12.62	2.70	102.515	1903.390	88.985
GS-9	0.70	11.40	2.63	95.365	1575.714	96.754
GS-10	0.92	08.12	2.07	93.722	841.304	95.320

Experimental trials were conducted using each of the 10 potential combinations. Calculations were made for the yield, grafting, and efficiency of the graft. The yield for 10 different grafted gum formulations ranged from 92.59% to 106.07%. The percentage of grafting was discovered to range from 791.66% to 2267.64%. The grafting efficiency was observed to range from 88.98% to 109.98%. ANOVA was used to find insignificant variables.

C. Fitting the model to data

All formulation's response data were fitted to a quadratic model. According to Design Expert software, the best-fitted model for responses R1, R2, and R3 (percentage yield, percentage grafting, and percentage efficiency) was quadratic. All responses were fitted to the model in order to create the full model (FM) polynomial equation:

D. Final Quadratic Polynomial Equations for the process

Percentage yield $= 100.71 + 4.32 * A + 0.64 * B + 0.67 * C - 0.59 * A * B - 0.58 * A * C - 2.61 * B * C + 1.33 * A^2 - 0.80 * B^2 - 6.30 * C^2$

Percentage grafting $= 1370.40 - 434.12 * A + 692.63 * B + 7.08 * C - 227.75 * A * B - 12.50 * A * C - 25.00 * B * C + 166.01 * A^2 - 8.16 * B^2 - 95.91 * C^2$

Percentage Efficiency $= 102.78 + 4.80 * A - 0.70 * B + 1.02 * C - 0.98 * A * B - 0.63 * A * C - 2.58 * B * C + 1.94 * A^2 - 0.50 * B^2 - 7.29 * C^2$

5.2.2 Responses

A. Response: Statistical analysis results of percentage yield, percentage grafting and percentage efficiency

ANOVA (analysis of variance) for the quadratic response model

Table 5.20: Statistical analysis results of percentage yield, percentage grafting and percentage efficiency (ANOVA) [Type III- partial sum of squares]

| Source	percentage yield		Percentage grafting		Percentage Efficiency		
	Sum of Squares	p-value Prob>F	Sum of Squares	p-value Prob>F	Sum of Squares	p-value Prob>F	
Model	362.9357	0.0071	5704756	<0.0001	465.3256	0.0074	Significant
A-Gum	149.6395	0.0011	1507716	<0.0001	184.0001	0.0013	
B-Monomer	3.271436	0.4596	3837835	<0.0001	3.92	0.4766	
C-Time	3.578206	0.4401	401.3889	0.7898	8.336806	0.3092	
AB	1.39921	0.6246	207480.3	0.0004	3.867778	0.4795	
AC	1.364748	0.6288	625	0.7397	1.5625	0.6495	
BC	27.20422	0.0586	2500	0.5116	26.69444	0.0905	
A^2	7.39226	0.2780	116036.9	0.0022	15.83313	0.1745	
B^2	2.723452	0.4984	280.2459	0.8236	1.063184	0.7070	
C^2	167.3652	0.0008	38730.14	0.0297	224.0205	0.0007	
Residual	37.4052		36611.28		48.5405		
Lack of Fit	3.654439	0.9281	29416.97	0.0675	8.0725	0.8474	Non-significant
Pure Error	33.7507		7194.311		40.468		
Cor Total	400.3409		5741367		513.866		

Table 5.21: Evaluation of design parameters for Optimized Numerical Solutions

Number of solutios	Design Parameters (DP)			Observed Parameters (OP)			SD Between DP and OP		
	% Yield	% Grafting	% Efficiency	% Yield	% Grafting	% Efficiency	% Yield	% Grafting	% Efficiency
1	**98.21**	**1861.245**	**101.23**	**97.31**	**1801.69**	**98.97**	**0.63**	**42.10**	**1.59**
2	97.83	3142.29	100.57	92.59	2267.64	93.79	3.69	618.46	4.79
3	97.08	1456.03	102.95	99.08	1023.57	102.54	1.41	305.79	0.29
4	92.74	1961.60	96.21	100.00	1496.29	100.00	5.12	329.02	2.67
5	100.24	2327.45	103.17	92.95	1600.70	94.08	5.15	513.89	6.42
6	104.64	1185.09	112.38	106.07	791.66	109.98	1.00	278.19	1.69
7	95.06	1930.19	98.20	99.21	1473.43	101.28	2.93	322.97	2.18
8	71.29	2846.80	100.28	102.51	1903.39	88.98	2.07	667.09	7.99
9	99.67	2225.91	102.83	95.36	1575.71	96.75	3.04	459.76	4.29
10	98.50	1228.01	103.90	93.72	841.30	95.32	3.38	273.44	6.06

*SD=Standard deviation

5.2.3 Response surface (3D) and Contour plot analysis

The impact of independent factors on response is displayed in Figures 5.10 and 5.27 together with contour and three-dimensional (3D) plots. The fact that all of the observed response surfaces were slopes with substantial curvatures implies that they were all impacted by the interaction effect of dependent component concentrations.
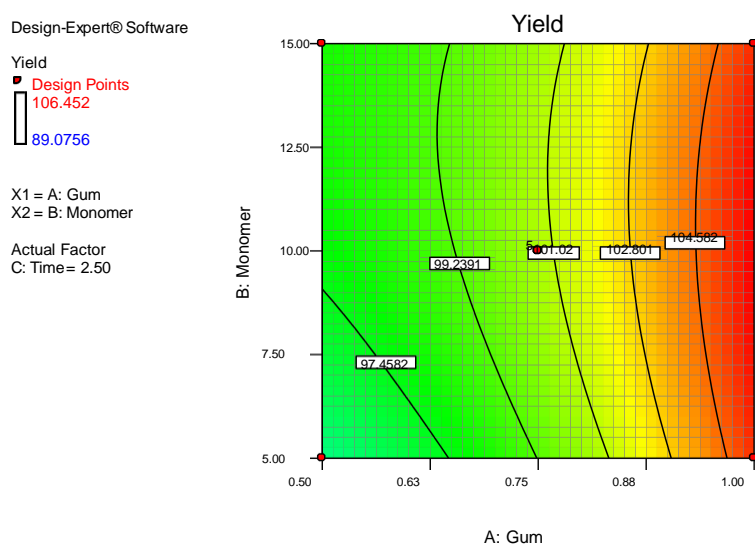
Figure 5.10: The impact of gum amount (A) and monomer (B) concentration on the % Yield of grafted gum is shown in a contour plot
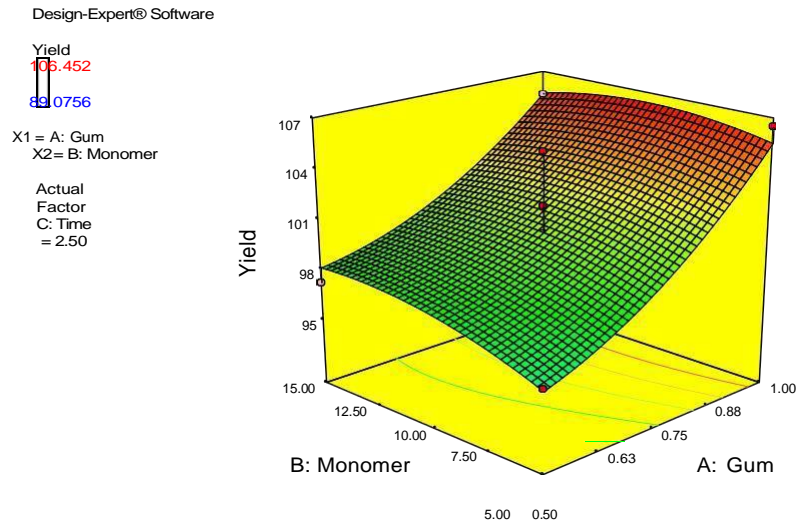
Figure 5.11: 3D Surface Response Graph displays the effect of gum amount (A), and monomer amount (B) on % Yield of grafted gum
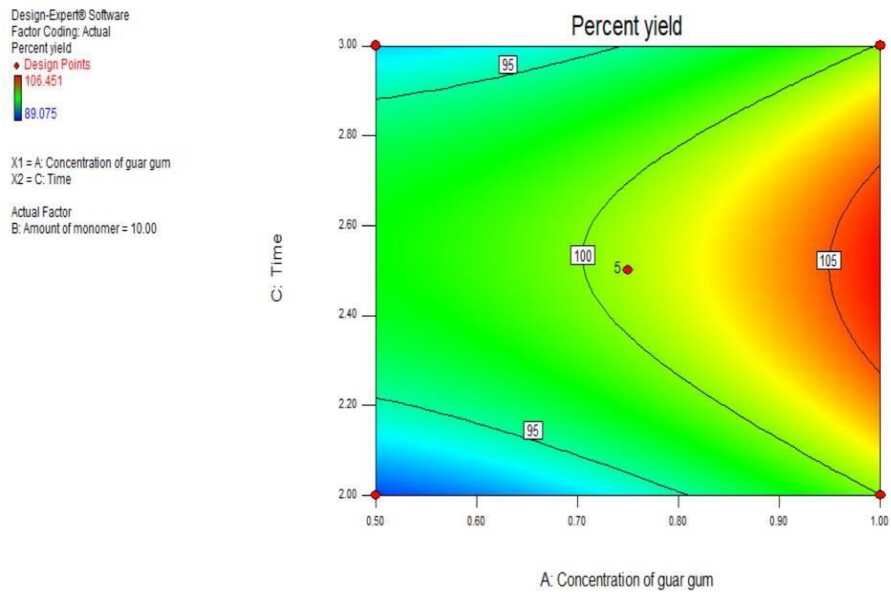
Figure 5.12: The impact of amount of gum (A) and time (C) on the % Yield of grafted gum is shown in contour plot
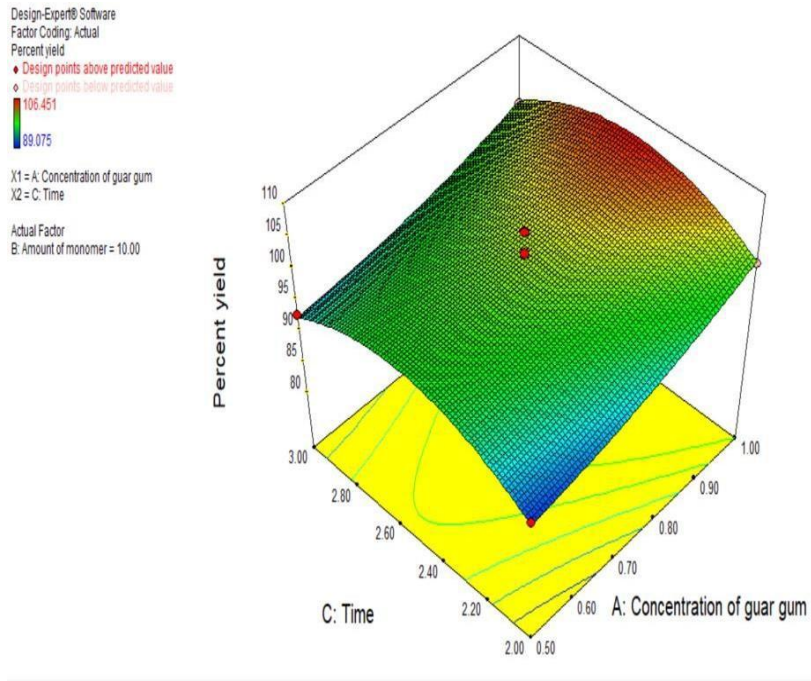
Figure 5.13: 3D Surface Response Graph displays the effect of gum amount (A),
and time (C) on % Yield of grafted gum

Figure 5.14: The impact of amount of monomer (B) and time (C) on the %
Yield of grafted gum is shown in contour plot
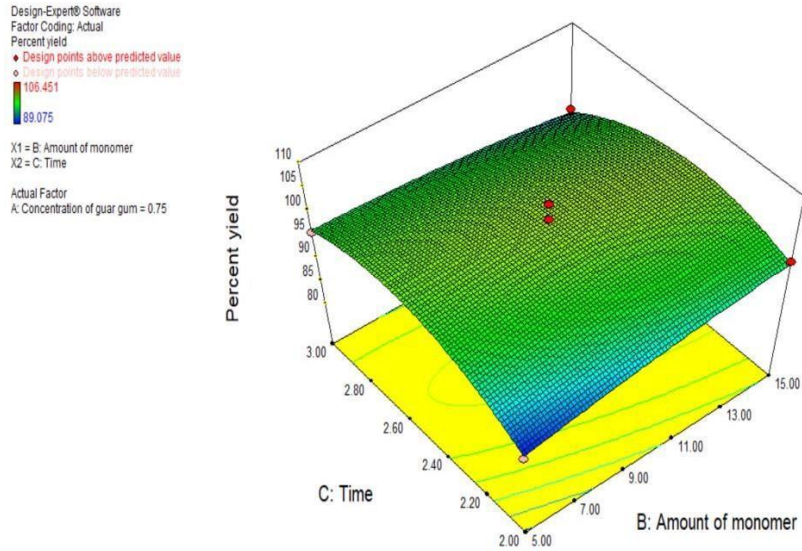
Figure 5.15: 3D Surface Response Graph displays the effect monomer amount (B) and time (C) on % Yield of grafted gum

Figure 5.16: The contour plot illustrates how the amount of gum (A) and monomer (B) affect the % grafting of grafted gum

Figure 5.17: 3D Surface Response Graph displays the effect of gum amount (A), and monomer amount (B) on % grafting of grafted gum

Figure 5.18: The contour plot illustrates how the amount of gum (A) and the Time (C) affect % grafting of grafted gum
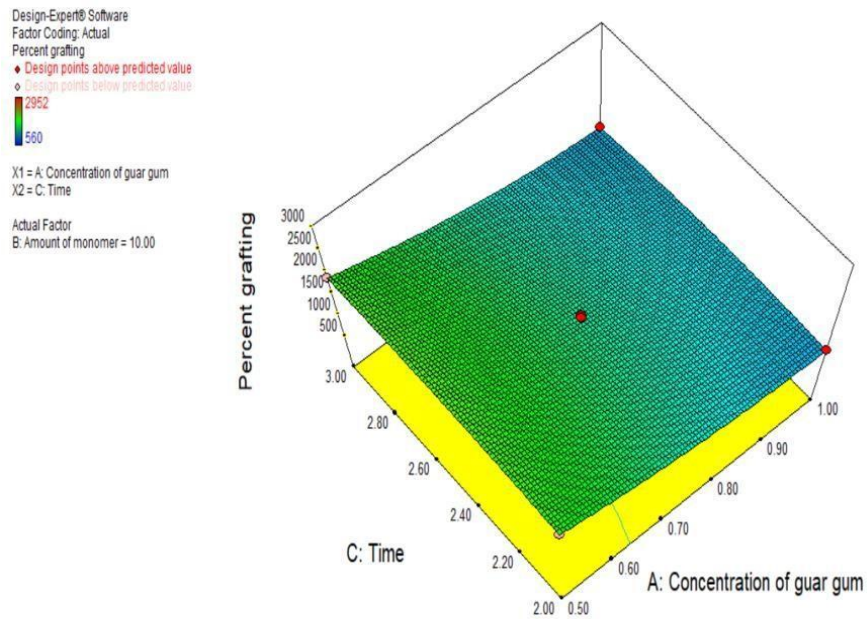
Figure 5.19: 3D Surface Response Graph displays the effect of gum amount (A), and time (C) on % grafting of grafted gum
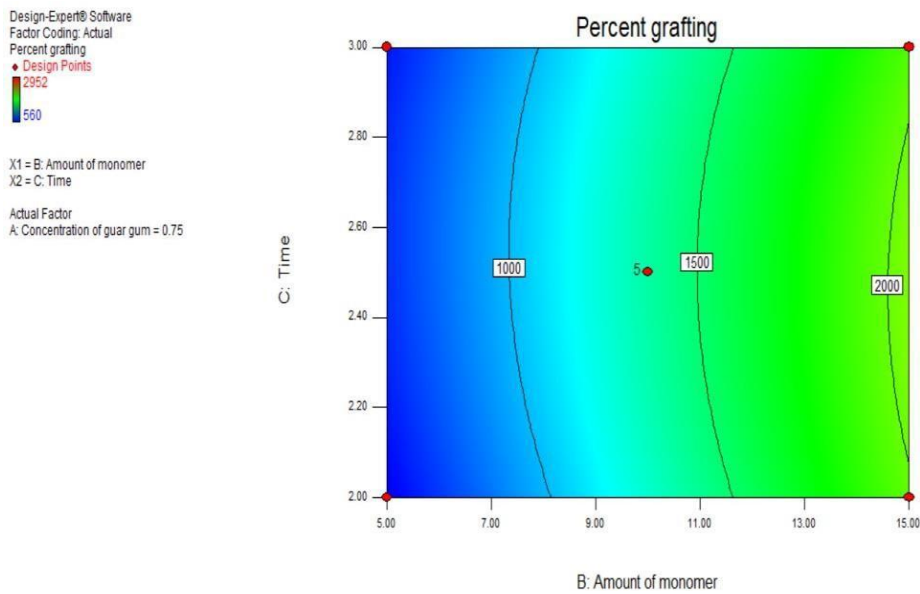
Figure 5.20: The contour plot illustrates how the amount of monomer (B) and the Time (C) affect % grafting of grafted gum
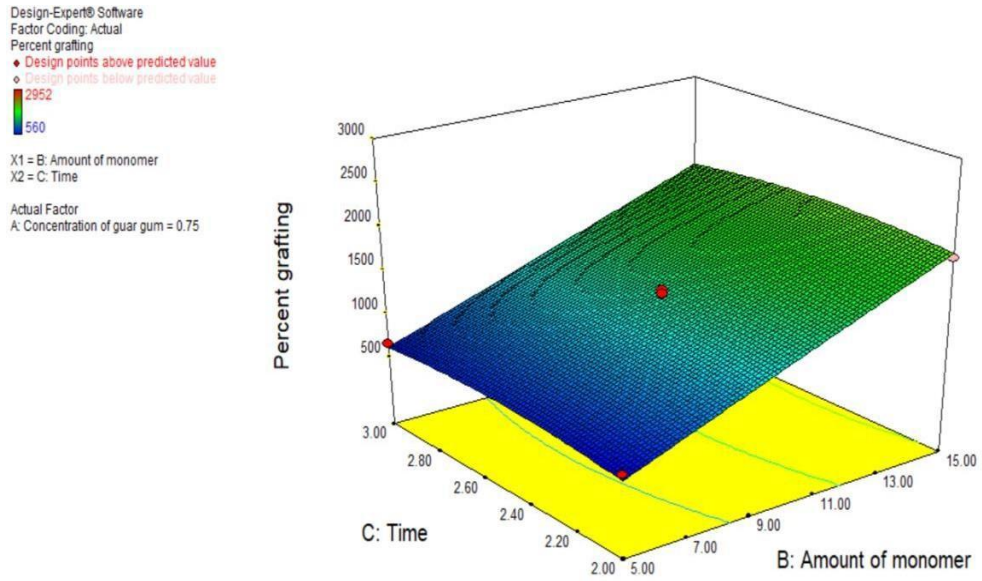
Figure 5.21: 3D Surface Response Graph displays the effect of monomer
amount (B) and time (C) on % grafting of grafted gum
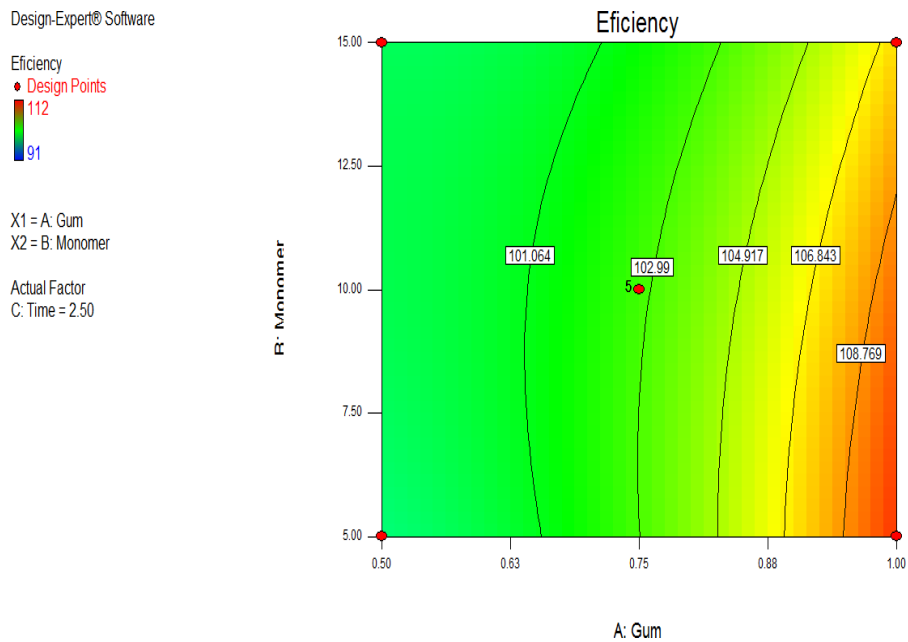
Figure 5.22: Contour Plot exhibits the effect of gum amount (A), and
monomer amount (B) on % efficiency of grafted gum
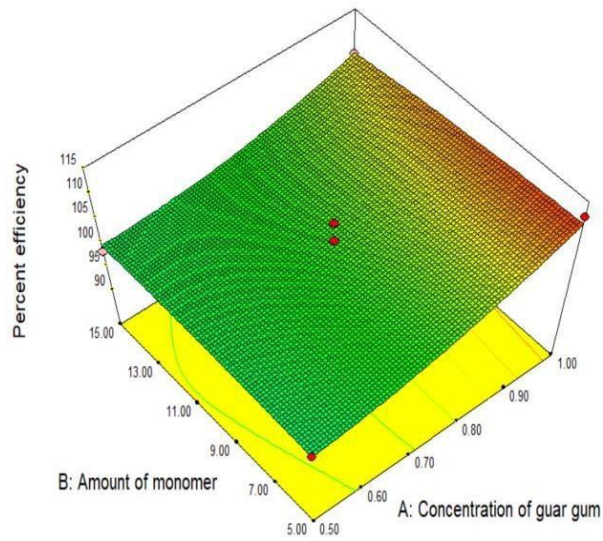
Figure 5.23: 3D Surface Response Graph displays the effect of gum amount (A) and monomer amount (B) on % efficiency of grafted gum
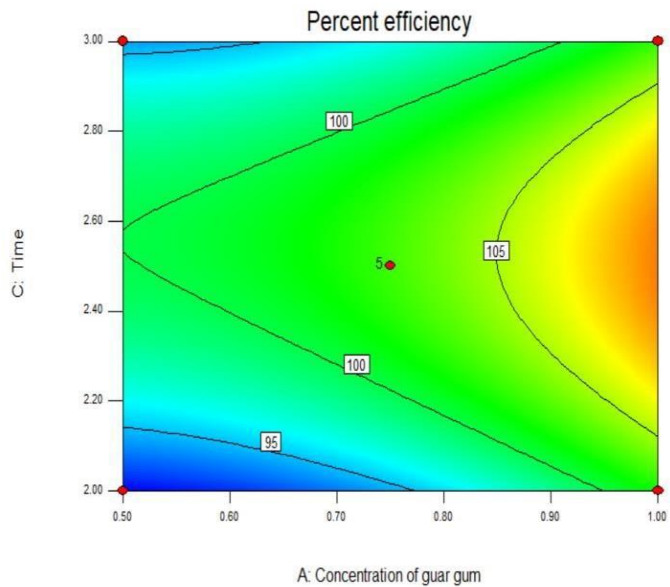
Figure 5.24: Contour Plot exhibits the effect of gum amount (A) and time (C) on % efficiency of grafted gum
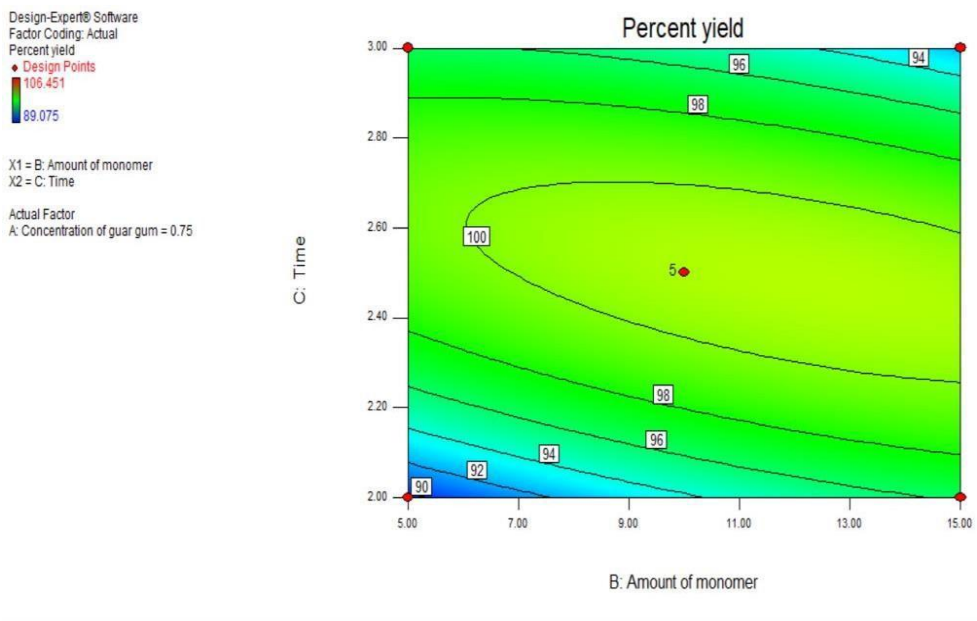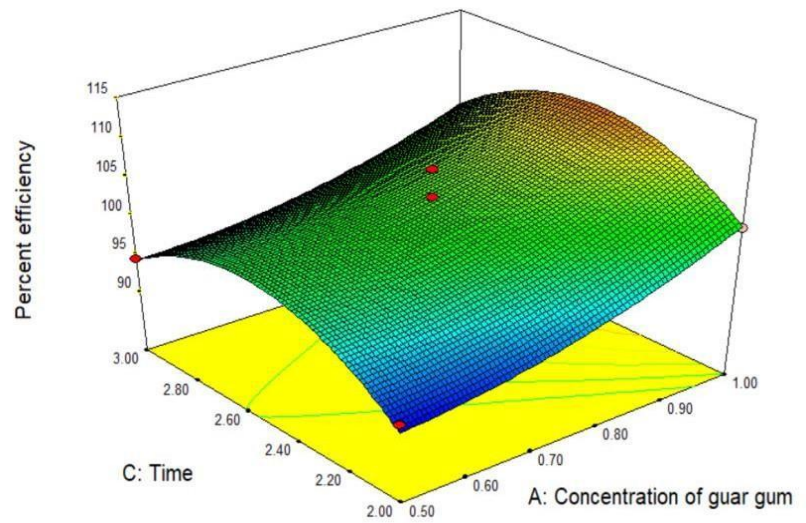
Figure 5.25: 3D Surface Response Graph displays the effect of gum

amount (A) and time (C) on % efficiency of grafted gum

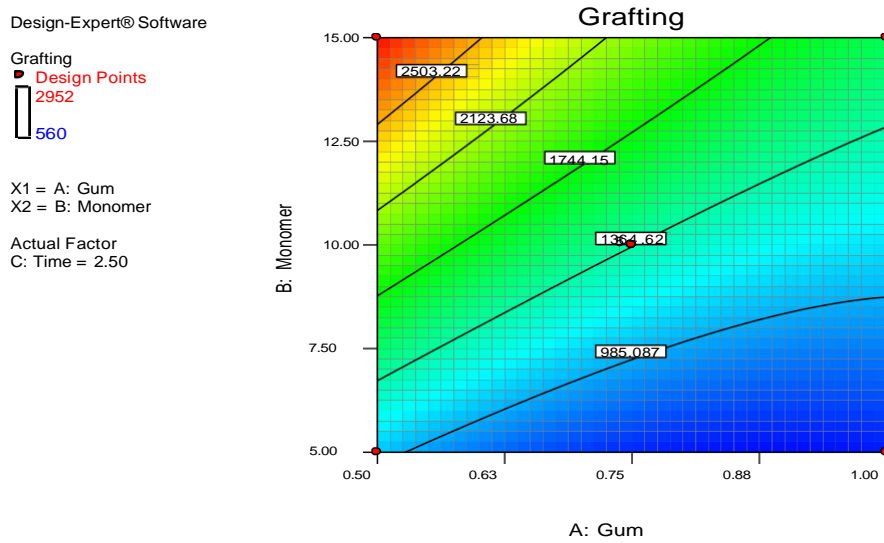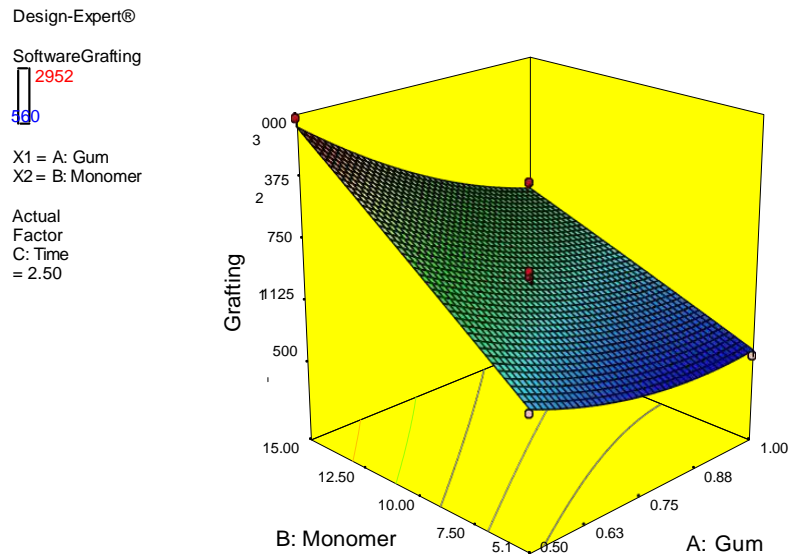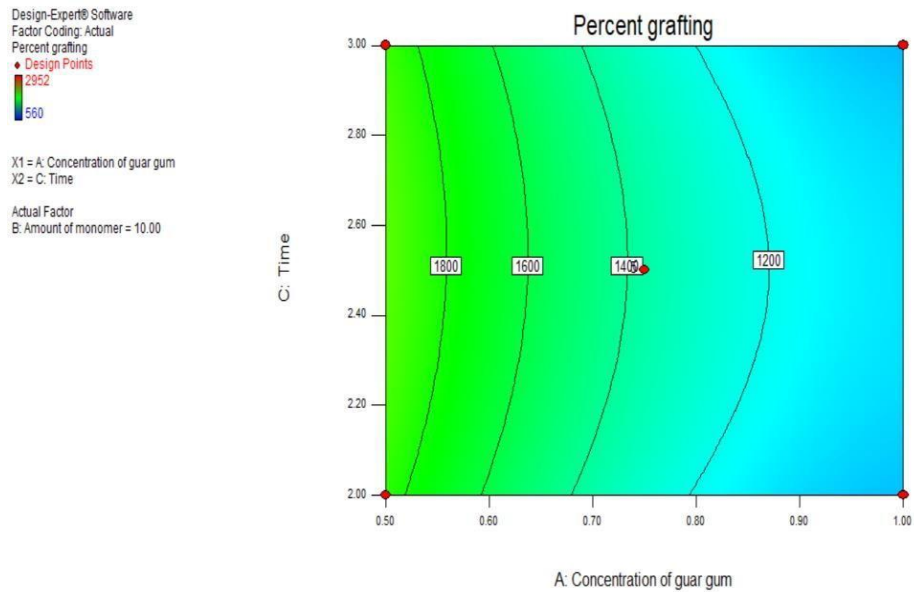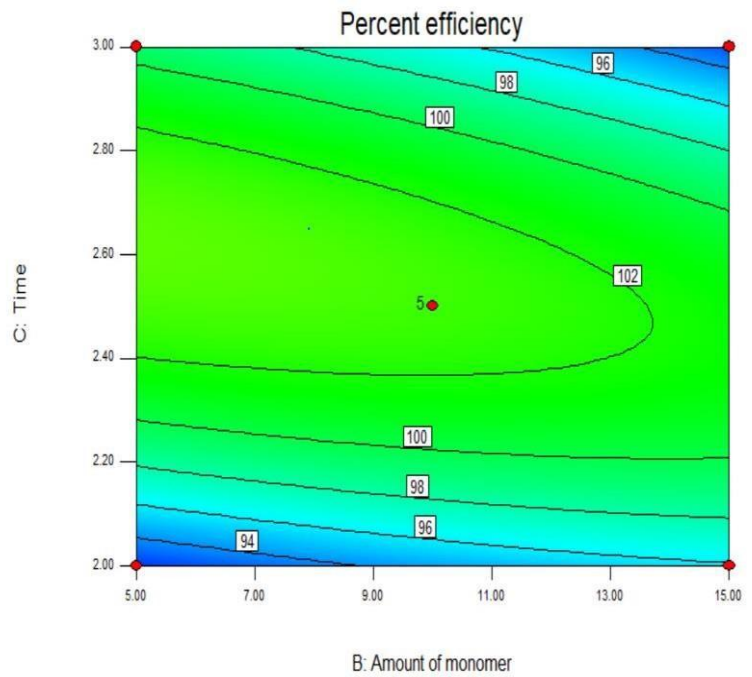**Figure 5.26:** Contour Plot exhibits the effect of monomer amount (B), and

time (C) on % efficiency of grafted gum
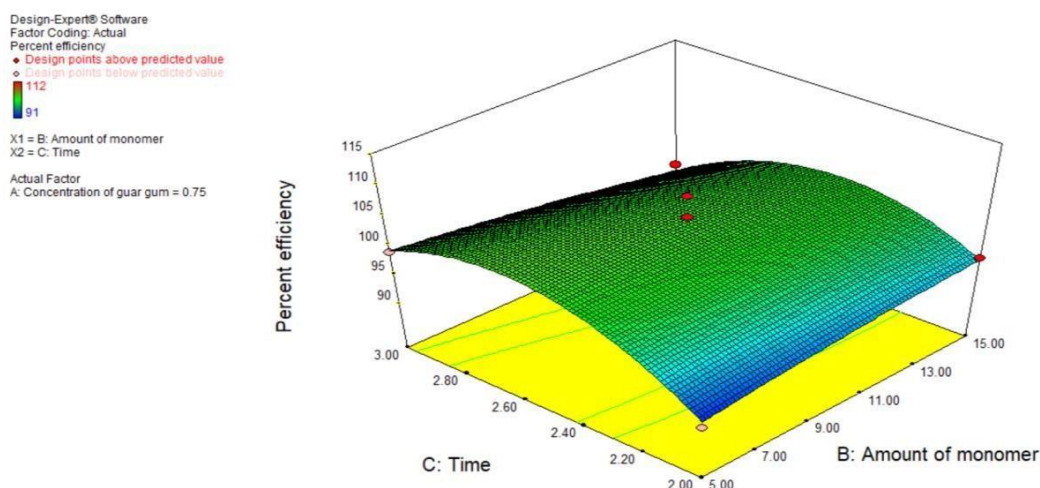
Figure 5.27: 3D Surface Response Graph displays the effect of monomer amount (B) and time (C) on % efficiency of grafted gum

5.2.4 Check point Analysis

The optimized Grafting (GS-1) displayed the experimentally determined percentage yield values of 97.311 ± 0.635%, percentage grafting of 1801.695 ± 42.10%, and percentage efficiency of 98.975 ± 1.59%. These experimental percentage yield, percentage grafting, and percentage efficiency values produced by the optimized grafting solutions were found to agree with the predicted percentage yield (97.311%), percentage grafting (1801.695%), and percentage efficiency (98.975%), respectively, generated by design expert software, indicating that the optimised formulation was rational and reliable.

Table 5.22: Optimized Numerical Solution GS-1

S. No.	Formulation	Guar Gum amount (g)	Monomer amount (g)	Time (min)
1	GS-1	0.59	10.74	2.4

5.2.5 Characterization of ungrafted gum and optimized grafted gum

The ungrafted gum and the optimized grafted gum were further characterised using FTIR, DSC, SEM and XRD techniques.

5.2.5.1 FTIR spectra analysis of different excipients and grafted gum

The FTIR spectra of Guar Gum (Figure 5.28) revealed the characteristic peak of Guar Gum. The spectra contains all of Guar Gum's characteristic peaks of $3610.53 cm^{-1}$ (O-H stretch structure), $2883.23 cm^{-1}$ (C-H stretch), and $1012.30 cm^{-1}$ (C-O-C Stretch). Figure 5.29 displays the FTIR spectrum of acrylamide.The NH group was stretched symmetrically and asymmetrically in the acrylamide spectra, with absorption peaks at $3199.23 cm^{-1}$. CO stretching began at $1668.37 cm^{-1}$. Additionally, the spectra revealed CH stretching at $1651.95 cm^{-1}$ with a $1350.69 cm^{-1}$ bend, which is attributable to CN stretching. All of the drug and excipient characteristics peaks were present in the FTIR spectra (Figure 5.30), indicating that there is no interaction between the drug and excipients. Figure 5.31 depicts the FTIR spectrum of grafted gum. The polyacrylamide chain's amide groups and the guar gum O-H stretching bond may have overlapped, according to the broad band at $3191.03 cm^{-1}$ in the grafted gum spectra. High-intensity bands in the grafted gum spectra, centred at $1553.27 cm^{-1}$ and $1421.51 cm^{-1}$, were ascribed to the C-O and C-N stretching of the polyacrylamide chain, respectively.
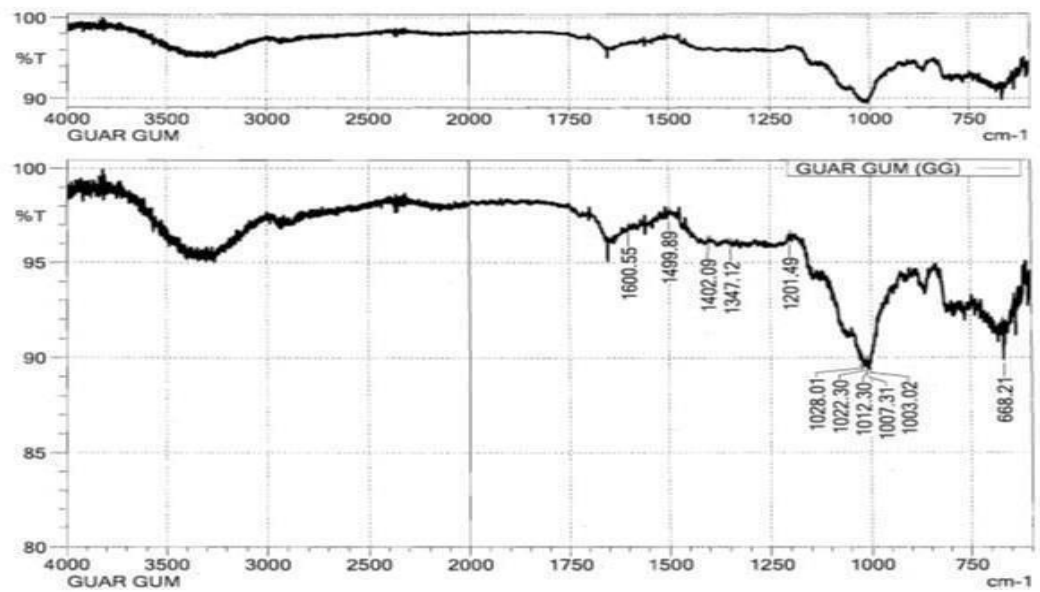
Figure 5.28: FT-IR spectra of Guar Gum
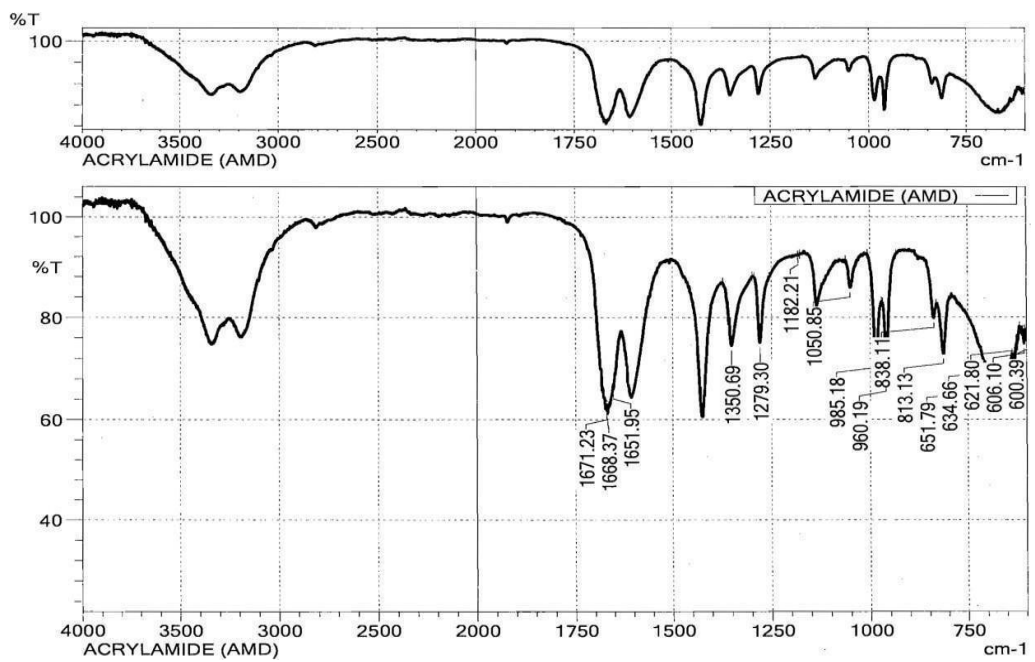
Figure 5.29: FT-IR spectra of Acrylamide
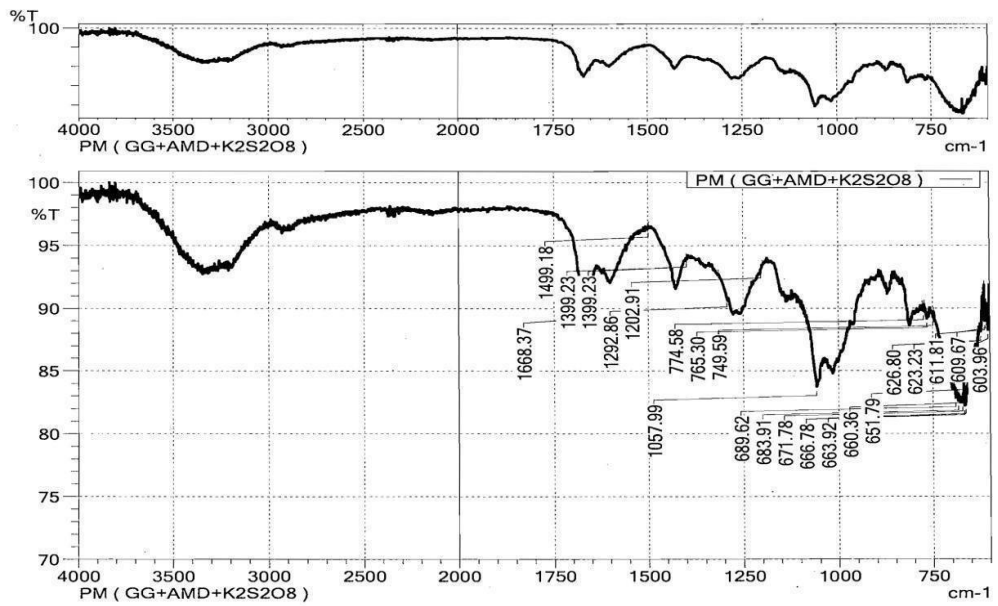
Figure 5.30: FT-IR spectra of Physical mixture
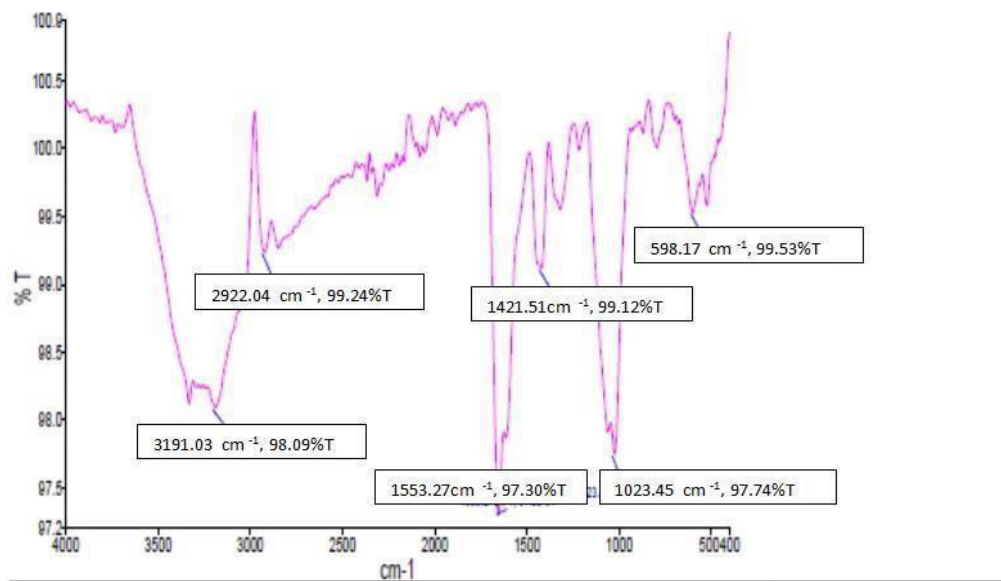
Figure 5.31: FT-IR spectra of Grafted gum

5.2.5.2 DSC Analysis

The DSC thermograms of guar gum, acrylamide, and grafted gum are displayed in Figures 5.32, 5.33, and 5.34. In the case of guar gum, two peaks (77.30°C and 307.59°C) were found. When it came to acrylamide, there was only one endothermic peak visible at 91.77°C. Figure 5.34 shows that two broad exothermic peaks (at 65.57°C and 284.73°C) and one less intense exothermic peak (at 390°C) are produced during the grafted gum heat transition mechanism. For the first exothermic peak, the starting and ending temperatures are, respectively, 29.44 °C and 98.17 °C. The temperature is 237.33 °C at the beginning and 328.47 °C at the end in second exothermic peak. This change in heat enthalpy is the outcome of the breakdown of acrylamide molecules. Extremely high temperatures cause grafted gum to entirely disintegrate, demonstrating its thermal durability and assisting in the grafting process.
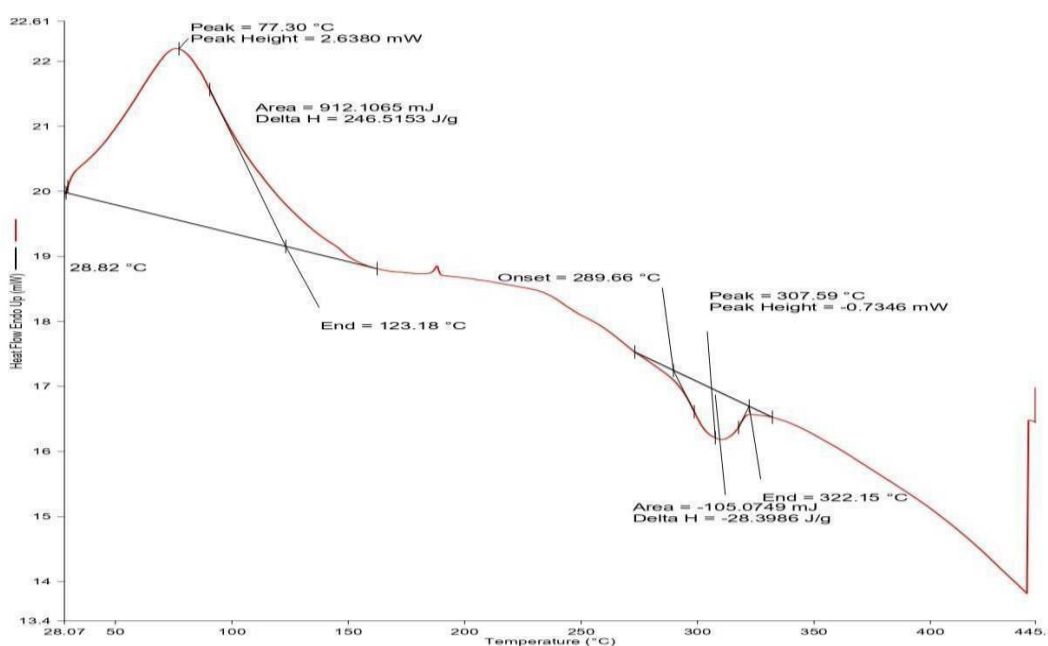
Figure 5.32: DSC of Guar gum
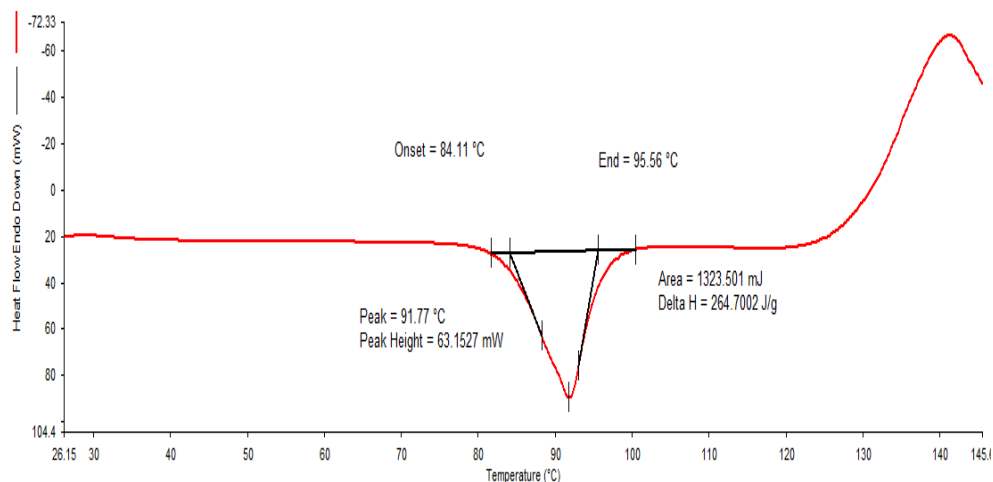
Figure 5.33: DSC of Acrylamide
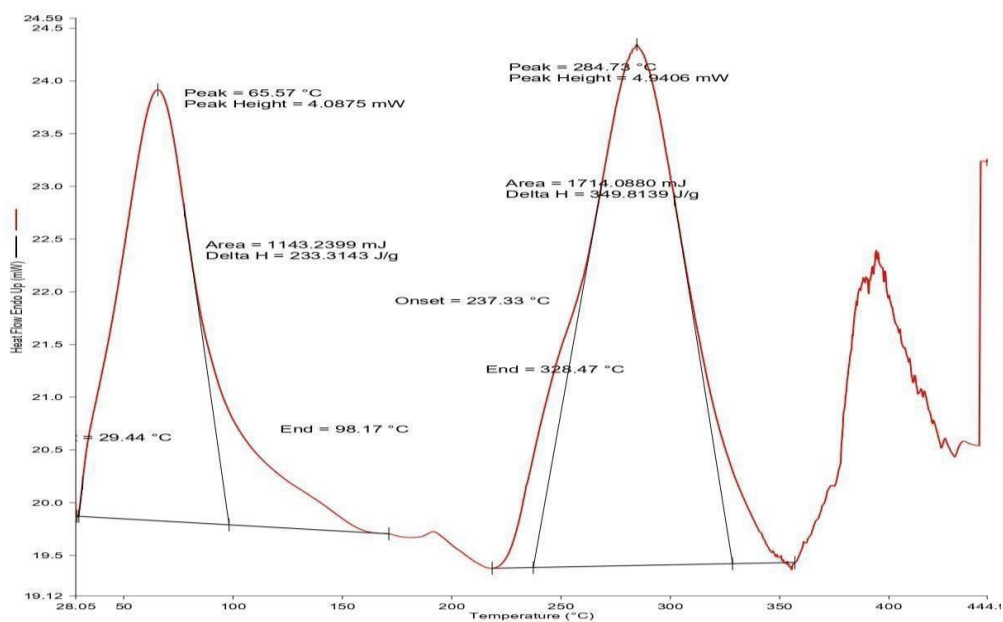
Figure 5.34: DSC of Grafted gum

5.2.5.3 X-ray diffraction studies (XRD)

X-ray diffractometer was used to acquire XRD patterns of guar gum, acrylamide, and optimised grafted gum (figures 5.35 to 5.37).The XRD spectra (Figure 5.35) revealed that Guar gum is amorphous, since no distinctive peaks were identified in the spectrum, but the diffractogram of acrylamide (Figure 5.36) revealed that it is crystalline. The grafted gum XRD spectrum (Figure 5.37) revealed the less intense peak of acrylamide confirming the development

of graft co-polymer and indicating that grafted gum is amorphous in nature.The broad peak was shifted from $2\theta = 20$ to $2\theta =24.5$ after the grafting of acrylamide and acrylic acid on to polymeric backbone of guar gum.
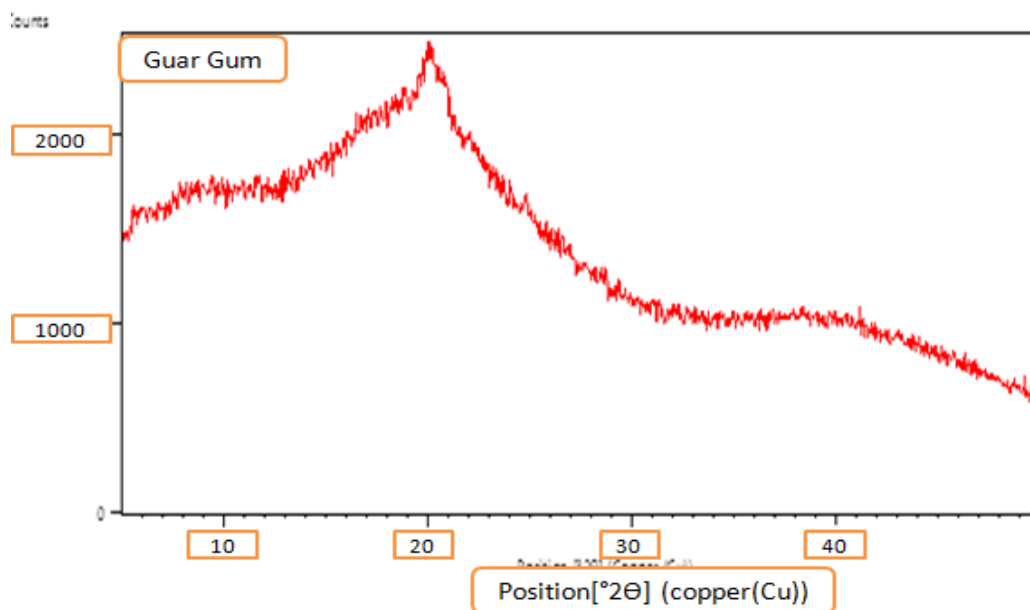
Figure 5.35: XRD of Guar Gum
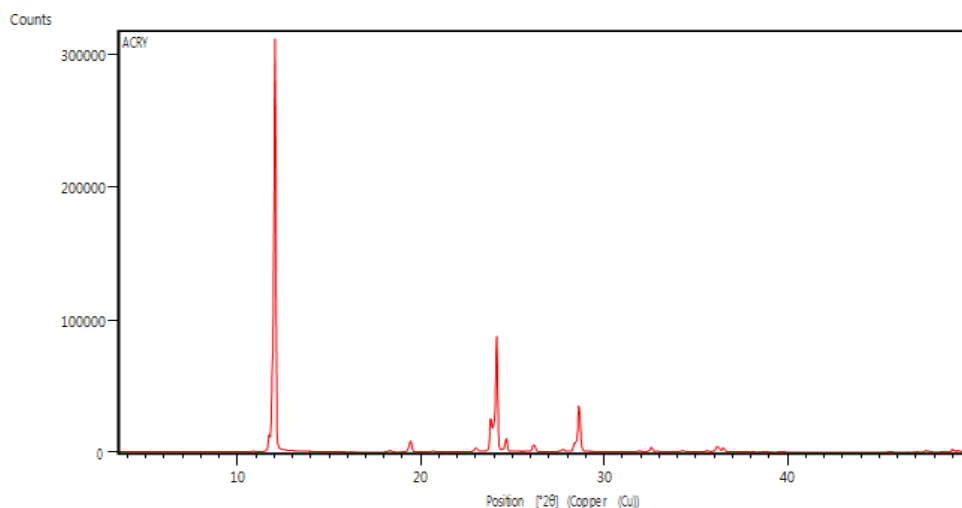
Figure 5.36: XRD of Acrylamide
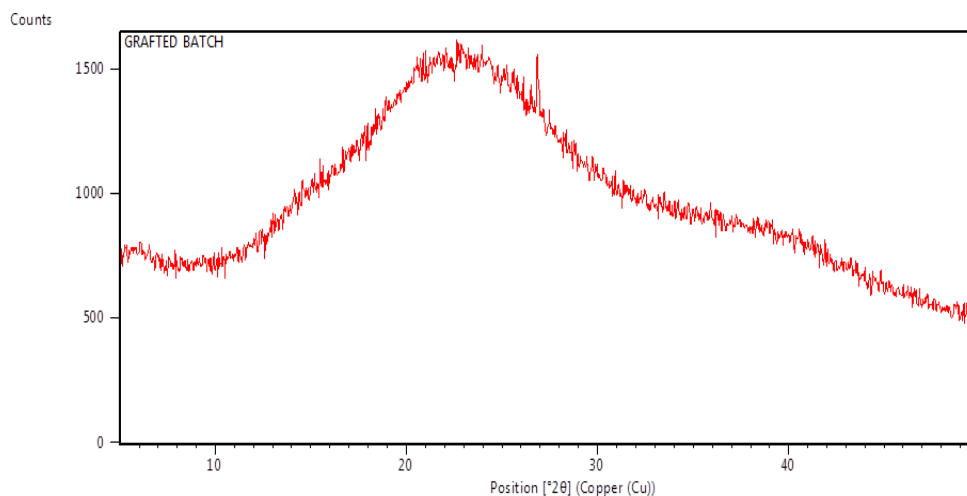
Figure 5.37: XRD of Grafted Gum

5.2.5.4 Scanning electron microscopy (SEM) of Grafted Gum

SEM analysis of Grafted Gum (Figure 5.38) revealed a change in surface morphology, suggesting that the grafting process successfully introduced acrylamide onto the gum. The increased roughness and unevenness may have implications for the gum's texture and overall performance. The surface morphology of pure guar gum was uniform and smooth, but this vanished after grafting of acrylamide onto the polymeric backbone of guar gum, resulting in a heterogeneous, rigid, dispersed morphology.
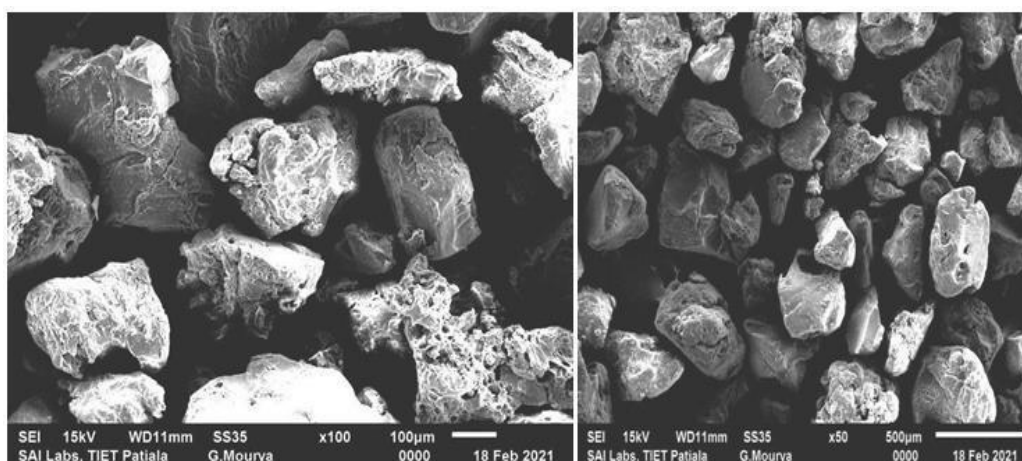
Figure 5.38: SEM of grafted gum

116

5.3 PREPARATION AND CHARACTERIZATION OF BBH LOADED MICROSPHERES USING GRAFTEDAND UNGRAFTED GUAR GUM

5.3.1 Preparation and optimization of microspheres by employing Box-Behnken design

Table 5.23: Box-Behnken design of experiment

Formulation Code	Polymer 2% (w/v) A: Grafted Gum: PVA (w/w)	B:RPM	C: Span 20 (%w/w)	% EE (%)	% DL (%)	Particle Size (µm)
FM 1	35:65	1000	0.75	77.88	15.45	1.17
FM 2	30:70	1000	0.50	65.74	10.77	1.84
FM 3	35:65	600	1.00	72.12	11.16	1.13
FM 4	35:65	1400	0.50	75.63	10.76	1.08
FM 5	35:65	1400	1.00	75.84	11.35	1.09
FM 6	35:65	600	0.50	67.68	9.53	1.18
FM 7	35:65	1000	0.75	78.85	15.48	1.17
FM 8	35:65	1000	0.75	78.90	15.5	1.17
FM 9	30:70	600	0.75	72.48	12.66	1.81
FM 10	35:65	1000	0.75	77.89	15.49	1.18
FM 11	30:70	1400	0.75	69.01	11.37	1.79
FM 12	35:65	1000	0.75	78.75	15.47	1.15
FM 13	40:60	1000	0.50	87.94	17.30	0.88
FM 14	40:60	600	0.75	79.08	16.49	0.88
FM 15	30:70	1000	1.00	73.65	12.59	1.86
FM 16	40:60	1000	1.00	84.68	17.71	0.85
FM 17	40:60	1400	0.75	94.93	19.20	0.75

A. Numerical Optimization Solution

Table 5.24: Numerical Optimization Solution

No. of solution	Polymer 2% (w/v) Gum: PVA (w/w)	RPM	Span 20 (%)	% EE	% DL	Particle Size (μm)
1	38.11:61.89	1206.08	0.61	86.75	16.96	0.89
2	32.70:67.30	1163.36	0.59	72.51	12.61	1.41
3	35.12:64.88	705.04	0.84	75.31	14.01	1.15
4	34.74:65.26	901.84	0.78	77.35	15.16	1.19
5	36.16:63.84	1067.92	0.55	78.69	14.22	1.06
6	36.96:63.04	1225.92	0.78	83.99	16.58	0.96
7	36.21:63.79	975.44	0.52	77.17	13.69	1.07
8	30.26:69.74	674.08	0.95	74.54	12.48	1.77
9	30.74:69.26	794.80	0.69	72.36	13.53	1.71
10	37.78:61.89	1206.08	0.61	86.75	16.96	0.89

B. Evaluation of Optimized Numerical Solutions

Table 5.25: Evaluation of Optimized Numerical Solutions FMS1 to FMS10

Formulation	%EE (%)	%DL (%)	Particle Size (μm)
FMS 1	81.94	16.60	1.10
FMS 2	68.50	15.80	1.88
FMS 3	77.05	16.84	1.84
FMS 4	79.59	14.28	1.63
FMS 5	74.08	12.40	1.31
FMS 6	82.79	16.48	1.10
FMS 7	74.62	12.6	0.89
FMS 8	71.66	15.44	1.34
FMS 9	75.57	16.60	0.66
FMS 10	80.36	14.64	1.24

C. Fitting the model to data

All formulations' response data were fitted to a quadratic model. According to Design Expert software, the best-fitted model for response R1, R2, and R3 (% Entrapment Efficiency, % Drug Loading, and Particle Size) was quadratic. All responses were fitted to the model in order to create the full model (FM) polynomial equation.

Coded Equation:

$$\% \text{ Entrapment Efficiency} = 78.45 + 8.22 * A + 3.01 * B + 1.16 * C + 4.83 * A * B - 2.79 * A * C - 1.06 * B * C + 2.80 * A^2 - 2.38 * B^2 - 3.25 * C^2$$

$$\% \text{ Drug Loading} = 15.48 + 2.91 * A + 0.36 * B + 0.56 * C + 1.00 * A * B - 0.35 * A * C - 0.26 * B * C + 1.67 * A^2 - 2.22 * B^2 - 2.56 * C^2$$

$$\text{Particle Size} = 1.17 - 0.49 * A - 0.036 * B - 6.250E\text{-}003 * C - 0.028 * A * B - 0.013 * A * C + 0.015 * B * C + 0.19 * A^2 - 0049 * B^2 + 1.000E\text{-}003 * C^2$$

D. Responses: Statistical analysis results of % EE, % DL and particle size.

ANOVA (Analysis of variance) for the response surface (quadratic) model

Table 5.26 Statistical analysis results of % EE, % DL and particle size

Source	%EE (R1)		% DL (R2)		Particle Size(R3)		
	Sum of Squares	p-value Prob> F	Sum of Squares	p-value Prob> F	Sum of Squares	p-value Prob> F	
Model	850.854	< 0.0001	135.512	< 0.0001	2.112	< 0.001	Significant
A-Grafted Gum	540.382	< 0.0001	67.919	< 0.0001	1.940	< 0.001	
B-rpm	72.300	< 0.0001	1.008	< 0.0001	0.010	< 0.001	
C-span	10.811	< 0.0001	2.475	< 0.0001	0.001	0.099	
AB	93.315	< 0.0001	4.000	< 0.0001	0.003	0.001	
AC	31.192	< 0.0001	0.497	< 0.0001	0.001	0.031	
BC	4.473	0.0014	0.270	< 0.0001	0.001	0.014	

A^2	33.081	< 0.0001	11.774	< 0.0001	0.149	< 0.001	
B^2	23.890	< 0.0001	20.755	< 0.0001	0.010	< 0.001	
C^2	44.596	< 0.0001	27.545	< 0.0001	4.210	0.831	
Residual	1.216		0.001		0.001		
Lack of Fit	0.126	0.921	2.505	0.994	0.001	0.794	Not signif icant
Pure Error	1.090		0.001		0.001		
Cor Total	852.071		135.513		2.112		

Table 5.27: Evaluation of design parameters for Optimized Numerical Solutions

Number of solutions	Design Parameters (DP)			Observed Parameters (OP)			Between DP and OP		
	% EE	%DL	Size (µm)	% EE	%DL	Size (µm)	% EE	% DL	Size(µm)
FMS1	86.75	16.96	0.89	81.94	16.60	1.10	3.42	0.26	0.13
FMS2	72.51	12.62	1.41	68.50	15.80	1.88	2.83	2.25	0.32
FMS3	75.31	14.01	1.15	77.05	16.84	1.84	1.23	1.99	0.48
FMS4	77.35	15.16	1.19	79.59	14.28	1.63	1.58	0.62	0.30
FMS5	78.69	14.22	1.06	74.08	12.40	1.31	3.26	1.29	0.17
FMS6	**83.99**	**16.58**	**0.96**	**82.79**	**16.48**	**1.10**	**0.85**	**0.07**	**0.10**
FMS7	77.17	13.69	1.07	74.62	12.60	0.89	1.80	0.77	0.12
FMS8	74.54	12.48	1.77	71.66	15.44	1.34	2.03	2.08	0.30
FMS9	72.36	13.53	1.71	75.57	16.60	0.66	2.24	2.16	0.74
FMS10	86.75	16.96	0.89	80.36	14.64	1.24	3.87	2.08	0.22

5.3.2 Response surface (3D) and Contour plot analysis

Figures 5.39 to 5.56 illustrate 3D plots and contour plots that show the influence of independent variables on response. All of the observed response surfaces formed hillsides with large curvatures, indicating that they were typically impacted by the interaction effect of dependent variables.
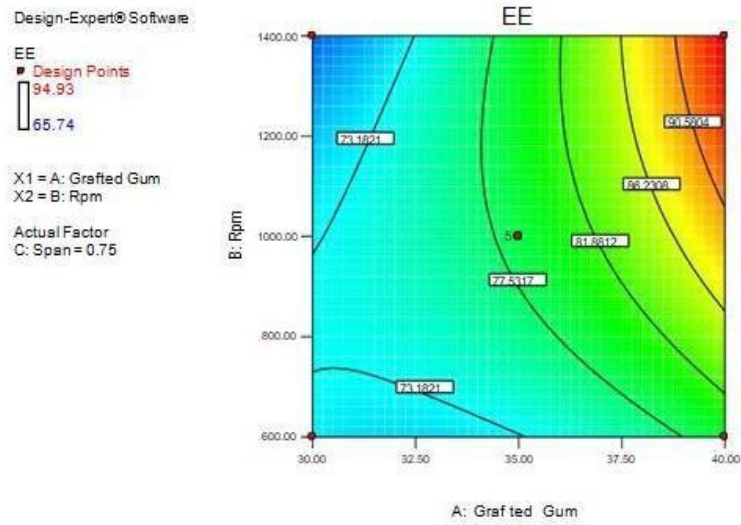
Figure 5.39: Contour plot displays the effect of grafted gum ratio (A) and RPM (B) on % EE
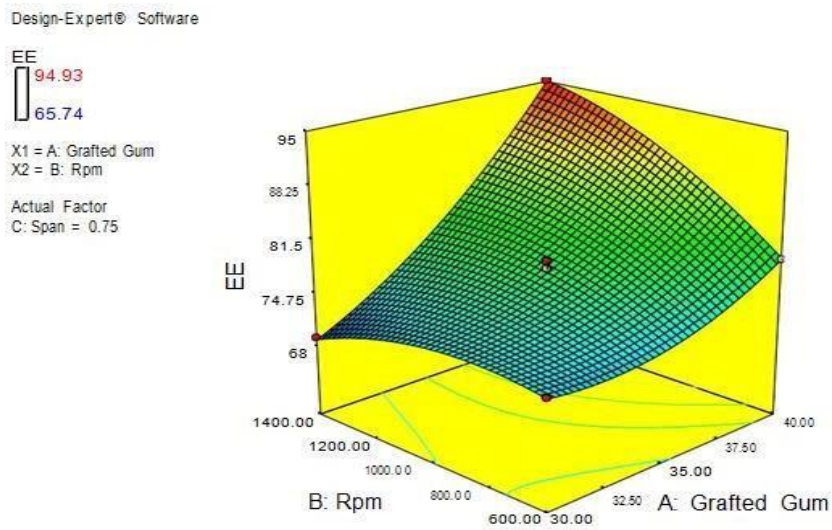
Figure 5.40: 3D surface response graph displays the effect of grafted gum ratio (A) and RPM (B) on % EE
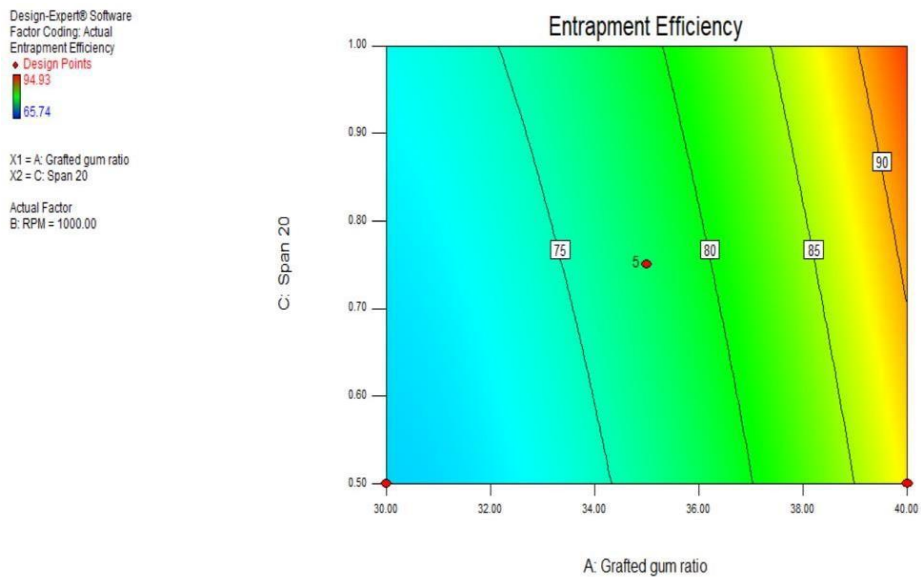
Figure 5.41: Contour plot displays the effect of grafted gum ratio (A) and concentration of span 20 (C) on % EE
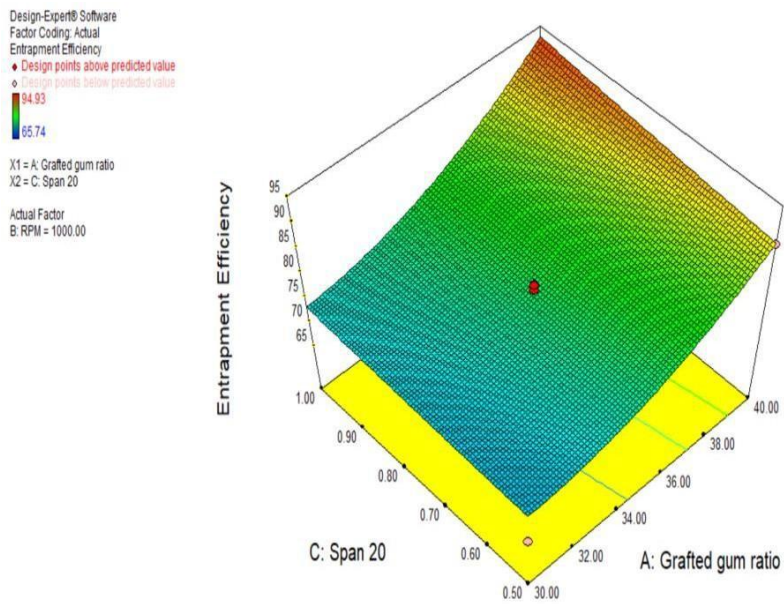
Figure 5.42: 3D surface response graph displays the effect of grafted gum ratio (A) and concentration of span 20 (C) on % EE
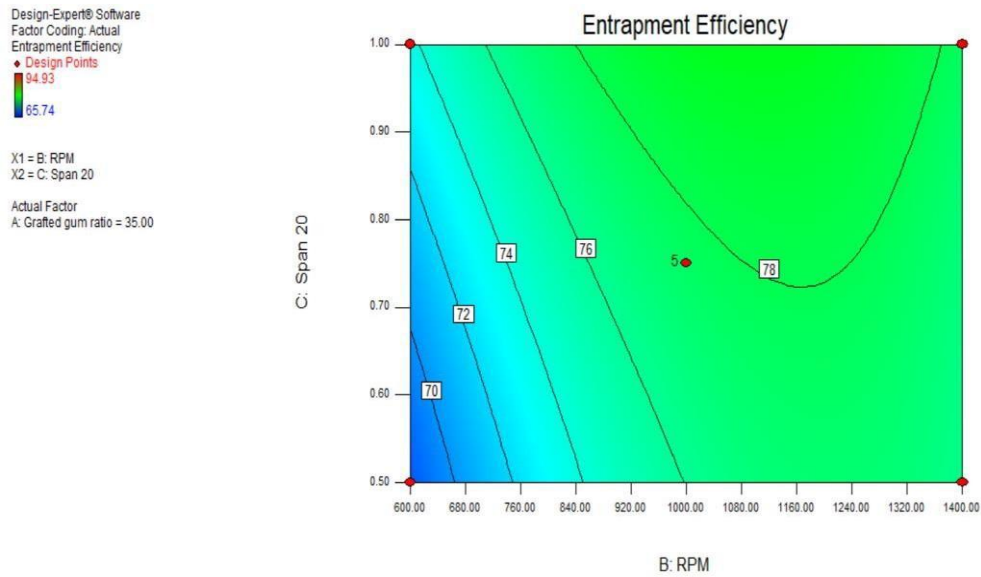
Figure 5.43: Contour plot displays the effect of RPM (B) and concentration of span 20 (C) on % EE
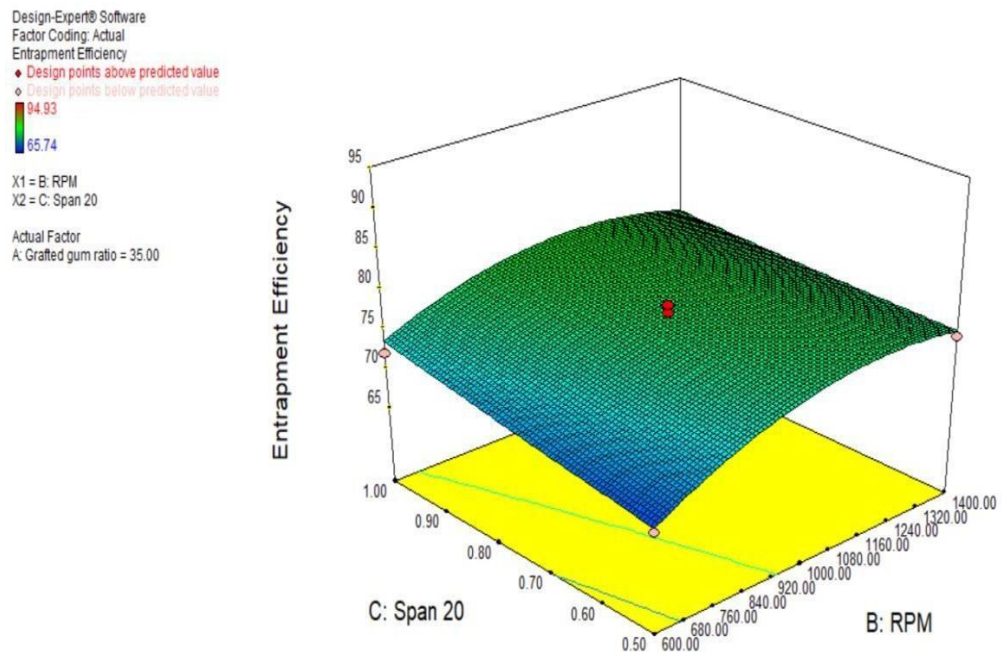
Figure 5.44: 3D surface response graph displays the effect of RPM (B) and concentration of span 20 (C) on % EE
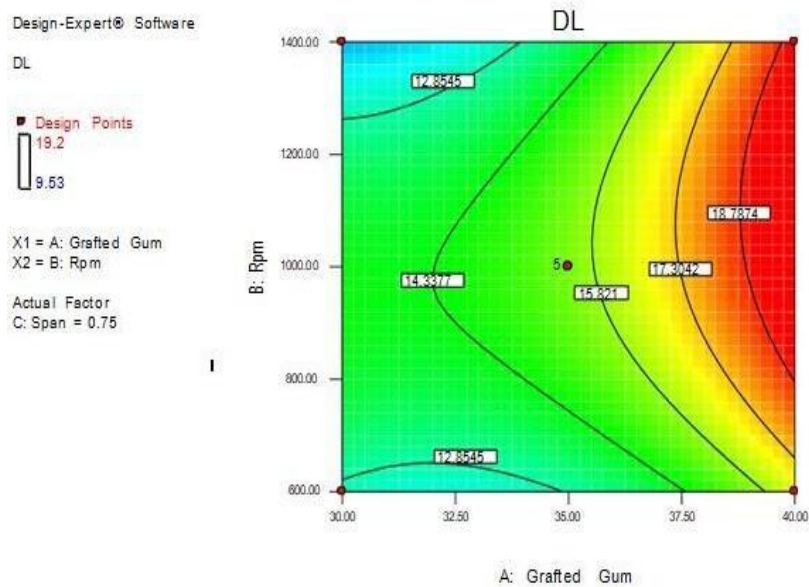
Figure 5.45: Contour plot displays the effect of grafted gum ratio (A) and RPM (B) on % DL
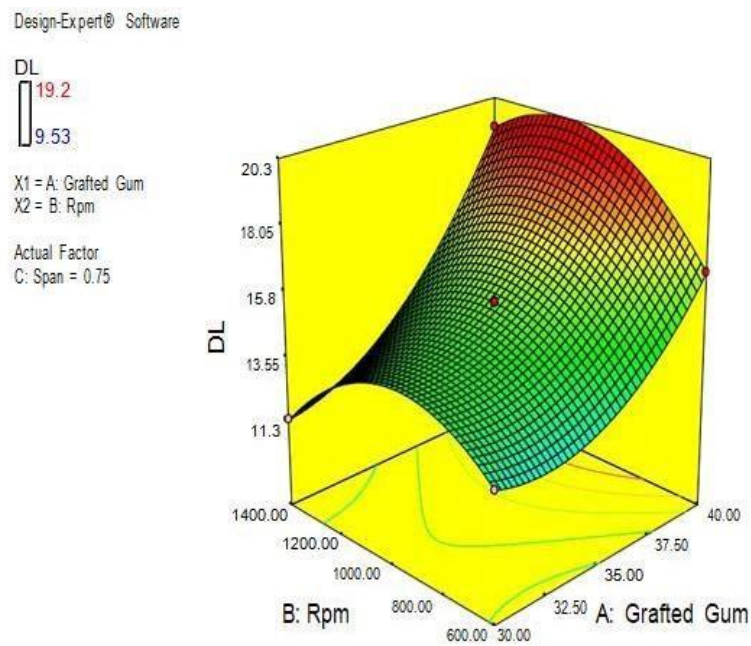
Figure 5.46: 3D surface response graph displays the effect of grafted gum ratio (A) and RPM (B) on % DL
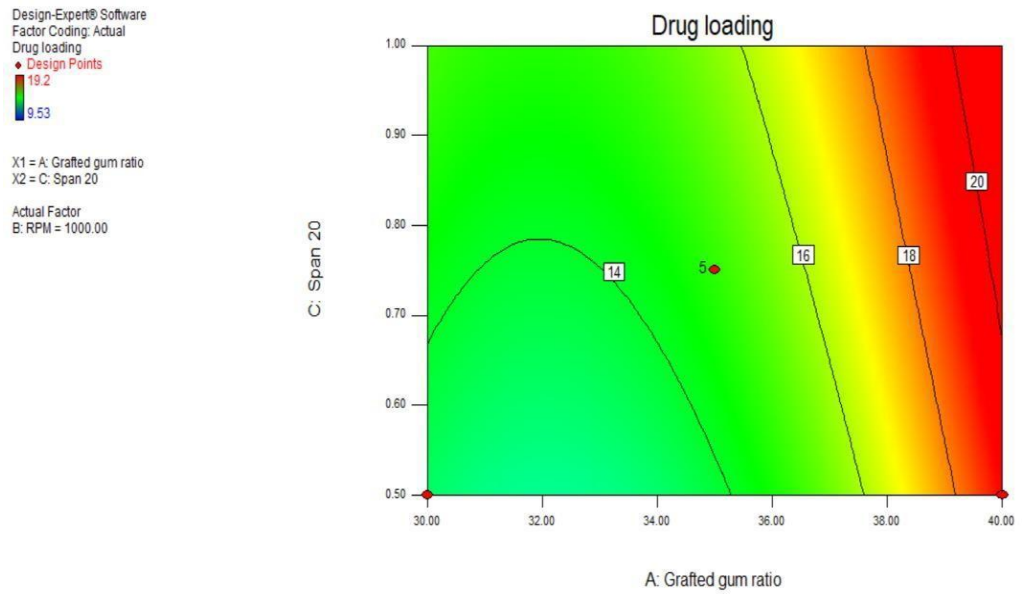
Figure 5.47: Contour plot displays the effect of grafted gum ratio (A) and concentration of span 20 (C) on % DL
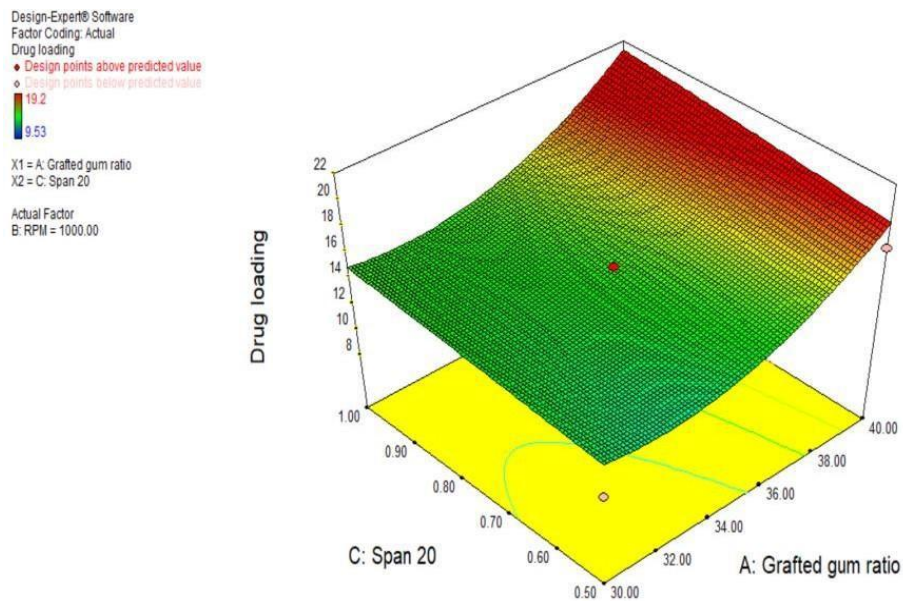
Figure 5.48: 3D surface response graph displays the effect of grafted gum ratio (A) and concentration of span 20 (C) on % DL
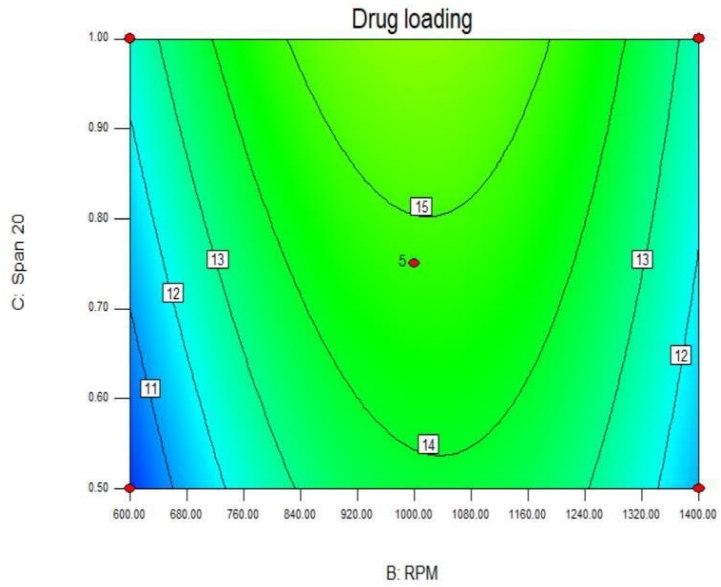
Figure 5.49: Contour plot displays the effect of RPM (B) and concentration of span 20 (C) on % DL
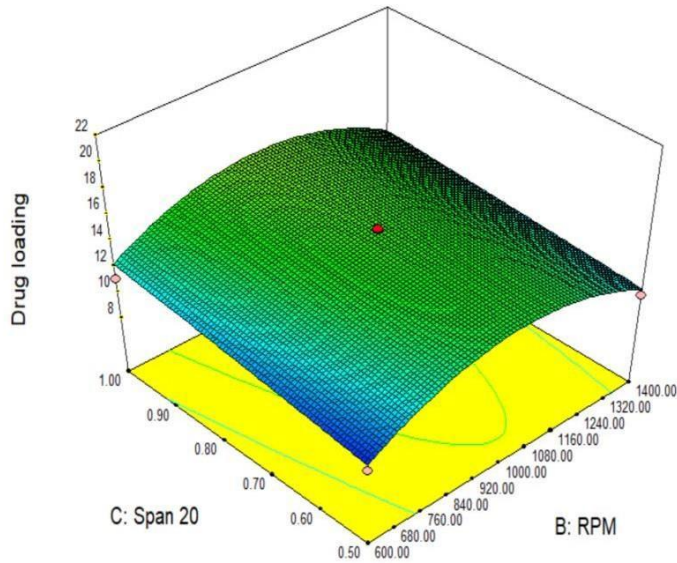
Figure 5.50: 3D surface response graph displays the effect of RPM (B) and concentration of span 20 (C) on % DL
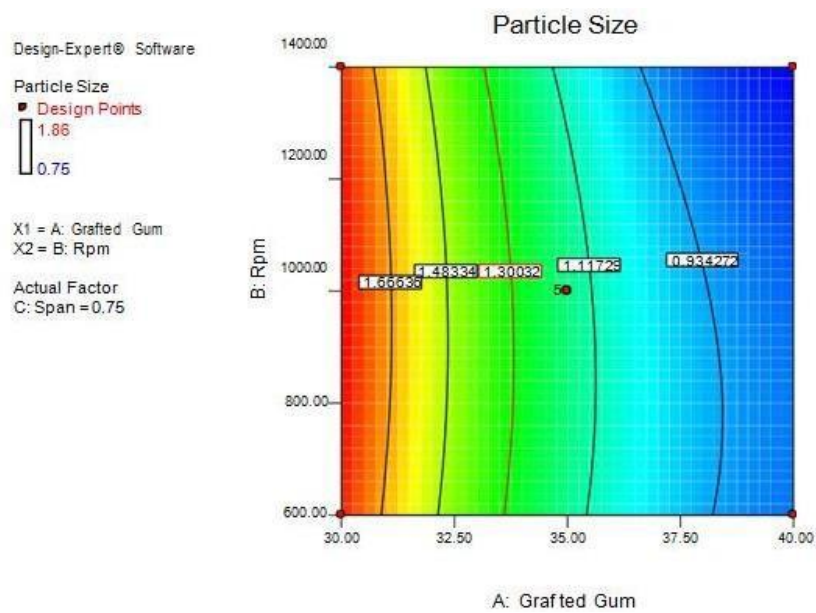
Figure 5.51: Contour plot displays the effect of grafted gum ratio (A) and RPM (B) on particle size (µm)
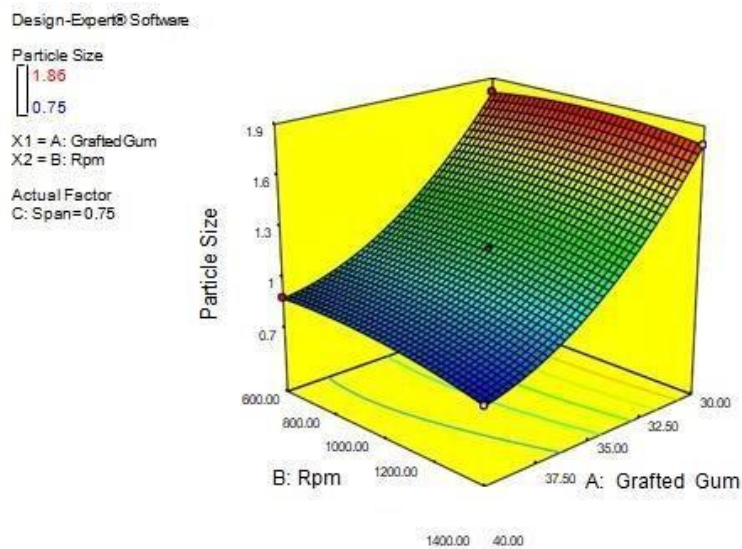
Figure 5.52: 3D surface response graph displays the effect of grafted gum ratio (A) and RPM (B) on particle size (µm)
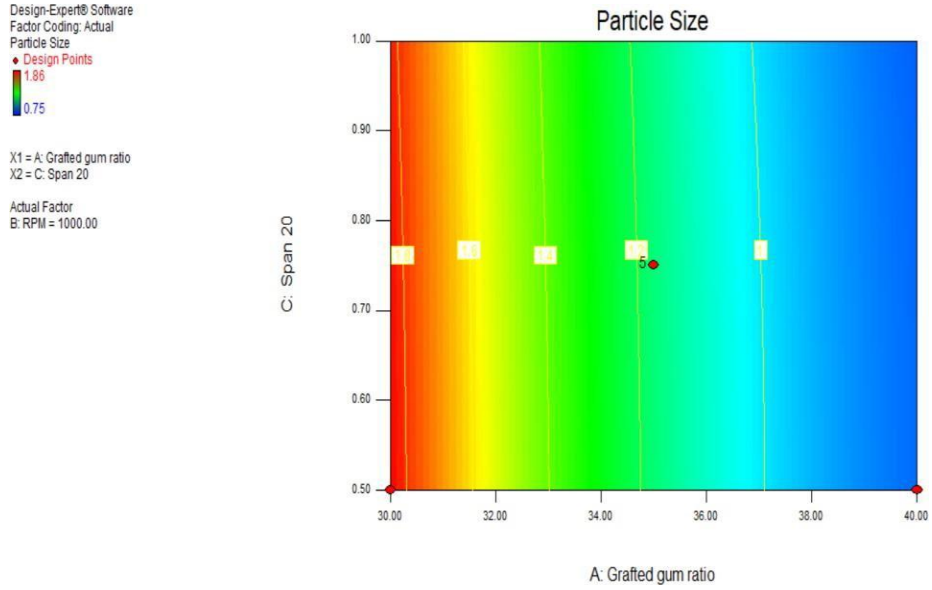
Figure 5.53: Contour plot displays the effect of grafted gum ratio (A) and concentration of span 20 (C) on particle size (µm)
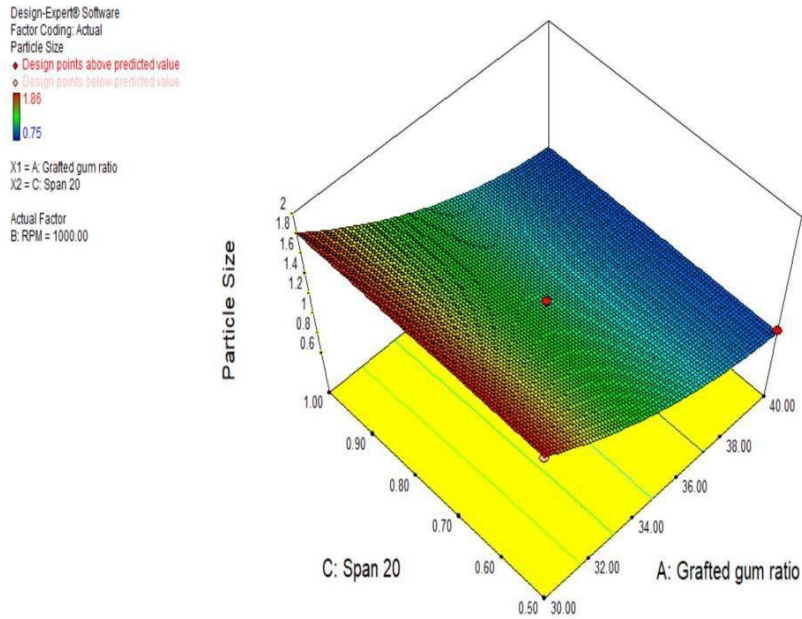
Figure 5.54: 3D surface response graph displays the effect of grafted gum ratio (A) and concentration of span 20 (C) on particle size (µm)
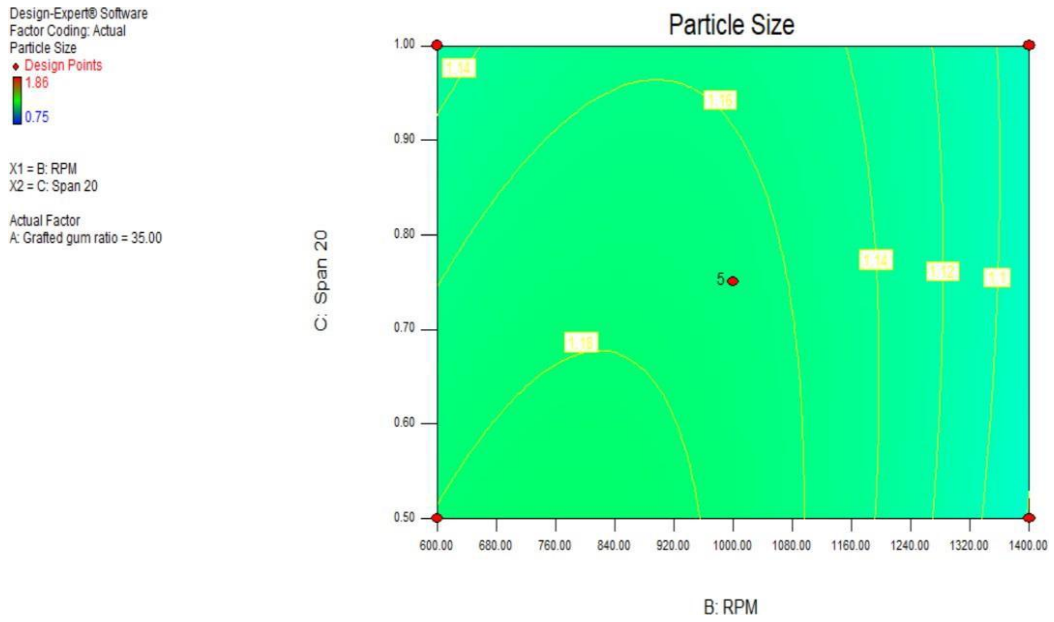
Figure 5.55: Contour plot displays displays the effect of RPM (B) and concentration of span 20 (C) on particle size (μm)
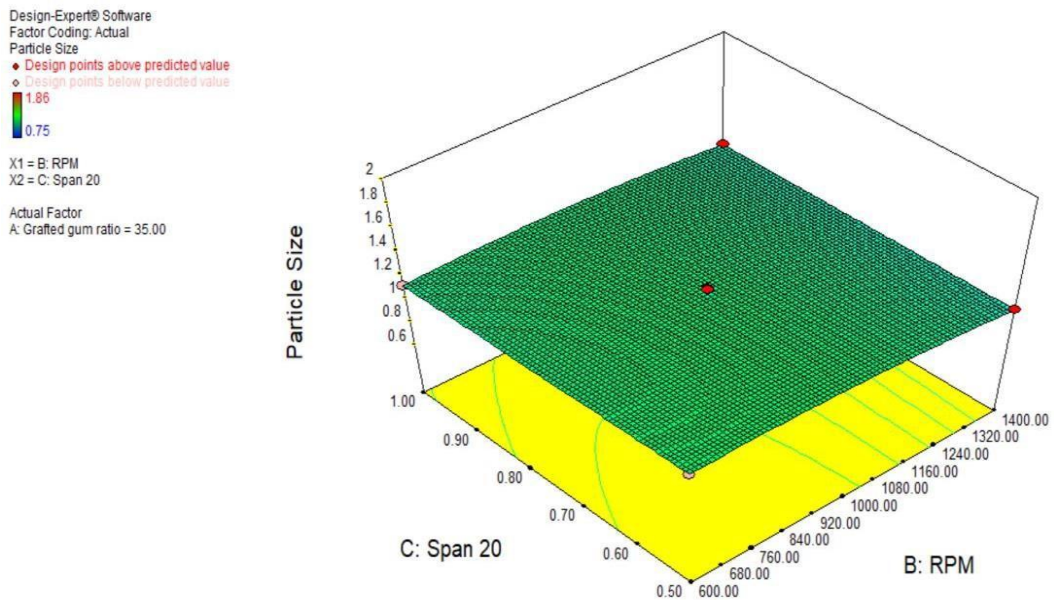
Figure 5.56: 3D surface response graph displays the effect of RPM (B) and concentration of span 20 (C) on particle size (μm)

5.3.3 Check Point Analysis

These experimental values of % EE, %, % DL, and Size (in µm) by the optimised grafting solutions (Table 5.28) were obtained to be consistent with the predicted values were found to be in agreement with the predicted values of % EE, % DL and size generated by design expert software, indicating that the optimised formulation was rational and reliable.

Table 5.28: Optimized Numerical Solution

Formulation code	Polymer 2%(w/v) Grafted Gum: PVA (w/w)	RPM	Span 20 (%)
FMS6	36.96:63.04	1225.92	0.78

Table 5.29: BBH Microsphere formulation (FMS11) by using ungrafted gum

Formulation code	Polymer Solution 2%(w/v)		GA (mL)	HCl (mL)	Span 20 (%w/w)	Liquid paraffin (%w/w)	RPM
	Guar gum (%w/v)	PVA (% w/v)					
FMS11	36.96	63.04	5	0.5	0.78	100	1225.92

Formulation code FMS6 and FMS11 were used for further coating using Eudragit S-100 polymer.
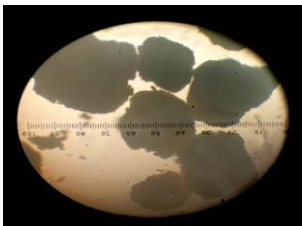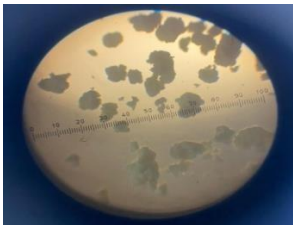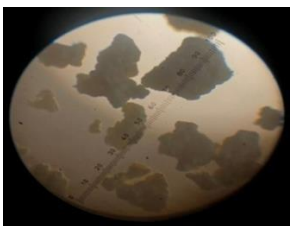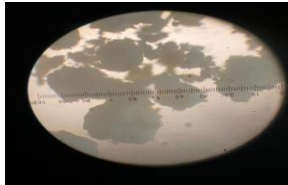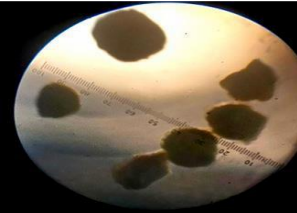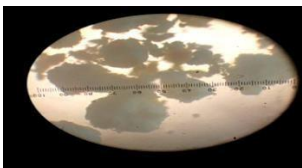
5.4 EUDRAGIT COATING OF PREPARED MICROSPHERES AND CHARACTERIZATION

5.4.1 Evaluation of coated microsphres

A. Microscopic examination and Surface appearance

Prepared microspheres were examined under optical microscope at 10 X. the microscopic images was given in Table no.5.30.

Table 5.30: Microscopic evaluation and surface appearance of Coated Microsphere

S.N	Formulation Code	Surface appearance	Appearance of Microsphere	Particle Size (µm)±SD
1	C1	Non-Uniformly coated		7.59±0.34
2	C2	Non-Uniformly coated		10.29±0.44
3	C3	Non-Uniformly coated		15.91±0.34
4	C4	Non-Uniformly coated		18.90±0.10
5	C5	Uniformly coated		19.98±0.60
6	C6	Cluster formation		27.47±0.17

*SD=Standard deviation

Discussion: From the microscopic as well as visual observation it was found thatmicrosphere formulation C5 was uniformly coated.

B. **Percentage yield:** From table 5.31 and figure 5.57, Formulation C5 (found highly significant $p < 0.05$) showed a higher Percentage yield (99.23±0.58) as compared to theother formulations.

C. **Entrapment efficiency:** From Table 5.31 and Figure 5.58, the maximum Percent Entrapment efficiency (92.90±0.87%) was reported by formulation C5 (found highly significant $p < 0.05$) as compared to the other formulations.

D. **Drug Loading:** From Table 5.31 and Figure 5.59, maximum Percent Drug Loading (15.47±0.15) was reported by C5 (found highly significant $p < 0.05$) formulation as compare to the other formulations.

Table 5.31: Percentage Yield, % EE, % DL of different formulations

Formulation code	Percentage yield ± SD	%EE±SD*	%DL±SD*
C1	92.27±0.50	61.80±0.21	10.29±0.03
C2	96.66±0.35	73.80±0.68	12.29±0.11
C3	91.23±0.30	74.93±0.19	12.48±0.03
C4	95.10±1.44	85.94±0.88	14.31±0.14
C5	**99.23±0.58**	**92.90±0.87**	**15.47±0.15**
C6	88.60±0.26	80.73±0.19	12.49±0.03

*SD=Standard deviation, n=3, C5**-Significant (p<0.05)
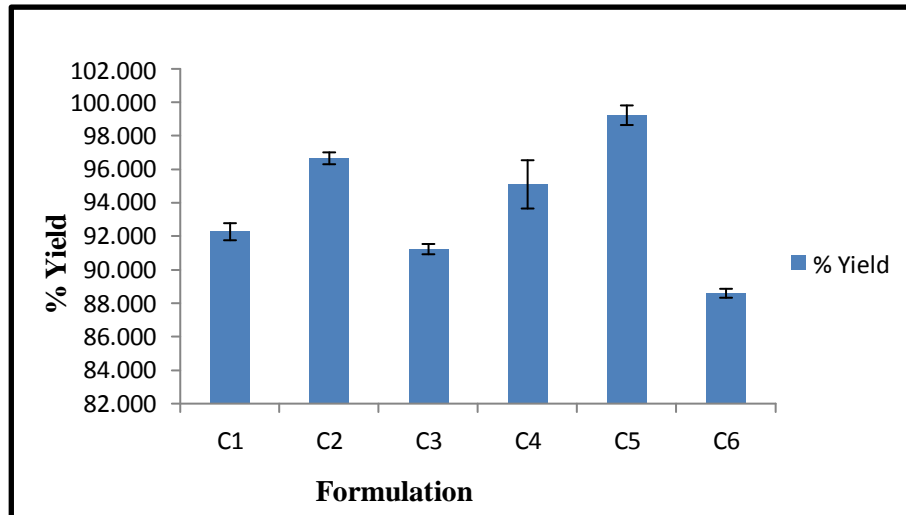
Figure 5.57: Percentage Yield of Different formulations
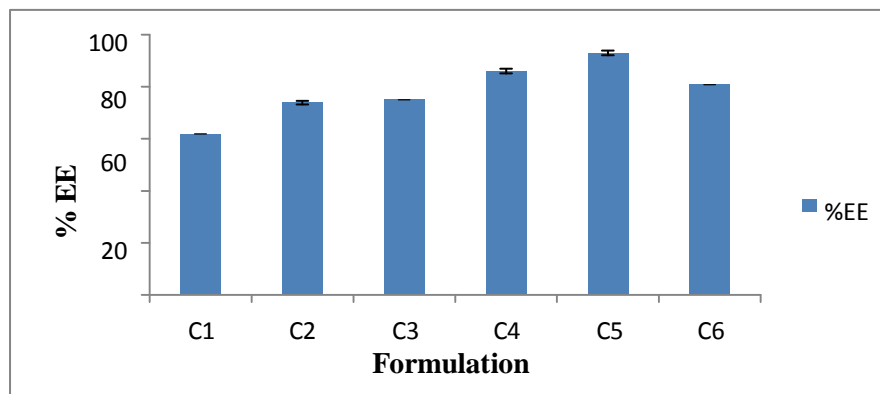
Figure 5.58: Percentage entrapment efficiency (%EE)
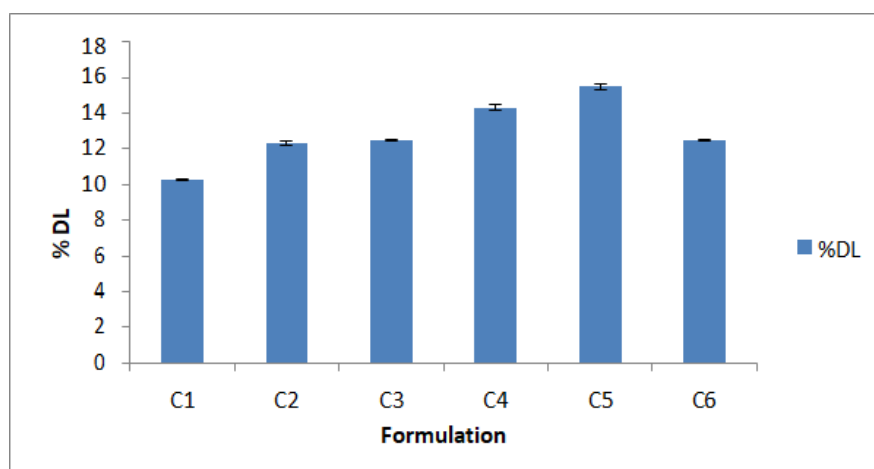
Figure 5.59: Percentage Drug Loading Capacity (%DL)

E. Micromeritic study

1. Angle of repose

The angle of repose of the various formulations (C1–C6) was determined using the fixed funnel standing technique, and the results ranged from 25.89 to 33.01. Formulation C5, which was determined to have highly significant flow characteristics ($p < 0.05$), is displayed in Table 5.32.

2. Compressibility index (Ci)

Ci for every formulation was calculated and is displayed in Table 5.32. The Ci ranged from 12.51 to 36.21, per the table. Formulation C5, which was determined to have highly significant flow characteristics ($p < 0.05$), is displayed in Table 5.32.

3. H.ratio

For every formulation (C1–C6), the H.ratio was calculated; the results are shown in Table 5.32. The formulation's H.ratio was found to be between 1.14 to 1.56. The outcome demonstrates that formulation C5 had excellent flow properties and was deemed to be extremely significant ($p < 0.05$).

Table 5.32: Micromeretic parameters of formulation (C5)

S.No	Formulation Code	Angle of repose ±SD*	Carr's Index ± SD*	H. ratio ± SD*
1	C1	30.41±0.05	36.21±0.54	1.56±0.01
2	C2	27.40±0.10	19.59±1.25	1.24±0.01
3	C3	32.29±0.15	27.82±1.35	1.38±0.02
4	C4	32.56±0.16	24.34±0.71	1.32±0.01
5	**C5****	**25.89±0.15**	**12.51±0.72**	**1.14±0.01**
6	C6	33.01±0.11	16.11±0.65	1.19±0.02

SD=Standard deviation, n=3 C5**-Significant ($p<0.05$)

5.4.2 Characterization of optimized coated microspheres (C5)

Formulation C5 was chosen for further analysis based on the results mentioned

above. FTIR, XRD and SEM studies were used to further characterise the optimised Eudragit coated formulation (C5).

A. X-Ray diffraction study

The XRD pattern of coated microspheres shows absence of sharp and intense diffraction peaks, which indicates that coated microspheres are amorphous in nature.
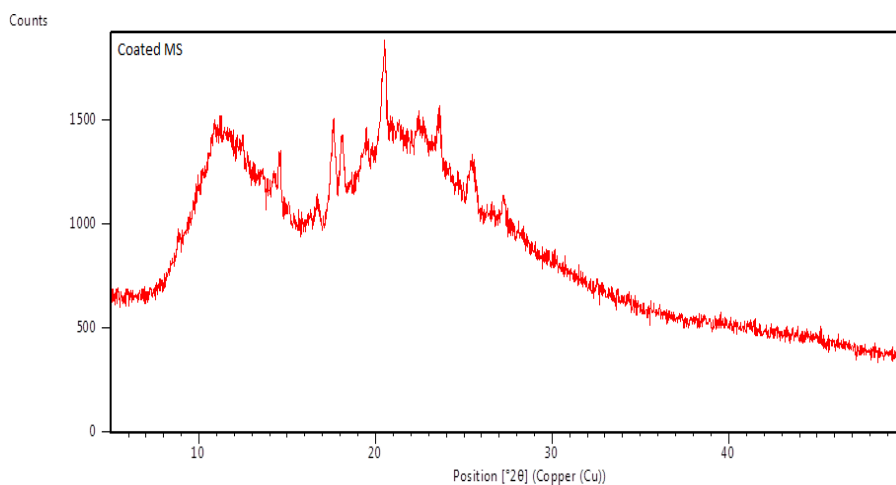
Figure 5.60: XRD Chromatogram of Coated microspheres (C5)

B. FTIR Spectroscopy

In the spectra above, none of the drug's characterstic peaks could be found, proving that it had been entirely encapsulated inside the coated microsphere that had been made.
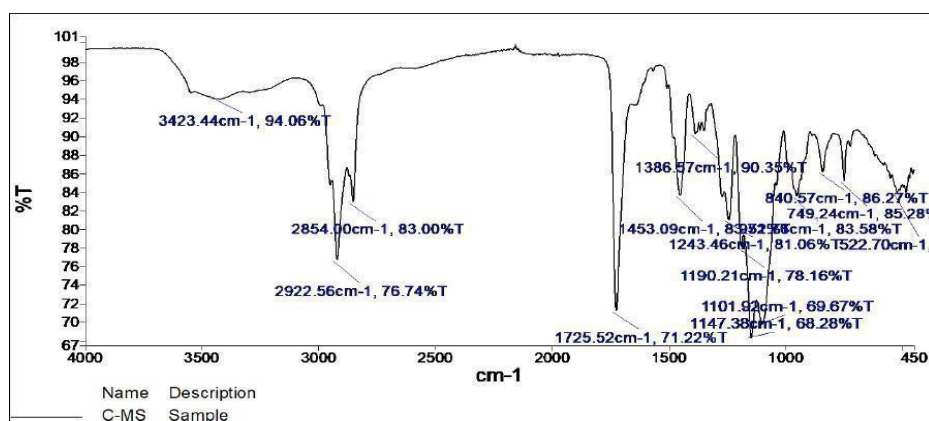
Figure 5.61: FT-IR spectra of optimized formulation C5

C. Scanning electronic microscopy of optimized formulation

SEM of eudragit coated microsphere (C5) shows smooth surface and sphereical shapewhich confirms the effective coating of microspheres.
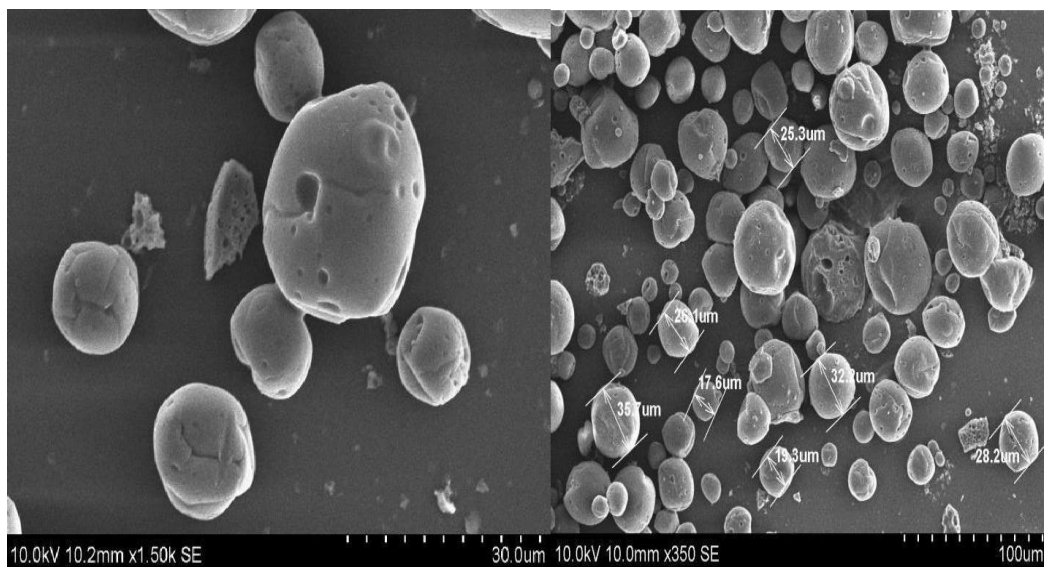
Figure 5.62: SEM of optimized formulation C5

5.5 *IN VITRO* DRUG RELEASE STUDIES

In vitro studies for dissolution were performed using the USP dissolution apparatus basket type-1 (Model DS-8000 Lab India). In the first two hours, the total percent drug release (% DR) from the pure drug was found to be 95.295±1.42%. At an acidic pH, drugrelease from uncoated BBH microspheres (grafted) began in the first hour, and the % DR in 2 hours was 39.235± 0.53% and 85.568±1.917 at 12 hours. % DR from ES-coated BBH microspheres (ungrafted) and ES-coated BBH microspheres (grafted) began after the fourth hour and reached 87.651±0.401 and 61.853±0.348, respectively, up to 12 hours, and 98.514±0.194 and 96.143±1.419, respectively, up to 24 hours.

Table 5.33: *In vitro* Release of BBH from various formulations in pH 1.2, 6.4 and 7.4

Time (Hrs.)	pH of Dissolution medium	% DR of pure Berberine HCl±SD	% Drug release of uncoated microspheres of BBH (grafted) ±SD (FMS6)	% DR of ES-Coated microspheres of BBH(ungrafted) ±SD (FMS11)	% DR of ES-Coated microspheres of BBH(grafted) ±SD (C5)
0		0	0	0	0
0.25	1.2	31.438±0.456	06.548±0.093	0.931±0.036	0.416±0.008
0.5		55.953±0.510	18.657±0.110	1.209±0.083	0.788±0.001
1		85.201±1.078	25.045±0.286	2.233±0.267	1.072±0.011
2		95.295±1.422	39.235±0.532	4.818±0.017	2.107±0.109
3	6.4	97.163±0.129	46.375±0.830	6.333±0.185	4.377±0.185
4		**97.684±0.211**	**52.396±1.741**	**7.898±0.001**	**6.440±0.107**
6	7.4	98.586±0.705	61.350±1.484	28.339±0.959	23.958±0.756
8		98.690±0.443	69.619±0.920	55.875±0.472	38.263±1.799
10		99.156±0.123	78.895±0.755	76.335±0.852	50.555±1.028
12		**99.358±0.135**	**85.568±1.917**	**87.651±0.401**	**61.853±0.348**
18		99.411±0.011	98.715±0.830	96.385±0.471	83.609±0.921
24		99.532±0.151	99.192±0.881	98.514±0.194	96.143±1.419

SD=Standard deviation

For dissimilarity (f1) and similarity (f2), the drug release study of C5 was compared with that of pure drug, FMS6, and FMS11. When C5 was compared to pure drug, the values of f1 and f2 were 40.41 and 16.39; when C5 was compared to FMS6 , the values were 28.16 and 29.43; and when C5 was compared to FMS11, the value were 20.02 and 37.86. Results were clearly indicated the significant difference in the release behavior of drug from C5 to pure drug, FMS6 and FMS11.
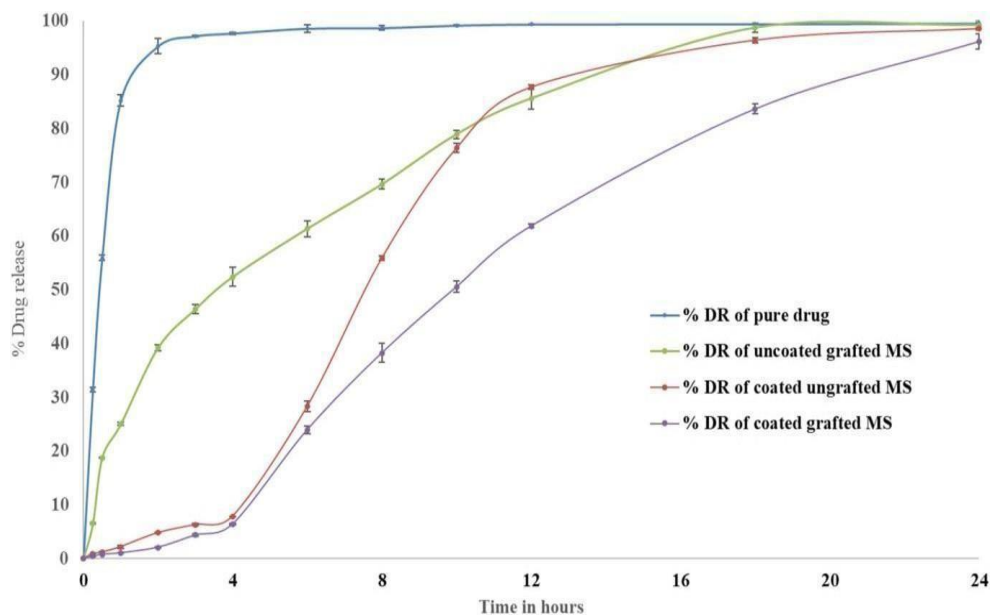
Figure 5.63: *In vitro* Release of BBH from pure drug and different
formulation of BBH in pH 1.2, 6.4 and 7.4
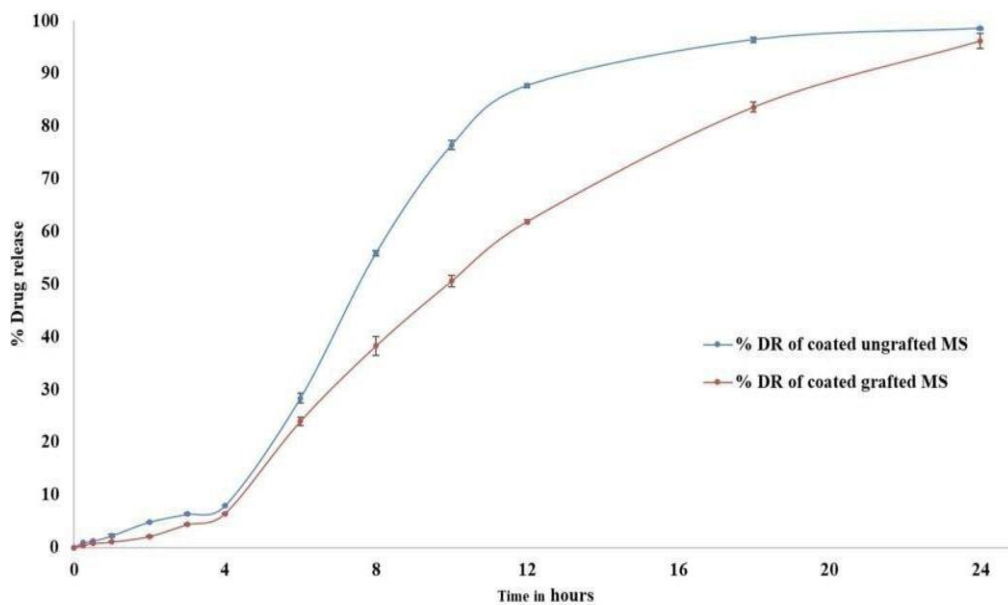
Figure 5.64: *In vitro* Release of BBH from ES-coated BBH microsphere
(grafted) (C5) and ES-coated BBH microsphere (ungrafted) (FMS11) in pH 1.2,
6.4 and 7.4

Discussion: To ensure the highest dosage of medication reaches the colon, there should be little drug release as it passes through the upper GIT.The dissolving trials' pH parameters were selected to closely resemble GI conditions. After 4 hours, % DR from uncoated BBH microspheres (grafted) was 52.396%, indicating brust drug release, indicating brust drug release. These dissolution patterns are inappropriate for colon- targeted delivery. The solubilization of the grafted copolymer at an acidic pH might explain the burst release of BBH from microspheres. In the colonic region, where the pH is usually higher than 7.4, the coating of microspheres with Eudragit S-100 enabled controlled drug release. This pH-dependent coating substance made sure that the drug was only released where it was actually required, preventing BBH from being released too early in the upper GIT, increasing its effectiveness, and lowering the possibility of side effects. After 4 hours, BBH release from C5 (Eudragit-coated microspheres) increased because the pH of the medium was raised to 7.4, that is greater than the pH at which the Eudragit S-100 polymer dissolves. For the drug release mechanism from the produced microspheres, the following pattern was expected.The controlled release of BBH from the grafted gum gel is largely dependent on these three mechanisms. The grafted copolymer is exposed when the Eudragit covering dissolves above pH 7.0, and this causes swelling. This swelling creates a porous network that facilitates the diffusion of BBH, resulting in its gradual release from the gel. Additionally, the higher concentration of the grafted copolymer may create a denser network within the microspheres, impeding the diffusion of drug molecules. This could explain the slower release rate observed with increasing concentration.

5.6 DRUG RELEASE AND KINETICS

Out of all the formulations, the most effective one (C5) was selected based on cumulative drug release. The application of release kinetics was then carried out using the optimal formulation. All four models' regression coefficient values were evaluated, and the model with the best fit was chosen. Figures 5.65-5.68

display the results that were attained. According to the highest correlation coefficient(r^2), the zero-order model appears to fit the *in vitro* release data better , with the highest value of r^2 (0.9674), thus suggesting a reservoir-type system is generated due to the coating of microspheres.

A. Zero Order Kinetics
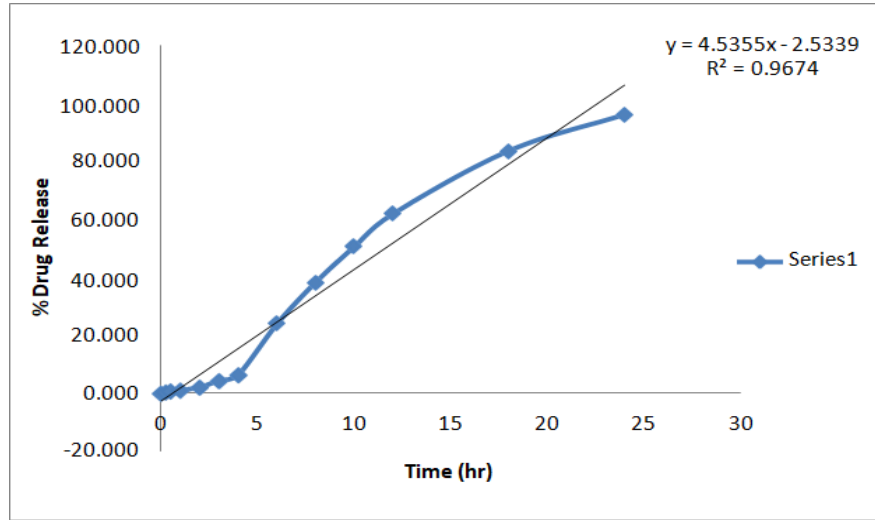
Figure 5.65: Zero order release kinetics of C5 formulation

B. First Order Kinetics model
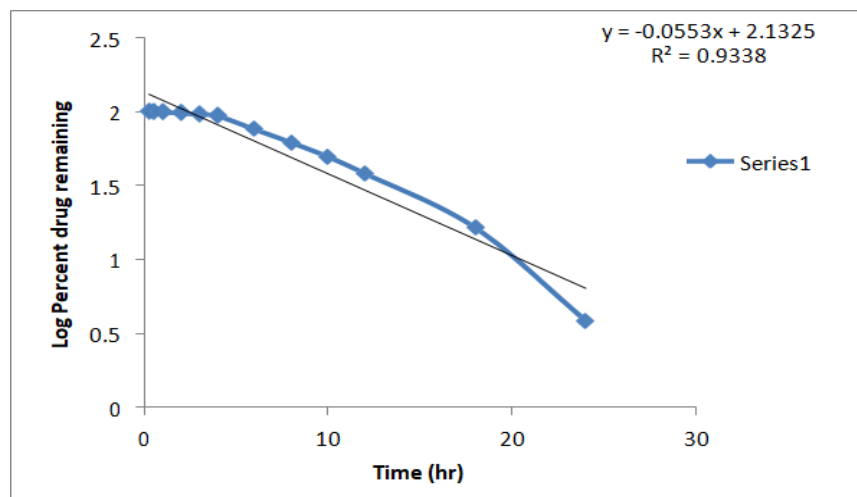
Figure 5.66: First order release kinetics of C5 formulation

C. Higuchi's Model
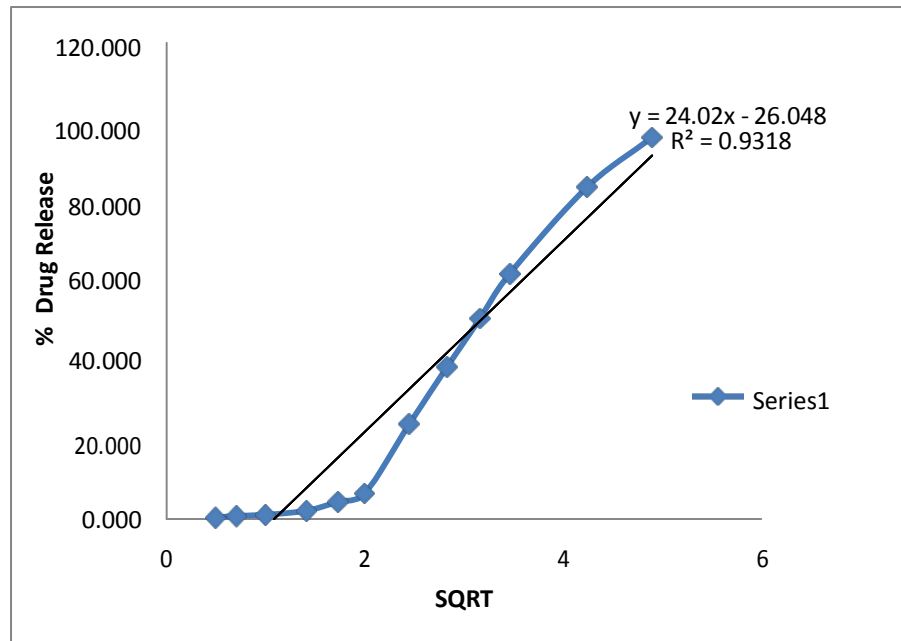
Figure 5.67: Higuchi release kinetics of formulation (C5)

D. Korsmeyer and Peppas Model
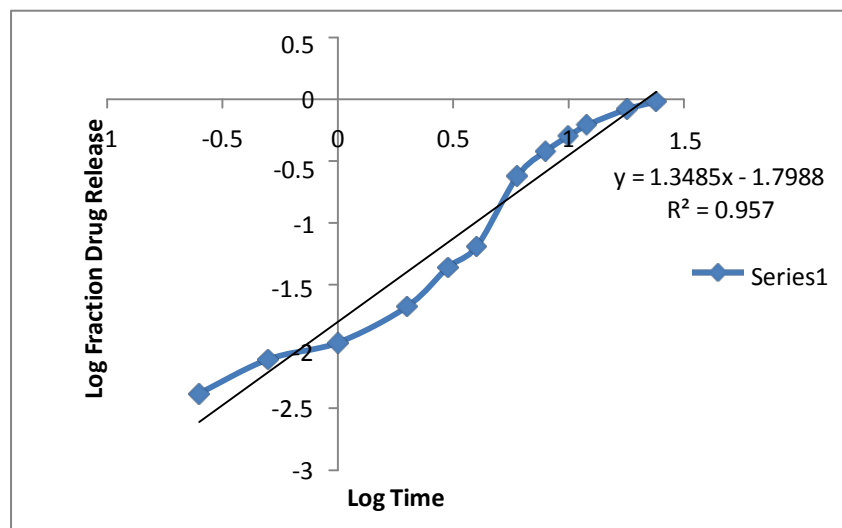
Figure 5.68: Korsmeyer and Peppas Model kinetics of optimised formulation (C5)

Table 5.34: R^2 values obtained for different kinetic models

Formulation code	Kinetics models				
	Zero Order (R^2)	First Order (R^2)	Higuchi Model (R^2)	Korsmeyer-Peppas (R^2)	(n)
C5 (Coated grafted)	**0.9674**	0.9338	0.9318	0.957	1.34
FMS6 (Uncoated grafted)	0.8154	0.9557	**0.9657**	0.943	0.54

As per the result from Table 5.34, in the case of coated formulation C5, the mechanism of drug release was discovered to be a supercase-II transport with n values greater than one, According to the highest correlation coefficient (r2), the zero-order model appearsto fit the *in vitro* release data better, with the highest value of r^2 (0.9674), thus suggesting a reservoir-type system is generated due to the coating of microspheres.The erosion and swelling of the polymer dominate the drug release process. But in the uncoated formulation, the FMS6 value of n was found to be less than one, suggesting that the formulation of FMS6 followed the Higuchi model.

5.7 STABILITY STUDIES

5.7.1 Physical appearance of microspheres

The chosen formulation C5 was subjected to storage conditions in accordance with ICH recommendations. For 180 days, the temperature was 40°C ± 2°C at 75 ± 5% RH (accelerated stability testing) and 30 ± 2 C/65 ± 5% RH for 360 days (long term stability testing).The influence of temperature and ageing on physical appearance, flow characteristics, % EE, % DL and *in vitro* release parameters were studied by obtaining samples at regular intervals, as indicated in the table 5.35 below:

Table 5.35: Stability test data of Physical appearance (0-180/360 days)

Time (Days)	Effect of storage on Visual appearance	
	40±2°C/75±5% RH	30 ± 2 °C/65 ± 5% RH
0 days	Light yellow colour Microsphere	Light yellow colour Microsphere
30 days	No change in colour	No change in colour
60 days	No change in colour	No change in colour
90 days	No change in colour	No change in colour
180 days	No change in colour	No change in colour
270 days	---	No change in colour
360days	-----	No change in colour

5.7.2 Flow properties

The results of stability studies at 40±2 ° C/75±5% RH for 0-180 days and 30 ± 2 C/65 ± 5% RH for 0-360 days of formulation C5 are shown in Table 5.36-5.37. The selected optimized formulation was evaluated for flow properties (Angle of repose, Hausner's ratio and Carr's index) after regular interval. After 180 days of storage under accelerated stability conditions or 360 days of storage under long-term stability conditions, no appreciable changes were found in the various parameters. According to the findings, the formulation of the chosen batch was discovered to be stable even after 180 days of storage under accelerated stability conditions as well as 360 days under long-term stability study conditions.

Table 5.36: Stability test data for flow properties of optimized formulation C5

Accelerated stability study (0-180 days)

Storage conditions	Accelerated stability study 40±2°C/75±5% RH		
Time (Days)	Angle of repose (θ) (Mean ±SD*)	Ci (%) (Mean ±SD*)	H.Ratio (Mean ±SD*)
0	25.89±0.15	12.51±0.72	1.14±0.01
30	26.77±0.33	12.90±1.24	1.14±0.21
60	24.28±0.73	13.33±1.21	1.15±0.32
90	25.97±0.18	12.12±1.32	1.13±0.10
180	26.78±0.32	11.76±1.14	1.13±0.02

SD=Standard deviation

Table 5.37: Stability test data for flow properties of optimized formulation C5

Long term stability study (0-360 days)

Storage conditions	Long term stability study 30 ± 2 °C/65 ± 5% RH)		
Time (Days)	Angle of repose (θ) (Mean ±SD*)	Ci (%) (Mean ±SD*)	H. Ratio (Mean ±SD*)
0	25.89±0.15	12.51±0.72	1.14±0.01
30	26.47±0.61	13.43±1.02	1.15±0.02
60	25.89±0.31	13.04±1.04	1.15±0.03
90	27.12±0.11	12.50±0.87	1.14±0.02
180	26.75±0.19	12.13±0.21	1.13±0.15
270	25.89±0.21	12.91±0.11	1.14±0.21
360	26.73±0.47	11.76±0.21	1.13±0.10

SD=Standard deviation

5.7.3 Percent Entrapment Efficiency (%EE) and Percent Drug Loading

Table 5.38 displays the findings of stability studies conducted at 40°C/75% RH for 0-180 days, and 30°C/65% RH for one year after formulation. After 0–6 months of storage, the choosen optimised formulation (C5) was assessed for a number of parameters (% EE and % DL). After 180 days of storage under accelerated stability circumstances and after 360 days of storage under long-term stability settings, no appreciable changes in the drug content or other parameters were found. According to the results, the C5 formulation was still stable after 6 months and 1 year of storage under accelerated stability conditions and long-term stability conditions, respectively.

Table 5.38: Stability test (Accelerated and long term stability) data of % EE and % DL (0-180/360 days)

Storage conditions	Accelerated stability study 40±2°C/75±5% RH		Long term stability study 30 ± 2 ∘C/65 ± 5% RH)	
Time (Days)	% EE (Mean+SD*)	% DL (Mean+ SD*)	% EE (Mean+SD*)	% DL (Mean+SD*)
0	92.905±0.888	15.478±0.148	92.905±0.888	15.478±0.148
30	92.369±0.165	15.389±0.027	92.213±0.687	15.363±0.114
60	91.458±1.210	15.237±0.202	92.350±0.452	15.385±0.075
90	91.834±0.422	15.300±0.07	92.681±1.069	15.441±0.178
180	92.057±0.938	15.337±0.156	92.453±0.799	15.403±0.133
270	---	---	92.653±0.219	15.213±0.124
360	---	---	92.771±0.329	15.363±0.013

*SD=Standard deviation

145

5.7.4 Stability test data of *in vitro* dissolution study

Table 5.39-5.40 displays the outcomes of *in vitro* dissolution studies conducted at 40°C/75% RH for 0-180 days, and 30°C/65% RH for 0-360 days of formulation. After 180 days of storage under accelerated stability circumstances and after 360 days of storage under long-term stability settings, no appreciable changes in the drug content and other parameters were found. According to the results, the coated microsphere from batch C5 is still stable after 6 months and 1 year of storage under accelerated stability conditions and long-term stability conditions, respectively.

A. Accelerated stability test data of *in vitro* dissolution study (0-180 days)

Table 5.39: Accelerated stability test data of *in vitro* dissolution study (0-180 days)

Time (Hrs.)	pH (Diss. medium)	% DR of Eudragit S-100 Coated microspheres of BBH (grafted) ±SD*(C5) ((40±2°C/75±5% RH))				
		0 days	30days	60 days	90 days	180 days
0		0	0	0	0	0
0.25		0.416±0.008	0.423±0.002	0.342±0.021	0.373±0.043	0.427±0.058
0.5	1.2	0.788±0.001	0.801±0.121	0.824±0.064	0.776±0.237	0.754±0.141
1		1.072±0.011	1.163±0.162	1.121±0.015	1.263±0.026	1.112±0.051
2		2.107±0.109	2.262±0.093	2.356±0.123	3.013±0.439	2.377±0.137
3	6.4	4.377±0.185	5.542±0.121	4.149±0.085	4.873±0.075	3.987±0.184
4		6.440±0.107	7.082±0.235	6.125±0.116	8.275±0.124	6.870±0.162
6		23.958±0.756	24.064±0.532	19.925±0.631	23.042±0.156	23.572±0.436
8		38.263±1.799	39.013±1.082	40.123±1.739	39.062±0.961	37.213±1.098
10	7.4	50.555±1.028	47.315±1.123	54.275±0.58	49.835±1.076	51.645±0.378
12		61.853±0.348	59.573±0.238	60.998±1.128	62.343±0.642	63.003±0.118
18		83.609±0.921	84.112±0.231	79.354±0.654	86.149±0.885	83.546±0.237
24		96.143±1.419	97.003±1.129	95.764±0.769	94.123±1.032	96.321±1.810

A. Long term stability test data of *in vitro* dissolution study (0-360 days)

Table 5.40: Long term stability test data of *in vitro* dissolution study (0-360 days)

Time (Hrs.)	pH (Diss .med ium)	% DR of ES-Coated microspheres of BBH (grafted) ±SD (30±2°C/65±5% RH) long term stability						
		0 days	30days	60 days	90 days	180 days	270 days	360 days
0		0	0	0	0	0	0	0
0.25	1.2	0.416±0.01	0.420±0.02	0.319±0.01	0.443±0.01	0.341±0.01	0.323±0.01	0.311±0.03
0.5		0.788±0.01	0.812±0.01	0.856±0.01	0.636±0.02	0.754±0.04	0.716±0.001	0.724±0.01
1		1.072±0.01	1.123±0.01	1.321±0.12	1.287±0.04	1.272±0.01	1.007±0.03	1.212±0.01
2		2.107±0.10	3.432±0.12	2.476±0.10	3.213±0.12	2.877±0.11	2.913±0.12	3.177±0.17
3	6.4	4.377±0.18	5.112±0.13	4.899±0.11	4.923±0.12	3.867±0.151	4.813±0.15	3.997±0.18
4		6.440±0.10	7.132±0.12	6.955±0.15	8.765±1.14	7.120±0.13	5.324±0.03	6.820±0.12
6	7.4	23.958±0.75	22.134±0.15	21.958±0.65	23.112±0.32	24.312±0.82	20.102±0.61	22.716±0.75
8		38.263±1.79	33.233±1.12	40.433±0.71	42.452±1.35	35.873±1.53	39.092±1.38	37.243±1.09
10		50.555±1.02	52.125±1.21	54.075±1.32	50.175±0.26	51.145±1.07	55.145±1.11	52.165±0.98
12		61.853±0.34	59.873±0.32	63.998±0.54	62.343±0.53	61.063±0.21	64.213±0.09	62.003±0.07
18		83.609±0.92	81.112±0.87	79.354±0.32	85.609±0.45	82.976±0.76	85.549±0.98	86.976±0.76
24		96.143±1.41	92.013±1.13	94.834±0.24	97.143±0.92	91.121±1.07	97.143±1.13	93.171±1.10

SD=Standard deviation

5.8 *IN VIVO* EVALUATION OF OPTIMIZED FORMULATION

Pharmacodynamic parameters were evaluated by macroscopic scoring and histopathology.

5.8.1 Macroscopic examination

A. Mean Body Weight

Figure-5.69 depicts that the body weights of all experimental animals visually displayed as a percentage weight reduced. The results revealed that animal groups 8 and 9 treated with ES-coated BBH microsphere (grafted) low and high dose showed minimum body weights reduction, 4.75% and 1.197% after the 5 days of regular treatment as compared to group II colitis group (12.93%) and found highly significant different (p   0.05). Furthermore, mean body weight for groups 3, 4, 5, 6, and 7 improved slightly, with percent body weights reduction, 10.85%, 10.49%, 12.64%, 11.38%, and 10.71%, respectively, from colitis induction to the last day of dose administration.
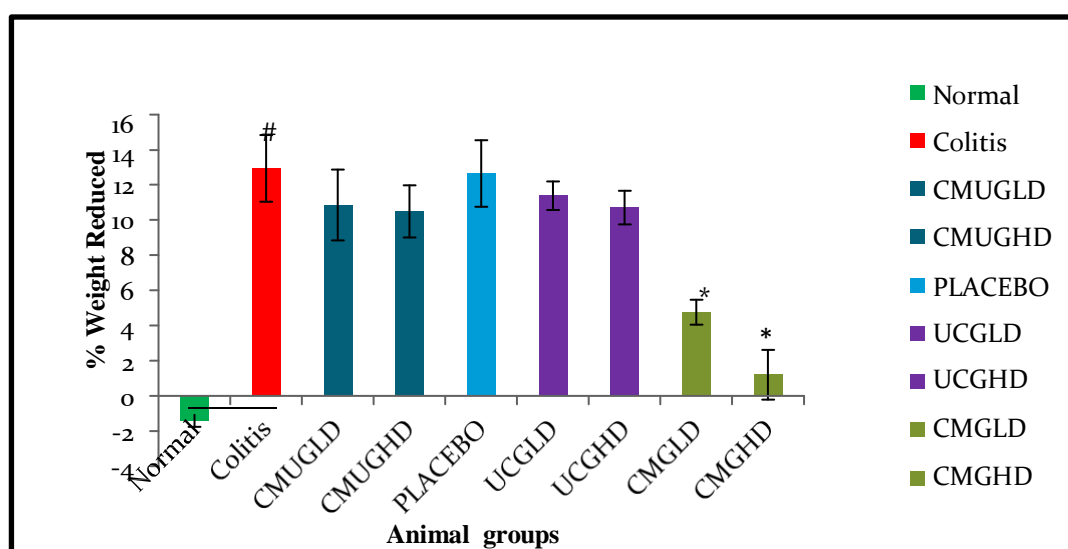
Figure 5.69: Percent weight reduction of various animal groups

The values were presented as mean ± standard deviation (n = 6).
# indicates a statistical significant (p < 0.05) in comparison to the control (Normal) group.
*indicates a highly significant difference (p < 0.05) in comparison to the colitis group

Table-5.41: Photographs of the colons

Group No.	Name of the group	Colon picture
1	Normal (No colitis induced)	
2	Experimental control (Acetic acid induced colitis)	
3	BBH Coated microsphere (ungrafted) low dose	
4	BBH Coated microsphere (ungrafted) high dose	
5	Placebo control (Grafted copolymer)	
6	BBH uncoated microsphere (grafted) Low dose	
7	BBH uncoated microsphere (grafted) High dose	
8	BBH coated microsphere (grafted) Low dose	
9	BBH coated microsphere (grafted) High dose	

B. Colon weight and colon length ratio and colon weight and body weight ratio

The colons of the studied rats (6 cm long, distal colons) were removed from the bodyand washed (Table 5.41). Using colon weight and colon length data, a colon weight/length ratio and a colon weight/body weight ratio were computed, and the results of both parameters were utilised to quantify colonic inflammation.

Animals treated with the optimised (C5) formulations (groups 8 and 9) were shown to be significantly different from colitis (group 2), with a lower colon weight/colon length ratio of 0.25 and 0.24, respectively, whereas colitis (group 2) had a higher ratio of 0.37. The ratios for resected specimens from groups 3, 4, 5, 6, and 7 were higher than in the normal group, and they differed significantly from the normal group but not from the colitis group. They were 0.32, 0.32, 0.36, 0.35, and 0.33 in that order. Furthermore, when compared to the colitis group (0.01), the colon weight/body weight ratios for groups 8 (0.007) and 9 (0.006) were found to be significant ($P < 0.05$), but not significant when compared to the healthy group (0.006) (Figure 5.70 & 5.71).
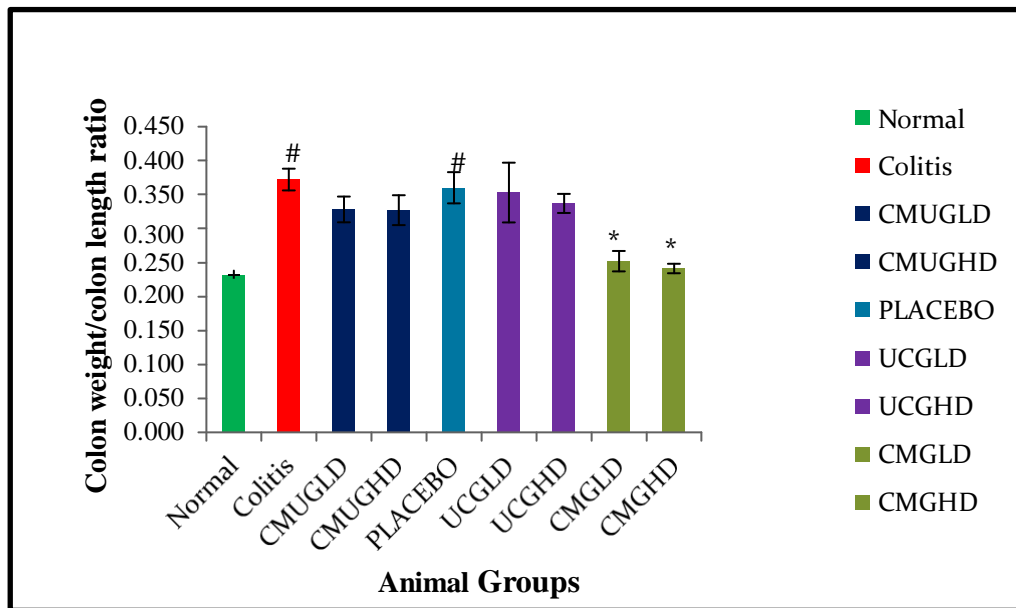
Figure-5.70: The ratio of colon weight to colon length as an inflammatory marker

\# indicates statistical significance (p < 0.05), when compared to the normal group
* Indicates statistical significance (p < 0.05), when compared to the colitis group
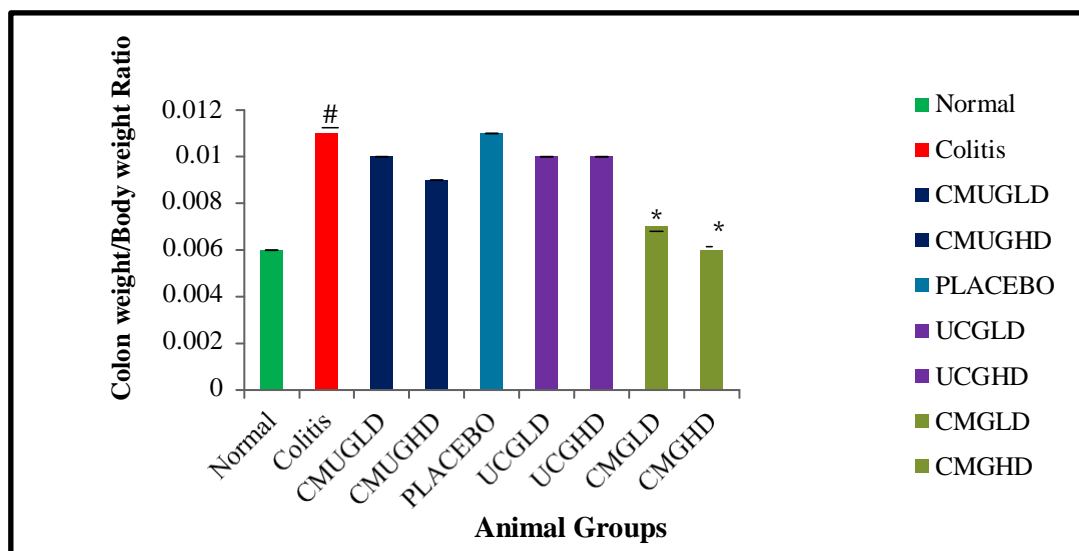
Figure 5.71: The ratio of colon weight to body weight as an inflammatory marker

Values were expressed as Mean ± SD. n = 6

\# indicates statistical significance (p < 0.05), when compared to the normal group.
* Indicates statistical significance (p < 0.05), when compared to the colitis group.

C. Disease activity index

The findings indicated that animals treated with the optimized (C5) formulation (groups 8 and 9) had a reduced DAI score of 5.33 and 0.66, respectively, which was significantly different (P   0.05) when compared to the colitis group, which had a DAI score of 10.83. Likewise when other resection specimens from groups 3, 5, 6, and 7 were compared withcolitis group, the difference was found to be non-significant See Figure 5.72).
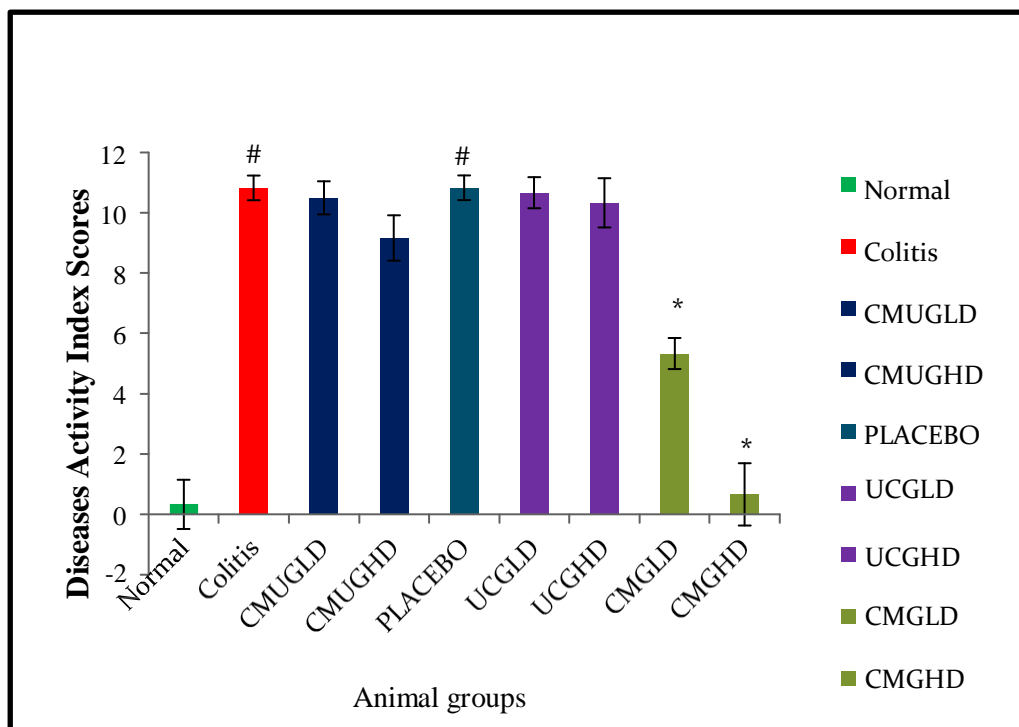
Figure-5.72: Disease activity index of animal groups

\# indicates statistical significance (p< 0.05), when compared to the normal group
 * indicates statistical significance (p< 0.05), when compared to the colitis group

D.Histopathology

From all treatment groups (8 and 9), the mucosa had mild inflammation as evidenced bythe infiltration of neutrophils, acute inflammatory cells. The

serosa, musculosa, and submucosa lacked inflammation. Some of the specimens under examination had crypt damage, but it only affected the basal 1/3 of the crypt. When compared to other groups, animal group 1 had a histopathology score (H.score) of 0.33, while colitis group 2 and placebo group 5 had the highest H.scores of 9.5 and 9.1, respectively. Animal groups 3 and 4 treated with ES-coated BBH (ungrafted) microsphere demonstrated H.scores of 7.8 and 6.8, while animal groups 6 and 7 demonstrated H.scores of 8.8 and 8.6, respectively, when treated with uncoated BBH (grafted) microsphere. When animal groups 8 and 9 treated with ES-coated grafted microsphere of BBH compared with the normal as well as colitis group, showed the lowest H. scores of 5.5 and 2.3, a reduction in crypt damage and also reduction in inflammatory cell invasion, muscle deterioration and mucosal edema. The treated groups 8 and 9 displayed a highly significant difference (P 0.05) in comparison to the colitis group scores (figure 5.73).
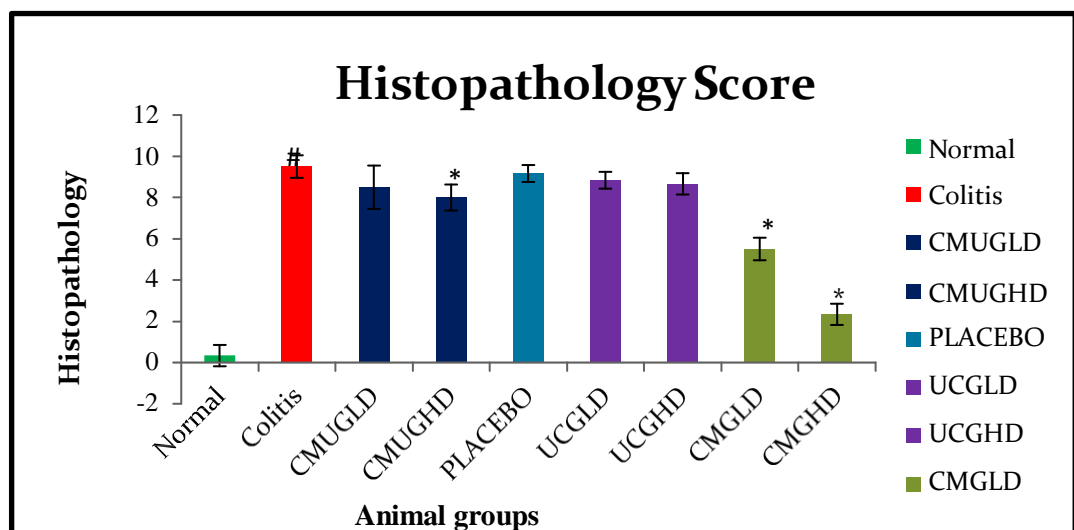
Figure-5.73: Animals' histopathological score system (Total score= 10). Scores based ondifferent criteria for inflammation .All the Values were presented as Mean ± SD. (n = 6)

# indicates statistical significance $p < 0.05$, when compared to the normal group

* Indicates statistical significance $p < 0.05$, when compared to the colitis group
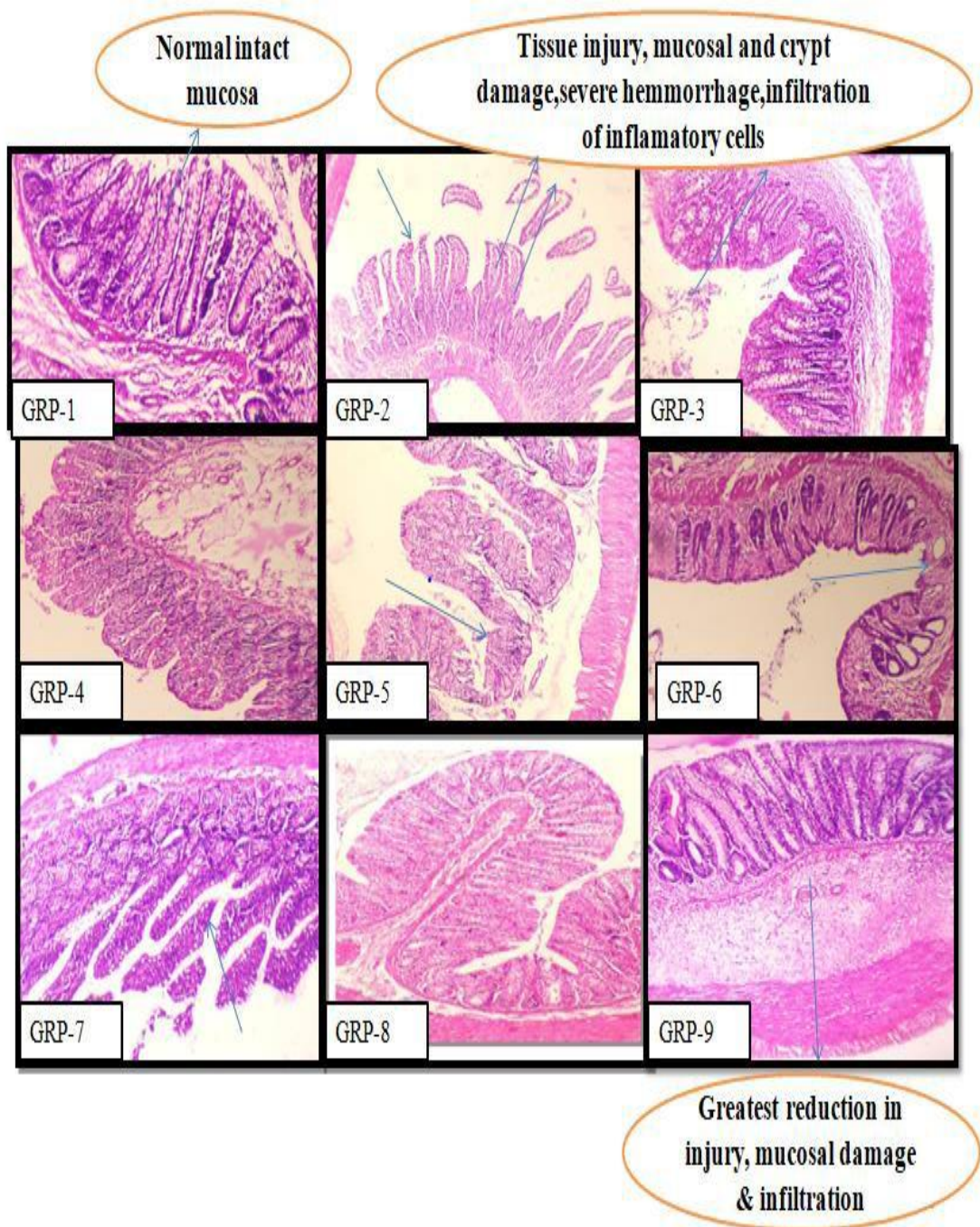
Figure-5.74: Histopathological examination for colitis of all animals groups
(1 to 9)

The presence of normal, intact mucosa with colonic glands and goblet cells in the healthy group (group-1) indicates the absence of any significant damage or abnormalities in the colon. However, it is worth noting that a few specimens did show mild inflammation, although it was limited to the mucosa and not present in the submucosa or musculosa (figure 5.74). The colitis group had acute inflammatory cell infiltration) in all layers, as well as necrosis and ulceration in the same sites on the mucosa. In the majority of the cases examined, surface epithelium had been destroyed, resulting in the total loss of crypts. In some cases, the musculosa was impacted by transmural inflammation.There was modest inflammation in the mucosa in treatment groups (8 and 9), as shown by the infiltration of neutrophils, acute inflammatory cells. No any inflammation was detected in submucosa, musculosa, and serosa.

CHAPTER -6

6.1 SUMMARY

The purpose of this study was to create and analyse graft copolymers of acrylamide and guar gum. Additionally, using the grafted gum to make Eudragit S-100 coated BBH microspheres. The *in vitro* release behaviour of coated versus uncoated BBH microspheres was compared .The entire research project was presented in six chapters, including an introduction, a review of the literature, a hypothesis & objective, a description of the materials and methods, results and discussion and summary & conclusion. Through preformulation studies, drug molecules' physical and chemical properties were identified. UV spectrum, FT-IR spectrum, and melting point were used to confirm the identity and purity of the drug's molecule. The partition coefficient's log P value supported its hydrophilic nature. The outcomes of preformulation studies indicated that BBH was good in quality and pure for the development of formulations. BBH was calculated using HPLC. It was discovered that the BBH calibration curve was linearly regressed. BBH's solubility was assessed using qualitative and quantitative methods. BBH was discovered to be soluble in methanol and ethanol. The microwave-assisted method was used to prepare guar gum with acrylamide grafting. The following procedures were followed in the grafted gums' preparation: (a) Preparation of preliminary experimental trial batches, (b) Optimisation of grafted guar gums, (c) Preparation of optimised graft copolymers and (d) Characertrization of optimized graft copolymers.

The amount of guar gum, the amount of acrylamide, and the passage of time were used as independent variables in the box-Behnken design, and % yield, % grafting, and % efficiency were used as dependent variables. Batch GS-1 was chosen as the most optimal batch of guar gum because of its guar gum concentration (0.59 g), monomer amount (10.74 g), and time (2.4 min). DSC, SEM, FT-IR, and XRD were used to further characterize the optimised

grafted copolymer, which confirmed its formation. Guar gum, acrylamide, and the grafted gum were represented on a DSC graph, which supported the grafting. Due to the overlap between the NH stretch band of acrylamide and the OH stretch band of guar gum, the FTIR spectra of gum that had been grafted with acrylamide showed a broad absorption band.

The XRD spectra revealed that Guar gum is amorphous, since no distinctive peaks were identified in the spectrum, but the diffractogram of acrylamide revealed that it is crystalline. The grafted gum XRD spectrum revealed the less intense peak of acrylamide confirming the development of graft co-polymer and indicating that grafted gum is amorphous in nature. Acrylamide was grafted onto guar gum, as seen in SEM images of the grafted copolymer.The grafted gum's altered shape and the variation in surface flaws served as grafting confirmation. W/O emulsion cross-linking was used to create BBH-loaded microspheres. A box-behnken design was used to optimize the BBH-loaded formulation with independent variables like guar gum and PVA ratio (A), RPM (B), and Span 20 (%) (C) and % EE (R1), % DL (R2) and Particle Size (µm) (R3). A solvent evaporation method known as oil-in-oil was used to coat the optimised formulation with various concentrations of Eudragit S-100. The C5 formulation was chosen for further study based on several evaluation characteristics, such as microscopic evaluation, micromeritic properties, percentage yield, percentage drug loading, and percentage entrapment efficiency. To ensure that the drug was entirely encapsulated inside the coated microsphere, FTIR, XRD, and SEM were utilised. The microspheres created had a homogeneous spherical shape and high entrapment efficiency. The X-ray diffractogram demonstrated that eudragit-coated BBH microspheres had less intense peaks than free BBH, demonstrating the incorporation of drug within the microsphere.

The coating and grafting outcome on release from various formulations *in vitro* release patterns were compared. Following zero-order kinetic models, uncoated BBH- microspheres displayed burst release within the first 4 hours. However, eudragit-coated BBH-microspheres restricted the formulation's early release of

the BBH in the upper GIT and only released the drug in the colon, demonstrating controlled release for up to 24 hours. According to *in vitro* research, the suggested formulations are a potential method for IBD patients' colonic pH-sensitive drug delivery.

A stability analysis of the optimised formulation (C5) was carried out (in accordance with ICH guidelines) to assess storage conditions and expiration dates. During the stability evaluation, various parameters were monitored to assess any changes or degradation in the optimised formulation batch (C5). The data collected at each interval (30 days) provided valuable insights into the batch's stability and its potential shelf life under different storage conditions.Both the accelerated stability conditions (180 days) and the long-term stability conditions (360 days) were chosen to be at 40 degrees Celsius(C°) and 75 percent relative humidity (RH), and 30 degrees Celsius(C°) and 65 percent RH, respectively. According to the findings, the coated microsphere from batch (C5) is stable throughout 6 months and 1 year of storage at accelerated stability settings and long-term stability conditions, respectively.

The *in vivo* study was carried out under the licence (800/PO/Re/S/03/CPCSEA) and with the approval of Lord Shiva College of Pharmacy's Institutional Animal Ethics Committee (IAEC). The animals (Wister albino rats) were housed in a variety of standard cages with unrestricted access to food and water in controlled environments. Before inducing colitis, Rats were starved for 48 hours with unrestricted water access. For the *in vivo* investigation; colitis-induced model was used. Different formulations were administered to each group for 5 days and assessed. Nine groups of rats were selected at random. Each group had six rats. The polyurethane tube of medical grade with a 2 mm external diameter was carefully inserted up to 6–8 cm (proximal to the anus margin) to avoid any damage to the surrounding tissues. Once in place, it allowed for the administration of substances that induced colitis, leading to inflammation in the animals' colons.

The colons of all animal groups (except the healthy one) were filled with a 2 mL solution of 3% v/v acetic acid to simulate an illness (IBD). To stop solution leakage, the rats were kept in inverted position for at least two minutes. Despite the presence of an acetic acid solution, the Normal group (Group-1) received 2 mL of a 0.5% carboxymethylcellulose (CMC) solution. To develop an IBD model, all the animals were kept untreated for a time interval of 24 hours during which food and water was provided in full access. Every group under treatment received a fixed volume of suspension of different formulations such as ES-coated BBH microsphere (ungrafted), uncoated BBH microsphere (grafted), placebo control (Blank microsphere), and ES-coated BBH microsphere (grafted). Each formulation was given one time per day for five continues days; these doses, which were equivalent to 20 mg/kg/day to 40 mg/kg/day, were administered orally via gavages. The administration of 1 mL of CMC was consistent across both the normal and colitis groups, regardless of the specific drug formulation used. In contrast, group V was given a blank microsphere solution that did not contain any active drug components. A 6 cm section of the colon was removed from each rat after it had been sacrificed under anaesthesia, 24 hours from the last dose. All samples (colons) were opened lengthwise, washed, and dried. Colonic inflammation was assessed by using disease activity index scoring system. Colon weight and length ratios, as well as colon weight to body weight ratios, were calculated from the weight and length of the colon to determine whether or not it was inflamed. The microscopic evaluation was determined by Animals' histopathological score system (inflammatory criteria).

6.2 CONCLUSION

Using this method, polysaccharides can be altered to improve certain aspects of their nature, such as solubility or stability. Additionally, microwave irradiation offers a quick and effective way to produce the desired grafting reactions, speeding up the process and using less energy. In most cases, the properties of microwave graft polysaccharides are better than those of their conventionally

synthesised derivatives. After four hours, there was an increase in BBH release from formulation C5 (coated formulation) as a result of the microspheres being exposed to colonic pH 7.4, which is higher than the pH at which Eudragit S-100 polymer is soluble. This shows that the formulations did not permit drug release into the upper GIT but instead only permitted drug release into the colon. It was anticipated that the C5 microspheres' drug release mechanism would proceed as follows: (a) the Eudragit coating dissolving above pH 7.0; (b) the grafted copolymer was supposed to be swollen; in addition to (c) BBH diffusion from the swollen gel due to the grafted gum. Additionally, the porosity and swelling behaviour of the microspheres may be influenced by the grafted copolymer concentration, which could further affect the rate of drug release. This might be because the medicine needs to traverse a path of more length when the grafted copolymer concentration is high. The finding that animal groups treated with optimized formulations (Groups 8 and 9) found reduced disease activity score, improvements in their body weight which is equivalent to normal rats, and also found enhanced therapeutic activity of drug verified by histological investigation, indicating treated colons with reduced inflammation. The optimised formulation's effectiveness in animal tests supported the *in vitro* release studies. More human research is necessary to demonstrate the efficacy of microspheres in treating IBD.

CHAPTER-7

REFERENCES

1. Dmochowska, N., Wardill, H. R., & Hughes, P. A. (2018). Advances in imaging specific mediators of inflammatory bowel disease. *International journal of molecular sciences*, *19*(9), 2471.

2. Colombel, J. F., Shin, A., & Gibson, P. R. (2019). AGA clinical practice update on functional gastrointestinal symptoms in patients with inflammatory boweldisease: expert review. *Clinical Gastroenterology and Hepatology*, *17*(3), 380- 390.

3. Wehkamp, J., Götz, M., Herrlinger, K., Steurer, W., & Stange, E. F. (2016). Inflammatory bowel disease: Crohn's disease and ulcerative colitis. *Deutsches Ärzteblatt International*, *113*(5), 72.

4. Roda, G., Chien Ng, S., Kotze, P.G., Argollo, M., Panaccione, R., Spinelli, A., Kaser, A., Peyrin-Biroulet, L. and Danese, S. (2020). Crohn's disease. *Nature Reviews Disease Primers*, *6*(1), 22.

5. Su, H. J., Chiu, Y. T., Chiu, C. T., Lin, Y. C., Wang, C. Y., Hsieh, J. Y., & Wei, S.C. (2019). Inflammatory bowel disease and its treatment in 2018: Global and Taiwanese status updates. *Journal of the Formosan Medical Association*, *118*(7),1083-1092.

6. Trivedi, P. J., & Adams, D. H. (2018). Chemokines and chemokine receptors as therapeutic targets in inflammatory bowel disease; pitfalls and promise. *Journal of Crohn's and Colitis*, *12*(suppl_2), S641-S652.

7. Lee, J. S., Kim, E. S., & Moon, W. (2019). Chronological review of endoscopic indices in inflammatory bowel disease. *Clinical endoscopy*, *52*(2), 129-136.

8. Lautenschläger, C., Schmidt, C., Fischer, D., & Stallmach, A. (2014). Drug delivery strategies in the therapy of inflammatory bowel disease. *Advanced drug delivery reviews*, *71*, 58-76.

9. Tiwari, G., Tiwari, R., Wal, P., Wal, A., & Rai, A. K. (2010). Primary and novel approaches for colon targeted drug delivery-A review. *International Journal of DrugDelivery*, *2*(1),1-11

10. Mehta, T. J., Patel, A. D., Patel, M. R., & Patel, N. M. (2011). Need of colon specific drug delivery system: review on primary and novel approaches. *IJPRD*, *3*(1), 134-153.

11. Challa, T., Vynala, V., & Allam, K. V. (2011). Colon specific drug delivery systems: a review on primary and novel approaches. *International Journal of Pharmaceutical Sciences Review and Research*, *7*(2), 171-181.

12. Qureshi, A. M., Momin, M., Rathod, S., Dev, A., & Kute, C. (2013). Colon targeted drug delivery system: A review on current approaches. *Indian Journal of Pharmaceutical and Biological Research*, *1*(04), 130-147.

13. Lautenschläger, C., Schmidt, C., Fischer, D., & Stallmach, A. (2014). Drug delivery strategies in the therapy of inflammatory bowel disease. *Advanced drug delivery reviews*, *71*, 58-76.

14. Philip, A. K., & Philip, B. (2010). Colon targeted drug delivery systems: a review onprimary and novel approaches. *Oman medical journal*, *25*(2), 79.

15. Amidon, S., Brown, J. E., & Dave, V. S. (2015). Colon-targeted oral drug delivery systems: design trends and approaches. *Aaps Pharmscitech*, *16*(4), 731-741.

16. Wahlgren, M., Axenstrand, M., Håkansson, Å., Marefati, A., & Lomstein Pedersen, B. (2019). *In vitro* methods to study colon release: State of the art and an outlook on new strategies for better in-vitro biorelevant release media. *Pharmaceutics*, *11*(2), 95.

17. Amidon, S., Brown, J. E., & Dave, V. S. (2015). Colon-targeted oral drug delivery systems: design trends and approaches. *Aaps Pharmscitech*, *16*(4), 731-741.

18. Anita, Singh, A., & Dabral, A. (2019). A review on colon targeted drug delivery system. *International journal of pharmaceutical sciences and research*, *10*(1), 47-56.

19. Ross and Wilson, "Anatomy and Physiology in Health and Illness", (2010); 11: 1- 512.

20. Wasnik, S., & Parmar, P. (2011). The design of colon-specific drug delivery system and different approaches to treat colon disease. *Int J Pharm Sci Rev Res*, *6*(2), 167- 77.

21. Qureshi, A. M., Momin, M., Rathod, S., Dev, A., & Kute, C. (2013). Colon targeted drug delivery system: A review on current approaches. *Indian J Pharm Biol Res*, *1*(4), 130-47.

22. Koziolek, M., Grimm, M., Becker, D., Iordanov, V., Zou, H., Shimizu, J., Wanke, C., Garbacz, G. & Weitschies, W. (2015). Investigation of pH and temperature profiles in the GI tract of fasted human subjects using the Intellicap® system. *Journal of pharmaceutical sciences*, *104*(9), 2855-2863.

23. Russell, T. L., Berardi, R. R., Barnett, J. L., Dermentzoglou, L. C., Jarvenpaa, K. M., Schmaltz, S. P., & Dressman, J. B. (1993). Upper gastrointestinal pH in seventy-ninehealthy, elderly, North American men and women. *Pharmaceutical research*, *10*, 187-196.

24. Helander, H. F., & Fändriks, L. (2014). Surface area of the digestive tract– revisited. *Scandinavian journal of gastroenterology*, *49*(6), 681-689.

25. Bergström, C. A., Box, K., Holm, R., Matthews, W., McAllister, M., Müllertz, A., Rades, T., Schäfer, K.J. & Teleki, A. (2019). Biorelevant intrinsic dissolution profiling in early drug development: Fundamental, methodological, and industrial aspects. *European journal of pharmaceutics and biopharmaceutics*, *139*, 101-114.

26. Bergström, C. A., Holm, R., Jørgensen, S. A., Andersson, S. B., Artursson, P., Beato, S. & Mullertz, A. (2014). Early pharmaceutical profiling to predict oral drug absorption: current status and unmet needs. *European Journal of Pharmaceutical Sciences*, *57*, 173-199.

27. Pentafragka, C., Symillides, M., McAllister, M., Dressman, J., Vertzoni, M., & Reppas, C. (2019). The impact of food intake on the luminal environment and performance of oral drug products with a view to *in vitro* and in silico simulations: a PEARRL review. *Journal of Pharmacy and Pharmacology*, *71*(4), 557-580.

28. Wahlgren, M., Axenstrand, M., Håkansson, Å., Marefati, A., & Lomstein Pedersen, B. (2019). *In vitro* methods to study colon release: State of the art and an outlook on new strategies for better in-vitro biorelevant release media. *Pharmaceutics*, *11*(2), 95.

29. Anita, Singh, A., & Dabral, A. (2019). A review on colon targeted drug delivery system. *International journal of pharmaceutical sciences and research*, *10*(1), 47-56.

30. Osmani, A. (2015). A review on grafting modification of polysaccharides by microwave irradiation-distinctive practice for application in drug delivery. *Int J CurrPharm Rev Res*, *6*(1), 8-17..

31. Bhardwaj, T. R., Kanwar, M., Lal, R., & Gupta, A. (2000). Natural gums and modified natural gums as sustained-release carriers. *Drug development and industrial pharmacy*, *26*(10), 1025-1038.

32. Sanghi, R., Bhatttacharya, B., & Singh, V. (2002). Cassia angustifolia seed gum as an effective natural coagulant for decolourisation of dye solutions. *Green Chemistry*, *4*(3), 252-254.

33. Sanghi, R., & Bhattacharya, B. (2005). Comparative evaluation of natural polyelectrolytes psyllium and chitosan as coagulant aids for decolourization of dye solutions. *Water Quality Research Journal*, *40*(1), 97-101.

34. Wang, W. B., & Wang, A. Q. (2010). Preparation, swelling and water-retention properties of crosslinked superabsorbent hydrogels based on guar gum. *Advanced Materials Research*, *96*, 177-182.

35. Gupta, S., Sharma, P., & Soni, P. L. (2004). Carboxymethylation of Cassia occidentalis seed gum. *Journal of Applied Polymer Science*, *94*(4), 1606-1611.

36. Edgar, K. J., Buchanan, C. M., Debenham, J. S., Rundquist, P. A., Seiler, B. D., Shelton, M. C., & Tindall, D. (2001). Advances in cellulose ester performance and application. *Progress in polymer science*, *26*(9), 1605-1688.

37. Sand, A., Yadav, M., Mishra, D. K., & Behari, K. (2010). Modification of alginate by grafting of N-vinyl-2-pyrrolidone and studies of physicochemical properties in terms of swelling capacity, metal-ion uptake and flocculation. *Carbohydrate Polymers*, *80*(4), 1147-1154.

38. Ramaprasad, A. T., Rao, V., Sanjeev, G., Ramanani, S. P., & Sabharwal, S. (2009). Grafting of polyaniline onto the radiation crosslinked chitosan. *Synthetic Metals*, *159*(19-20), 1983-1990.

39. Crescenzi, V., Dentini, M., Risica, D., Spadoni, S., Skjåk-Bræk, G., Capitani, D., Mannina, L. & Viel, S. (2004). C (6)-oxidation followed by C (5)-epimerization of guar gum studied by high field NMR. *Biomacromolecules*, *5*(2), 537-546.

40. Galanos, C., Lüderitz, O., & Himmelspach, K. (1969). The partial acid hydrolysis of polysaccharides: a new method for obtaining oligosaccharides in highyield. *European Journal of Biochemistry*, *8*(3), 332-336.

41. Shah, N., Shah, T., & Amin, A. (2011). Polysaccharides: a targeting strategy for colonic drug delivery. *Expert opinion on drug delivery*, *8*(6), 779-796.

42. Sinha, V. R., & Kumria, R. (2001). Polysaccharides in colon-specific drug delivery. *International journal of pharmaceutics*, *224*(1-2), 19-38.

43. Rana, V., Rai, P., Tiwary, A. K., Singh, R. S., Kennedy, J. F., & Knill, C. J. (2011). Modified gums: Approaches and applications in drug delivery. *Carbohydrate polymers*, *83*(3), 1031-1047.

44. Hoogenboom, R., & Schubert, U. S. (2007). Microwave-assisted polymer synthesis: recent developments in a rapidly expanding field of research. *Macromolecular RapidCommunications*, *28*(4), 368-386.

45. Wiesbrock, F., Hoogenboom, R., & Schubert, U. S. (2004). Microwave-assisted polymer synthesis: state-of-the-art and future perspectives. *Macromolecular Rapid Communications*, *25*(20), 1739-1764.

46. Sharma, K., & Ajay Kumar Mishra, A. (2010). Microwave assisted synthesis of chitosan-graft-styrene for efficient Cr (VI) removal. *Advanced Materials Letters*, *1*(1), 59-66.

47. Mahdavinia, G. R., Zohuriaan-Mehr, M. J., & Pourjavadi, A. (2004). Modified chitosan III, superabsorbency, salt- and pH-sensitivity of smart ampholytic hydrogels from chitosan-g-PAN. *Polymers for Advanced Technologies*, *15*(4), 173-180.

48. Tizzotti, M., Charlot, A., Fleury, E., Stenzel, M., & Bernard, J. (2010). Modification of polysaccharides through controlled/living radical polymerization grafting   towards the generation of high performance hybrids. *Macromolecular rapid communications*, *31*(20), 1751-1772.

49. Macchione, M. A., Biglione, C., & Strumia, M. (2018). Design, synthesis and architectures of hybrid nanomaterials for therapy and diagnosis applications. *Polymers*, *10*(5), 527.

50. Zhang, L. M., Tan, Y. B., Huang, S. J., Chen, D. Q., & Li, Z. M. (2000). Water-Soluble Ampholytic Grafted Polysaccharides. 1. Grafting of the Zwitterionic Monomer 2-(2-Methacrylo-Ethyldimethylammonio) Ethanoate onto HydroxyethylCellulose.

51. Maity, N., & Dawn, A. (2020). Conducting polymer grafting: Recent and key developments. *Polymers*, *12*(3), 709.

52. Singh, B., & Sharma, N. (2008). Development of novel hydrogels by functionalization of sterculia gum for use in anti-ulcer drug delivery. *Carbohydrate polymers*, *74*(3), 489-497.

53. Da Silva, D. A., de Paula, R. C., & Feitosa, J. P. (2007). Graft copolymerisation of acrylamide onto cashew gum. *European Polymer Journal*, *43*(6), 2620-2629.

54. Mishra, A., & Pal, S. (2007). Polyacrylonitrile-grafted Okra mucilage: A renewable reservoir to polymeric materials. *Carbohydrate polymers*, *68*(1), 95-100.

55. Mishra, A., & Malhotra, A. V. (2012). Graft copolymers of xyloglucan and methyl methacrylate. *Carbohydrate polymers*, *87*(3), 1899-1904.

56. Chavan, R. R., & Hosamani, K. M. (2018). Microwave-assisted synthesis, computational studies and antibacterial/anti-inflammatory activities of compounds based on coumarin-pyrazole hybrid. *Royal Society open science*, *5*(5), 172435.

57. Galema, S. A. (1997). Microwave chemistry. *Chemical Society Reviews*, *26*(3), 233- 238.

58. Hayward, D. (1999). Apparent equilibrium shifts and hot-spot formation for catalytic reactions induced by microwave dielectric heating. *Chemical Communications*, (11), 975-976.

59. Kappe, C. O. (2004). Controlled microwave heating in modern organic synthesis. *Angewandte Chemie International Edition*, *43*(46), 6250-6284.

60. Grant, E., & Halstead, B. J. (1998). Dielectric parameters relevant to microwave dielectric heating. *Chemical society reviews*, *27*(3), 213-224.

61. Lidström, P., Tierney, J., Watheyb, B., & Westmana, J. (2001). Microwave assisted organic synthesis.Đa review. *Tetrahedron*, *57*, 9225-9283.

62. Michael P áMingos, D. (1991). Tilden Lecture. Applications of microwave dielectric heating effects to synthetic problems in chemistry. *Chemical society reviews*, *20*(1), 1-47.

63. Kharlamova, T. V. (2018).Characteristics of microwaves, some aspects theory of microwave heating and the field of application of microwaves in organic chemistry and chemistry of natural compounds. *Khim Zh Kaz,* 3(63), 37-53.

64. Singh, V., Tiwari, A., Pandey, S., & Singh, S. K. (2007). Peroxydisulfate initiated synthesis of potato starch-graft-poly (acrylonitrile) under microwave irradiation. *Express Polymer Letters*, *1*(1), 51-58.

65. Tiwari, A., & Singh, V. (2008). Microwave-induced synthesis of electrical conducting gum acacia-graft-polyaniline. *Carbohydrate Polymers*, *74*(3), 427-434.

66. Prasad, K., Mehta, G., Meena, R., & Siddhanta, A. K. (2006). Hydrogel-forming agar-graft-PVP and κ-carrageenan-graft-PVP blends: Rapid synthesis and characterization. *Journal of Applied Polymer Science*, *102*(4), 3654-3663.

67. Sen, G., Singh, R. P., & Pal, S. (2010). Microwave-initiated synthesis of polyacrylamide grafted sodium alginate: Synthesis and characterization. *Journal of Applied Polymer Science*, *115*(1), 63-71.

68. Sen, G., & Pal, S. (2009). Microwave initiated synthesis of polyacrylamide grafted carboxymethylstarch (CMS-g-PAM): application as a novel matrix for sustained drug release. *International journal of biological macromolecules*, *45*(1), 48-55.

69. Singh, V., Tiwari, A., Tripathi, D. N., & Sanghi, R. (2004). Microwave assisted synthesis of guar-g-polyacrylamide. *Carbohydrate Polymers*, *58*(1), 1-6.

70. Sosnik, A., Gotelli, G., & Abraham, G. A. (2011). Microwave-assisted polymer synthesis (MAPS) as a tool in biomaterials science: how new and how powerful. *Progress in polymer science*, *36*(8), 1050-1078.

71. Singh, V., Kumar, P., & Sanghi, R. (2012). Use of microwave irradiation in the grafting modification of the polysaccharides–A review. *Progress in polymer science*, *37*(2), 340-364.

72. Singh, I., Rani, P., & Kumar, P. (2017). Microwave assisted grafting of gums and extraction of natural materials. *Mini Reviews in Medicinal Chemistry*, *17*(16), 1573- 1582.

73. Arsalani, N., Zare, P., & Namazi, H. (2009). Solvent free microwave assisted preparation of new telechelic polymers based on poly (ethylene glycol). *Express Polym Lett*, *3*(7), 429-436.

74. Dondi, D., Buttafava, A., Stagnaro, P., Turturro, A., Priola, A., Bracco, S., Galinetto, P. & Faucitano, A. (2009). The radiation-induced grafting of polybutadiene onto silica. *Radiation Physics and Chemistry*, *78*(7-8), 525-530.

75. Thostenson, E. T., & Chou, T. W. (1999). Microwave processing: fundamentals and applications. *Composites Part A: Applied Science and Manufacturing*, *30*(9), 1055- 1071.

76. White, J. B., Hausner, S. H., Carpenter, R. D., & Sutcliffe, J. L. (2012). Optimization of the solid-phase synthesis of [18F] radiolabeled peptides for positron emission tomography. *Applied Radiation and Isotopes*, *70*(12), 2720- 2729.

77. Schanche, J. S. (2003). Microwave synthesis solutions from personal chemistry. *Molecular Diversity*, *7*(2-4), 293.

78. Bharaniraja, B., Jayaram Kumar, K., Prasad, C. M., & Sen, A. K. (2011). Modified katira gum for colon targeted drug delivery. *Journal of Applied Polymer Science*, *119*(5), 2644-2651.

79. Mehra, S., Nisar, S., Chauhan, S., Singh, V., & Rattan, S. (2020). Soy protein-based hydrogel under microwave-induced grafting of acrylic acid and 4-(4-hydroxyphenyl) butanoic acid: a potential vehicle for controlled drug delivery in oral cavity bacterial infections. *ACS omega*, *5*(34), 21610-21622.

80. Shailaja, T., Latha, K., Sasibhushan, P., Alkabab, A. M., & Uhumwangho, M. U. (2012). A novel bioadhesive polymer: grafting of tamarind seed polysaccharide and evaluation of its use in buccal delivery of metoprolol succinate. *Der Pharmacia Lettre*, *4*(2), 487-508.

81. Fu, H., Xie, L., Dou, D., Li, L., Yu, M., & Yao, S. (2007). Storage stability and compatibility of asphalt binder modified by SBS graft copolymer. *Construction and Building Materials*, *21*(7), 1528-1533.

82. Rani, P., Mishra, S., & Sen, G. (2013). Microwave based synthesis of polymethyl methacrylate grafted sodium alginate: its application as flocculant. *Carbohydrate polymers*, *91*(2), 686-692.

83. Xing, J., Deng, L., Li, J., & Dong, A. (2009). Amphiphilic poly [-maleic anhydride- -methoxy-poly (ethylene glycol)]-co-(ethyl cyanoacrylate)} graft copolymer nanoparticles as carriers for transdermal drug delivery. *International Journal of Nanomedicine*, 227-232.

84. Homayun, B., Lin, X., & Choi, H. J. (2019). Challenges and recent progress in oral drug delivery systems for biopharmaceuticals. *Pharmaceutics*, *11*(3), 129.

85. Tiwari, S., & Batra, N. (2014). Oral drug delivery system: a review. *Am. J. Life. Sci. Res*, *2*(1), 27-35.

86. Mandhar, P., & Joshi, G. (2015). Development of sustained release drug delivery system: a review. *Asian Pacific Journal of Health Sciences*, *2*(1), 179-185.

87. Pandey, V., Gadeval, A., Asati, S., Jain, P., Jain, N., Roy, R. K., & Tekade, R. K. (2020). Formulation strategies for nose-to-brain delivery of therapeutic molecules. In *Drug delivery systems* (pp. 291-332). Academic press.

88. Kumar, A. R., & Aeila, A. S. S. (2019). Sustained release matrix type drug delivery system: An overview. *World J Pharma pharm Sci*, *8*(12), 470-80.

89. Begum, S. A., Bhargavi, B., Divya, J., Swetha, K., Zareena, S., Lohitha, S., & Ramya, S. S. (2019). Formulation and *In Vitro* Characterisation Oxcarbazepine Controlled Release Tablets. *Asian Journal of Pharmacy and Technology*, *9*(2).

90. Mishra, S. (2019). Sustained release oral drug delivery system: a concise review. *IntJ Pharm Sci Rev Res*, *54*, 5-15.

91. Nautyal, U., & Gupta, D. (2020). Oral sustained release tablets: an overview with a special emphasis on matrix tablet. *International Journal of Health and Biological Sciences*, *3*(1), 06-13.

92. Bhumarkar, L., & Patil, U. (2019). Colon targeted drug delivery systems: A boon forthe treatment of inflammatory bowel disease. The Pharma Innovation Journal 2019; 8(4): 549-557

93. Alange, V. V., Birajdar, R. P., & Kulkarni, R. V. (2017). Novel spray dried pH-sensitive polyacrylamide-grafted-carboxymethylcellulose sodium copolymer microspheres for colon targeted delivery of an anti-cancer drug. *Journal of Biomaterials science, Polymer edition*, *28*(2), 139-161.

94. Dhadde, G. S., Mali, H. S., Raut, I. D., Nitalikar, M. M., & Bhutkar, M. A. (2021). Areview on microspheres: Types, method of preparation, characterization and application. *Asian Journal of Pharmacy and Technology*, *11*(2), 149-155.

95. Heikal, E. J., Kaoud, R. M., Gad, S., Mokhtar, H. I., Alattar, A., Alshaman, R., & Hammady, T. M. (2023). Development of Novel pH-Sensitive Eudragit Coated Beads Containing Curcumin-Mesalamine Combination for Colon-Specific Drug Delivery. *Gels*, *9*(4), 264.

96. Freiberg, S., & Zhu, X. X. (2004). Polymer microspheres for controlled drug release. *International journal of pharmaceutics*, *282*(1-2), 1-18.

97. Hua, S., Marks, E., Schneider, J. J., & Keely, S. (2015). Advances in oral nano-delivery systems for colon targeted drug delivery in inflammatory bowel disease: selective targeting to diseased versus healthy tissue. *Nanomedicine: nanotechnology,biology and medicine*, *11*(5), 1117-1132.

98. Nikam, V. K., Kotade, K. B., Gaware, V. M., Dolas, R. T., Dhamak, K., Somwanshi, S. & Kashid, V. (2011). Eudragit a versatile polymer: a review. *Pharmacologyonline*, *1*(5), 152-164.

99. Patra, C. N., Priya, R., Swain, S., Jena, G. K., Panigrahi, K. C., & Ghose, D. (2017). Pharmaceutical significance of Eudragit: A review. *Future Journal of Pharmaceutical Sciences*, *3*(1), 33-45.

100. Thakral, S., Thakral, N. K., & Majumdar, D. K. (2013). Eudragit®: a technology evaluation. *Expert opinion on drug delivery*, *10*(1), 131-149.

101. Battu, S. K., Repka, M. A., Maddineni, S., Chittiboyina, A. G., Avery, M. A., & Majumdar, S. (2010). Physicochemical characterization of berberine chloride: a perspective in the development of a solution dosage form for oral delivery. *Aaps Pharmscitech*, *11*(3), 1466-1475.

102. Zhu, J. X., Tang, D., Feng, L., Zheng, Z. G., Wang, R. S., Wu, A. G., Duan, T.T., He, B. & Zhu,Q. (2013). Development of self-microemulsifying drug delivery system for oral bioavailability enhancement of berberine hydrochloride. *Drug Development and Industrial Pharmacy*, *39*(3), 499-506.

103. Tan, W., Li, Y., Chen, M., & Wang, Y. (2011). Berberine hydrochloride: anticancer activity and nanoparticulate delivery system. *International journal of nanomedicine*, 1773-1777.

104. Jia, L., Xue, K., Liu, J., Habotta, O. A., Hu, L., & Moneim, A. E. A. (2020). Anticolitic effect of berberine in rat experimental model: impact of PGE2/p38 MAPK pathways. *Mediators of Inflammation*, *2020*.1-12.

105. Zhang, L. C., Wang, Y., Tong, L. C., Sun, S., Liu, W. Y., Zhang, S., Wang, R.M., Wang, Z.B., & Li, L.(2017). Berberine alleviates dextran sodium sulfate-induced colitis by improving intestinal barrier function and reducing inflammation and oxidative stress. *Experimental and Therapeutic Medicine*, *13*(6), 3374-3382.

106. Li, H., Fan, C., Lu, H., Feng, C., He, P., Yang, X., Xiang, C., Zuo, J., & Tang, W. (2020). Protective role of berberine on ulcerative colitis through modulating enteric glial cells–intestinal epithelial cells–immune cells interactions. *Acta Pharmaceutica Sinica B*, *10*(3), 447-461.

107. Zhang, X., Zhao, Y., Zhang, M., Pang, X., Xu, J., Kang, C. & Zhao, L. (2012). Structural changes of gut microbiota during berberine-mediated prevention of obesity and insulin resistance in high-fat diet-fed rats.

108. Yan, F., Wang, L., Shi, Y., Cao, H., Liu, L., Washington, M. K. & Polk, D. B. (2012). Berberine promotes recovery of colitis and inhibits inflammatory responses in colonic macrophages and epithelial cells in DSS-treated mice. *American Journal of Physiology-Gastrointestinal and Liver Physiology*, *302*(5), G504-G514.

109. Wang, X., Feng, S., Ding, N., He, Y., Li, C., Li, M. & Li, Y. (2018). Anti-inflammatory effects of berberine hydrochloride in an LPS-induced murine model of mastitis. *Evidence-Based Complementary and Alternative Medicine*, *2018*.

110. Zhang, Y., Li, X., Zhang, Q., Li, J., Ju, J., Du, N., & Yang, B. (2014). Berberine hydrochloride prevents postsurgery intestinal adhesion and inflammation in rats. *Journal of Pharmacology and Experimental Therapeutics*, *349*(3), 417-426.

111. Cheng, X. X., Lui, Y., Hu, Y. J., Liu, Y., Li, L. W., Di, Y. Y., & Xiao, X. H. (2013). Thermal behavior and thermodynamic properties of berberine hydrochloride. *Journal of thermal analysis and calorimetry*, *114*, 1401-1407.

112. Bhardwaj, T. R., Kanwar, M., Lal, R., & Gupta, A. (2000). Natural gums and modified natural gums as sustained-release carriers. *Drug development and industrial pharmacy*, *26*(10), 1025-1038.

113. Mudgil, D., Barak, S., & Khatkar, B. S. (2014). Guar gum: processing, properties and food applications- a review. *Journal of food science and technology*, *51*, 409- 418.

114. Kolling, W. M. (2004). Handbook of pharmaceutical excipients. *American Journal of Pharmaceutical Education*, *68*(1-5), BF1.

115. Varma, V. N. S. K., Shivakumar, H. G., Balamuralidhara, V., Navya, M., & Hani, U. (2016). Development of pH sensitive nanoparticles for intestinal drug delivery using chemically modified guar gum Co-polymer. *Iranian Journal of Pharmaceutical Research: IJPR*, *15*(1), 83.

116. Friedman, M. (2003). Chemistry, biochemistry, and safety of acrylamide. A review. Journal of agricultural and food chemistry, 51(16), 4504-4526.

117. https://pubchem.ncbi.nlm.nih.gov/compound/Acrylamide assessed on dated 22-06-2023.

118. Lande, S. S., Bosch, S. J., Howard, P. H. (1979). Degradation and leaching of acrylamide in soil. J Environ Qual, 8(1), 133-137.

119. Smith, E. A., & Oehme, F. W. (1991). Acrylamide and polyacrylamide: a review of production, use, environmental fate and neurotoxicity. *Reviews on environmental health*, *9*(4), 215-228.

120. Nandi, G., Changder, A., & Ghosh, L. K. (2019). Graft-copolymer of polyacrylamide-tamarind seed gum: Synthesis, characterization and evaluation of flocculating potential in peroral paracetamol suspension. *Carbohydrate polymers*, *215*, 213-225.

121. Dan, S., Mandal, P., Bose, A., & Pal, T. K. (2018). Microwave Assisted Acrylamide Grafting on a Natural Gum Cassia Tora: Characterization and Pharmacokinetic Evaluation of the Formulation Containing Metformin and Sitagliptin in Rats by LC-MS/MS. *Analytical Chemistry Letters*, *8*(5), 622-641.

122. Singh, I., Rani, P., Sareen, G., & Kaur, S. (2018). Microwave assisted synthesis ofacrylamide grafted locust bean gum for colon specific drug delivery. *Current Microwave Chemistry*, *5*(1), 46-53.

123. Eswaramma, S., & Rao, K. K. (2017). Synthesis of dual responsive carbohydrate polymer based IPN microbeads for controlled release of anti-HIV drug. *Carbohydrate Polymers*, *156*, 125-134.

124. Bardajee, G. R., Azimi, S., & Sharifi, M. B. A. S. (2017). Application of central composite design for methyl red dispersive solid phase extraction based on silver nanocomposite hydrogel: Microwave assisted synthesis. *MicrochemicalJournal*, *133*, 358-369.

125. Shruthi, S. B., Bhat, C., Bhaskar, S. P., Preethi, G., & Sailaja, R. R. N. (2016). Microwave assisted synthesis of guar gum grafted acrylic acid/nanoclay superabsorbent composites and its use in crystal violet dye absorption. *Green and sustainable chemistry*, *6*(01), 11.

126. Badwaik, H. R., Sakure, K., Alexander, A., Dhongade, H., & Tripathi, D. K. (2016). Synthesis and characterisation of poly (acryalamide) grafted carboxymethyl xanthan gum copolymer. *International journal of biological macromolecules*, *85*, 361-369.

127. Sirajo, A. Z., & Vishalakshi, B. (2016). Microwave assisted synthesis of poly (diallyldimethylammonium chloride) grafted locust bean gum: Swelling and dye adsorption studies. *Indian J. Adv. Chem. Sci. S*, *1*, 88-91.

128. Setia, A., & Kumar, R. (2014). Microwave assisted synthesis and optimization of Aegle marmelos-g-poly (acrylamide): release kinetics studies. *International journal of biological macromolecules*, *65*, 462-470.

129. Kaity, S., Isaac, J., Kumar, P. M., Bose, A., Wong, T. W., & Ghosh, A. (2013). Microwave assisted synthesis of acrylamide grafted locust bean gum and its application in drug delivery. *Carbohydrate polymers*, *98*(1), 1083-1094.

130. Alvarez-Lorenzo, C., Blanco-Fernandez, B., Puga, A. M., & Concheiro, A. (2013). Crosslinked ionic polysaccharides for stimuli-sensitive drug delivery. *Advanced drug delivery reviews*, *65*(9), 1148-1171.

131. Vijan, V., Kaity, S., Biswas, S., Isaac, J., & Ghosh, A. (2012). Microwave assisted synthesis and characterization of acrylamide grafted gellan, application in drug delivery. *Carbohydrate polymers*, *90*(1), 496-506.

132. Ali, H., Weigmann, B., Neurath, M. F., Collnot, E. M., Windbergs, M., & Lehr, C. M. (2014). Budesonide loaded nanoparticles with pH-sensitive coating for improved mucosal targeting in mouse models of inflammatory bowel diseases. *Journal of Controlled Release*, *183*, 167-177.

133. Patel, J., & Gupta, R. A. (2021). Development and In-Vitro Evaluation of Budesonide Mucoadhesive Microsphere for Pulmonary Drug Delivery. *Journal of Drug Delivery and Therapeutics*, *11*(2-S), 76-81

134. Andremont, A., & Huguet, H. (2008). *U.S. Patent Application No. 11/985,465*.

135. Wu, F., Ju, X. J., He, X. H., Jiang, M. Y., Wang, W., Liu, Z., Xie, R., He, B. & Chu, L. Y. (2016). A novel synthetic microfiber with controllable size for cell encapsulation and culture. *Journal of Materials Chemistry B*, *4*(14), 2455-2465.

136. Liu, Y., & Zhou, H. (2015). Budesonide-loaded guar gum microspheres for colon delivery: preparation, characterization and *in vitro/in vivo* evaluation. *International Journal of Molecular Sciences*, *16*(2), 2693-2704.

137. Sandborn, W. J., & Rhodes, J. (1998). *U.S. Patent No. 5,846,983*. Washington, DC: U.S. Patent and Trademark Office.

138. Jeganath, S., & Senthilkumaran, K. (2014). Formulation development and *in vitro* evaluation of pulsatile release tablet of budesonide. *World Journal of Pharmaceutical Research*, *4*(1), 1197-1208.

139. Pandey, N., Sah, N. A., & Mahara, K. (2016). Formulation and evaluation of floating microspheres of nateglinide. *International Journal of Pharma Sciences and Research*, *7*(11), 453-464.

140. Owusu, G., Obiri, D. D., Ainooson, G. K., Osafo, N., Antwi, A. O., Duduyemi, B. M., & Ansah, C. (2020). Acetic acid-induced ulcerative colitis in Sprague Dawley rats is suppressed by hydroethanolic extract of Cordia vignei leaves through reduced serum levels of TNF- and IL-6. *International journal of chronic diseases*, *2020*.

141. Shalkami, A. S., Hassan, M. I. A., & Bakr, A. G. (2018). Anti-inflammatory, antioxidant and anti-apoptotic activity of diosmin in acetic acid-induced ulcerative colitis. *Human & experimental toxicology*, *37*(1), 78-86.

142. Adakudugu, E. A., Ameyaw, E. O., Obese, E., Biney, R. P., Henneh, I. T., Aidoo, D. B. & Obiri, D. D. (2020). Protective effect of bergapten in acetic acid-induced colitis in rats. *Heliyon*, *6*(8).

143. Thippeswamy, B. S., Mahendran, S., Biradar, M. I., Raj, P., Srivastava, K., Badami, S., & Veerapur, V. P. (2011). Protective effect of embelin against acetic acid induced ulcerative colitis in rats. *European journal of pharmacology*, *654*(1), 100-105.

144. Rahman, Z., Kohli, K., Zhang, S. Q., Khar, R. K., Ali, M., Charoo, N. A. & Renka, M. A. (2008). In-vivo evaluation in rats of colon-specific microspheres containing 5-fluorouracil. *Journal of Pharmacy and Pharmacology*, 60(3), 615-623.

145. Ali, J., Khar, R. K., & Ahuja, A. (2008). Dosage form and design. *CBS Publishersand Distributers. Delhi*, *1*, 2004-05.

146. Pandey, A., Rath, B., & Dwivedi, A. K. (2012). Pharmaceutical preformulation studies with special emphasis on excipients compatibility. *ChemInform*, *43*(23), 20- 25.

147. Indian Pharmacopoeia Volume III. (2010).Published by Indian Pharmacopoeia Commission, Ghaziabad, 2495-2497.

148. Canbay, H. S., & Do ant rk, M. (2018). Application of differential scanning calorimetry and Fourier transform infrared spectroscopy to the study of metoprolol- excipient and lisinopril-excipient compatibility. Eurasian J Anal Chem, 13(5), 39.

149. Meira, R. Z., Biscaia, I. F., Nogueira, C., Murakami, F. S., Bernardi, L. S., & Oliveira, P. R. (2019). Solid-state characterization and compatibility studies of penciclovir, lysine hydrochloride, and pharmaceutical excipients. Materials, 12(19), 3154.

150. Srinivas, L., Tenneti, V. V. K., & Rajasri, A. (2015). Preparation and evaluation of liposome formulations for poorly soluble drug itraconazole by complexation. Der Pharmacia Lettre, 7(8), 1-17.

151. Rani, T. N., Muzeeb, Y. I., Rani, P. S., & Pradesh, A. (2013). Solubility Enhancement of Poorly Soluble Drug Ezetimibe By Solid Dispersion Technique. J. Adv. Pharm. Educ. Res, 4, 75-81.

152. Pobudkowska, A., & Doma ska, U. (2014). Study of pH-dependent drugs solubility in water. Chemical Industry and Chemical Engineering Quarterly, 20(1), 115-126.

153. Battu, S. K., Repka, M. A., Maddineni, S., Chittiboyina, A. G., Avery, M. A., & Majumdar, S. (2010). Physicochemical Characterization of Berberine Chloride: A Perspective in the Development of a Solution Dosage Form for Oral Delivery. AAPSPharm Sci Tech.;11(3): 1466–1475.

154. Du, G. H., Yan, Y., Fang, L. H., & Du, G. H. (2018). Andrographolide. *Natural Small Molecule Drugs from Plants*, 357-362.

155. Mehta, A. (2013). Ultraviolet--visible (uv--vis) spectroscopy--woodward--fieser rules to calculate wavelength of maximum absorption (lambda--max) of polyenes. *Postet on May*, *13*.

156. Xia, X. R., Baynes, R. E., Monteiro-Riviere, N. A., & Riviere, J. E. (2005). Determination of the partition coefficients and absorption kinetic parameters of chemicals in a lipophilic membrane/water system by using a membrane-coated fiber technique. *European journal of pharmaceutical sciences*, *24*(1), 15-23.

157. Kesharwani, R., Ansari, M. S., & Patel, D. K. (2017). Novel technology used in the preformulation study: A review. *Journal of Drug Delivery and Therapeutics*, *7*(4), 20-33.

158. Pavia D.C., Lampman, G.M. Kriz, G.S. Vivian, J.R. (2009).Spectroscopy, 2nd edition, Cengage learning India Pvt. Ltd. New Delhi, 37-40.

159. Gupta, K. R., Pounikar, A. R., & Umekar, M. J. (2019). Drug excipient compatibility testing protocols and charaterization: a review. *Asian Journal of Chemical Sciences*, *6*(3), 1-22.

160. Sen, G., Mishra, S., Rani, G. U., Rani, P. & Prasad, R. (2012). Microwave initiated synthesis of polyacrylamide grafted Psyllium and its application as a flocculant. *International Journal of Biological Macromolecules*, *50*(2), 369-375.

161. Malik, S., & Ahuja, M. (2011). Gum kondagogu-g-poly (acrylamide): Microwave-assisted synthesis, characterisation and release behaviour. *Carbohydrate polymers*, *86*(1), 177-184.

162. Biswal, J., Kumar, V., Bhardwaj, Y. K., Goel, N. K., Dubey, K. A., Chaudhari, C. V. & Sabharwal, S. (2007). Radiation-induced grafting of acrylamide onto guar gumin aqueous medium: Synthesis and characterization of grafted polymer guar-g- acrylamide. *Radiation Physics and Chemistry*, *76*(10), 1624-1630.

163. Xie, W., Xu, P., Wang, W., & Liu, Q. (2002). Preparation and antibacterial activity of a water-soluble chitosan derivative. *Carbohydrate polymers*, *50*(1), 35-40.

164. Singh, V., Kumar, P., & Sanghi, R. (2012). Use of microwave irradiation in the grafting modification of the polysaccharides–A review. *Progress in polymer science*, *37*(2), 340-364.

165. Malviya, R., Sharma, P. K., & Dubey, S. K. (2016). Modification of polysaccharides: Pharmaceutical and tissue engineering applications with commercial utility (patents). *Materials Science and Engineering: C*, *68*, 929-938.

166. Kaity, S., Isaac, J., Kumar, P. M., Bose, A., Wong, T. W., & Ghosh, A. (2013). Microwave assisted synthesis of acrylamide grafted locust bean gum and its application in drug delivery. *Carbohydrate polymers*, *98*(1), 1083-1094.

167. Kaur, J., Kaith, B. S., Jindal, R. (2013).Evaluation of Physio-chemical and Thermal properties of Soy Protein Concentrate and Different Binary Mixtures Based Graft Copolymers. Int J Sci Engg Res, 4(10), 573-579.

168. Vijan, V., Kaity, S., Biswas, S., Isaac, J., & Ghosh, A. (2012). Microwave assisted synthesis and characterization of acrylamide grafted gellan, application in drug delivery. *Carbohydrate polymers*, *90*(1), 496-506.

169. Sullad, A. G., Manjeshwar, L. S., & Aminabhavi, T. M. (2010). Novel pH-sensitive hydrogels prepared from the blends of poly (vinyl alcohol) with acrylic acid-graft-guar gum matrixes for isoniazid delivery. *Industrial & Engineering Chemistry Research*, *49*(16), 7323-7329.

170. Sareen, R., Jain, N., Rajkumari, A., & Dhar, K. L. (2016). pH triggered delivery of curcumin from Eudragit-coated chitosan microspheres for inflammatory bowel disease: characterization and pharmacodynamic evaluation. *Drug Delivery*, *23*(1), 55-62.

171. Kemala, T., Budianto, E., & Soegiyono, B. (2012). Preparation and characterization of microspheres based on blend of poly (lactic acid) and poly (-caprolactone) with poly (vinyl alcohol) as emulsifier. *Arabian Journal of Chemistry*, *5*(1), 103-108.

172. Martin, A. (1993). Physical pharmacy. *Physical chemical principles in the pharmaceutical sciences*, 126-127.

173. Purushotham Rao, K., & PATIL, C. (2005). Colon specific delivery of naproxen through guar gum matrices. *The Indian pharmacist*, *4*(33), 70-72.

174. Martin, A. N., Sinko, P. J., & Singh, Y. (2006). Martin's physical pharmacy and pharmaceutical sciences: physical chemical and biopharmaceutical principles in the pharmaceutical sciences. *(No Title)*.

175. Yadav, P. S., Kumar, V., Singh, U. P., Bhat, H. R., & Mazumder, B. (2013). Physicochemical characterization and in vitro dissolution studies of solid dispersions of ketoprofen with PVP K30 and d-mannitol. *Saudi Pharmaceutical Journal*, *21*(1), 77-84.

176. Thakral, N. K., Ray, A. R., & Majumdar, D. K. (2010). Eudragit S-100 entrapped chitosan microspheres of valdecoxib for colon cancer. *Journal of Materials Science: Materials in Medicine*, *21*(9), 2691-2699.

177. Paharia, A., Yadav, A. K., Rai, G., Jain, S. K., Pancholi, S. S., & Agrawal, G. P. (2007). Eudragit-coated pectin microspheres of 5-fluorouracil for colon targeting. *Aaps Pharmscitech*, *8*(1), E87-E93

178. Rai, G., Yadav, A. K., Jain, N. K., & Agrawal, G. P. (2016). Eudragit-coated dextran microspheres of 5-fluorouracil for site-specific delivery to colon. *Drug delivery*, *23*(1), 328-337.

179. Nath, B., Nath, L. K., & Kumar, P. (2011). Preparation and *in vitro* dissolution profile of zidovudine loaded microspheres made of Eudragit RS 100, RL 100 and their combinations. *Acta Pol Pharm*, *68*(3), 409-415.

180. Dash, S., Murthy, P. N., Nath, L., & Chowdhury, P. (2010). Kinetic modeling on drug release from controlled drug delivery systems. *Acta Pol Pharm*, *67*(3), 217-223.

181. Rignall, A. (2017). ICHQ1A (R2) stability testing of new drug substance and product and ICHQ1C stability testing of new dosage forms. *ICH quality guidelines: an implementation guide*, 3-44.

182. Singh, A. V., & Nath, L. K. (2013). Evaluation of microwave assisted grafted sago starch as controlled release polymeric carrier. *International journal of biological macromolecules*, *60*, 62-68.

183. De, B., Bhandari, K., Katakam, P., Adiki, S. K., & Mitra, A. (2017). Developmentof an antidiabetic phytocomposite loaded phytoceutical formulation, its quality control and pharmacokinetic studies and establishing *in vitro-in vivo*

correlation. *IntJ Drug Deliv Technol*, *7*(1), 1-12.

184. Yuan, W., Feng, Y., Chen, D., Gharibani, P., Chen, J. D., Yu, H., & Li, X. (2022).*In vivo* assessment of inflammatory bowel disease in rats with ultrahigh-resolution colonoscopic OCT. *Biomedical optics express*, *13*(4), 2091-2102.

185. Qelliny, M. R., Aly, U. F., Elgarhy, O. H., & Khaled, K. A. (2019). Budesonide- loaded Eudragit S 100 nanocapsules for the treatment of acetic acid-induced colitis in animal model. *AAPS PharmSciTech*, *20*(6), 1-17.

186. Owusu, G., Obiri, D. D., Ainooson, G. K., Osafo, N., Antwi, A. O., Duduyemi, B.M., & Ansah, C. (2020). Acetic acid-induced ulcerative colitis in Sprague Dawley rats is suppressed by hydroethanolic extract of Cordia vignei leaves through reduced serum levels of TNF- and IL-6. *International journal of chronic diseases*, *2020*.

187. Badhana, S., Garud, N., & Garud, A. (2013). Colon specific drug delivery of mesalamine using eudragit S100-coated chitosan microspheres for the treatment of ulcerative colitis. *International Current Pharmaceutical Journal*, *2*(3), 42-48.

188. El-Bary, A. A., Aboelwafa, A. A., & Al Sharabi, I. M. (2012). Influence of some formulation variables on the optimization of pH-dependent, colon-targeted, sustained-release mesalamine microspheres. *AAPS PharmSciTech*, *13*(1), 75-84.

189. Shalkami, A. S., Hassan, M. I. A., & Bakr, A. G. (2018). Anti-inflammatory, antioxidant and anti-apoptotic activity of diosmin in aceti c acid-induced ulcerative colitis. *Human & experimental toxicology, 37*(1), 78-86.

190. Varshosaz, J., Emami, J., Fassihi, A., Tavakoli, N., Minaiyan, M., Ahmadi, F., & Dorkoosh, F. (2010). Effectiveness of budesonide-succinate-dextran conjugate as a novel prodrug of budesonide against acetic acid-induced colitis in rats. *International journal of colorectal disease*, *25*, 1159-1165.

191. Beloqui, A., Coco, R., Alhouayek, M., Solinís, M. Á., Rodríguez-Gascón, A., Muccioli, G. G., & Préat, V. (2013). Budesonide-loaded nanostructured lipid carriersreduce inflammation in murine DSS-induced colitis. *International journal of pharmaceutics*, *454*(2), 775-783.

192. Aslan, A., Temiz, M., Atik, E., Polat, G., Sahinler, N., Besirov, E., & Parsak, C. K. (2007). Effectiveness of mesalamine and propolis in experimental colitis. *Advances in therapy*, *24*, 1085-1097.

193. Gorgulu, S., Yagci, G., Kaymakcioglu, N., Özkara, M., Kurt, B., Ozcan, A., Kaya, O., Sadir, S. & Tufan, T. (2006). Hyperbaric oxygen enhances the efficiency of 5- aminosalicylic acid in acetic acid–induced colitis in rats. *Digestive diseases and sciences*, *51*, 480- 487.

194. Mohanta, S., Singh, S. K., Kumar, B., Gulati, M., Kumar, R., Yadav, A. K., & Pandey, N. K. (2019). Efficacy of co-administration of modified apple polysaccharide and probiotics in guar gum-Eudragit S100 based mesalamine mini tablets: A novel approach in treating ulcerative colitis. *International journal ofbiological macromolecules*, *126*, 427-435.

195. Dai, C., Zheng, C. Q., Meng, F. J., Zhou, Z., Sang, L. X., & Jiang, M. (2013). VSL3 probiotics exerts the anti-inflammatory activity via PI3k/Akt and NF- B pathway in rat model of DSS-induced colitis. *Molecular and cellular biochemistry*, *374*, 1-11.

196. Yue, G., Sun, F. F., Dunn, C., Yin, K., & Wong, P. Y. (1996). The 21-aminosteroid tirilazad mesylate can ameliorate inflammatory bowel disease in rats. *Journal of Pharmacology and Experimental Therapeutics*, *276*(1), 265-270.

197. Thiesen, A., Wild, G. E., Tappenden, K. A., Drozdowski, L., Keelan, M., Thomson, B. K. A. & Thomson, A. B. R. (2003). The locally acting glucocorticosteroid budesonide enhances intestinal sugar uptake following intestinal resection in rats. *Gut*, *52*(2), 252-259.

LIST OF PAPER PUBLICATION/PRESENTATION

Sr. No	Title of the paper/Conferencewith author names	Name of the journal/ institution	Published/ presented Date	ISSN No./ volume no, issue no
1	Guar Gum-g-Poly (Acrylamide):Microwave-Assisted Synthesis& Characterization	AIP conference proceeding	2023	0094243X, 1551 7616 2800(1)
2	Optimization and characterization of microspheres of Berberine Hydrochloride by using Box-Behnken Design	International journal of applied pharmaceutics	2023	Published
3.	International Conference on "Materials for Emerging Technologies" (ICMET-21)	Lovely professional university, Punjab	February 18-19, 2022	Paper presented
4	Two day 3RD International conference on "functional material manufacturing and performance" ICFMMP-22	Lovely professional university, Punjab	29-30 July 2022	Paper presented
5	3rd international conference on"Practice publication and promotion of innovation" ICP-2022	Lovely professional university ,Punjab	9-10 November 2022	Paper presented
6	Two days International Conference on "Recent Advances in Basic and AppliedSciences" ICRABAS-21	Baba Mastnath University, Asthal Bohar (Rohtak),	27th-28th August, 2021.	Poster presented
7	World Nano congress on advanced science and technology (WNCST-21)	Vellore institute of technology, Vellore	8-13 march 2021	Paper presented
8.	One day conference on artificialintelligence the new era in pharmaceutical sciences ASPERCON-2019	Abhilashi university Mandi(HP)	13April 2019	Participation

LIST OF WORKSHOPS ATTENDED

S. No	Title of Conference/workshop attended	Name of the institution	Date
1	Workshop on animal experimental models and ethics in preclinical research	Lovely professional university ,Punjab	July 6,2019
2	Workshop on Molecular Spectroscopy and Thermal Analysis for Innovation and Industrial Applications organized by PerkinElmer-LPU	Lovely professional university ,Punjab	27th November to 1st December 2020
3	Importance of Particle Characterization and Zeta Potential in Pharmaceutical	Lovely Professional University, Punjab	July 22, 2021
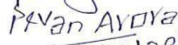
CERTIFICATE FOR APPROVAL BY IAEC

Name of student: **Gautam Kumar**

Certificate

This is to certify that the project proposal no. **01** entitled "**Solid dosages for** **evaluation of Berberine hydrochloride for colon delivery**" submitted by Kumar has been approved/recommended by the IAEC of **Lord Shiva Colleg** Sirsa in its meeting dated **27-12-2022** and has been sanctioned **54** (animals) und for a duration of next **6 months** (from the date of procurement).

Authorized by	Signature	Date
Chairman:		27/12/22
Member Secretary:		27/12/2L
Main Nominee of CPCSEA:	Pavan Arora	27/12/2022

(Kindly make sure that minutes of the meeting duly signed by all the parti maintained by Office)

PAPER PRESENTATION

3ICP2022ORAL PRESENTATION 33
Serial No. _____

Certificate of Participation

This is to certify that Prof./Dr./Mr./Ms. **Gautam Kumar** _____ has successfully participated as Delegate & Presented Poster/ Oral Presentation on **FORMULATION AND EVALUATION OF FAST DISSOLVING TABLETS OF AMOXICILLIN TRIHYDRATE USING NATURAL SUPERDISINTEGRANTS** in the 3rd International Conference of Pharmacy (ICP-2022) on the Theme of "Practice, Promotion & Publication of Innovation : A Way of Transforming Health" held on 09th & 10th November 2022 organized by School of Pharmaceutical Sciences in a collaboration with Indian Pharmaceutical Association (IPA) at Lovely Professional University, Punjab.

Mr. Suresh Khanna
National Hon. Gen. Secretary, IPA

Dr. Bimlesh Kumar
Organizing Secretary

Dr. T.V. Naryana
National President IPA

Dr. Monica Gulati
LOC Chairperson

Sri Herbasia Biotech | Tishk International University, Iraq

Certificate No.253391

Certificate of Presentation
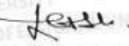
This is to certify that **Dr./Mr./Ms. Gautam Kumar** of School of Pharmaceutical Sciences, Lovely Professional University, Phagwara has presented a paper on **Gum Linum usitatissimum-g-poly (acrylamide): Microwave-assisted synthesis, characterization and release behaviour** in the **"3rd International Conference on Functional Materials, Manufacturing and Performances (ICFMMP-2022)"** held on July29-30th, 2022, organized by **Division of Research and Development, Lovely Professional University, Punjab.**

Date of Issue: 30-08-2022
Place: Phagwara (Punjab), India

Prepared by
(Administrative Officer-Records)

Dr. Hitesh Vasudev
Convenor

Dr. Pranav Kumar Prabhakar
Organizing Secretary

Dr. Chander Prakash
Conference Secretary

PAPER PRESENTATION

INTERNATIONAL CONFERENCE

Unique ID_ICR- 3281

ON
"RECENT ADVANCES IN BASIC AND APPLIED SCIENCES"
(ICRABAS-2021)

Celebrating
Azadi Ka
Amrit Mahotsav

Organized by

FACULTY OF SCIENCES, BABA MASTNATH UNIVERSITY, ROHTAK
In Association with Internal Quality Assurance Cell (IQAC)
On
27th-28th August, 2021

CERTIFICATE

This is to certify that Mr./Ms./Dr./Prof. **Gautam Kumar** of **Department of Chemistry/Pharmacy, Lovely Professional University Jalandhar (Punjab)** has presented **Poster** entitled **"Formulation and Evaluation of Floating Matrix Tablets of Tramadol Hydrochloride"** at the **International Conference on "Recent Advances in Basic and Applied Sciences"** held at Faculty of Sciences, Baba Mastnath University, Asthal Bohar (Rohtak), on 27th-28th August, 2021.

Dr. Manoj Antil
Convener
ICRABAS-2021

Dr. Praveen Bhatt
Organizing Secretary
ICRABAS-2021

Dr. Manoj Kumar
Dean
FACULTY OF SCIENCES

DIVISION OF RESEARCH AND DEVELOPMENT

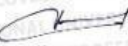[Under the Aegis of Lovely Professional University, Jalandhar-Delhi G.T. Road, Phagwara (Punjab)]

Certificate No.240300

Certificate of Participation

This is to certify that **Mr. Gautam Kumar** of **Lovely Professional University, Phagwara, Punjab, India** has presented paper on **Guar Gum-g-poly (acrylamide): Microwave-assisted synthesis & characterization** in the **International Conference on Materials for Emerging Technologies (ICMET-21)** held on February 18-19, 2022, organized by Department of Research Impact and Outcome, Division of Research and Development, Lovely Professional University, Punjab.

Date of Issue: 16-03-2022
Place: Phagwara (Punjab), India
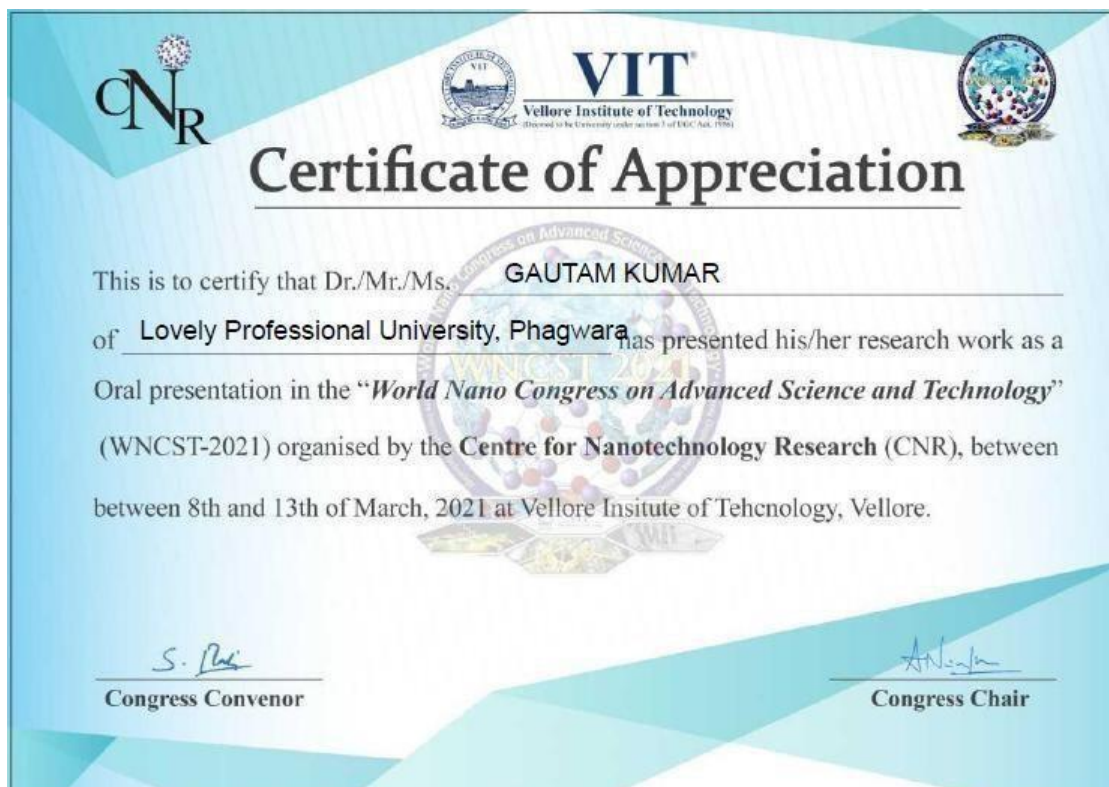
Prepared by
(Administrative Officer-Records)

Dr. Vipul Srivastava
Convener
(ICMET-21)

Dr. Manish Vyas
Organizing Secretary
(ICMET-21)

Dr. Chander Prakash
Co-Chairperson
(ICMET-21)

PAPER PRESENTATION

Appendix-7

PAPER PUBLISHED

(International Journal of Applied Pharmaceutics)

OPTIMIZATION AND CHARACTERIZATION OF MICROSPHERES OF BERBERINE HYDROCHLORIDE USING BOX-BEHNKEN DESIGN

GAUTAM KUMAR[1,3], NARENDRA KUMAR PANDEY[1*] , VIJAY MISHRA[1] , SURAJ PAL VERMA[2] , JITENDER SINGH[3], BIMLESH KUMAR[1] , SACHIN KUMAR SINGH[1] , DILEEP SINGH BAGHEL[1] , KALVATALA SUDHAKAR[1] , SAURABH SINGH[1]

[1]School of Pharmaceutical Sciences, Lovely Professional University, Punjab-144411, India. [2]School of Pharmaceutical Sciences, Delhi Pharmaceutical Sciences and Research University, Delhi, India. [3]Lord Shiva College of Pharmacy, Sirsa-125055, Haryana, India
*Corresponding author: Narendra Kumar Pandey; *Email: herenarendra4u@gmail.com

ABSTRACT

Objective: The current work sought to optimize Berberine hydrochloride (BBH)-loaded microspheres by examining the link between design parameters and experimental results.

Methods: BBH-loaded microspheres were prepared by using the water-in-oil emulsion cross-linking process and optimized with a three-factor, three-level Box-Behnken design (BBD). Grafted gum polyvinyl alcohol (PVA) ratio (w/w) (A), Revolutions per minute (RPM) (B), and Span 20 (%) (C) were independent variables. The dependent variables were Percent Entrapment Efficiency (% EE) (R1), Percent Drug Loading (% DL) (R2), and Particle Size (μm) (R3). The generated polynomial equations and response surface plots were used to relate the dependent and independent variables. Microscopic examination, %EE, and % DL were determined to evaluate the optimized formulation. Fourier transforms infrared (FT-IR) spectroscopy studies and stability studies of optimized formulation were also carried out.

Results: The optimized formulation (FMS6) had a polymer content of 2% w/v [Grafted gum (36.96): PVA (63.04)], a span 20 (0.78 %), and a prepared at the speed of 1225.92 rpm. The observed responses were close to the improved formulation's predicted values. The particle size, % EE, and % DL were found to be 1.10 μm, 82.79% and 16.48%, respectively. FT-IR spectroscopy study indicated that the drug was entrapped in microspheres.

Conclusion: BBD provides a systematic approach to optimize the BBH microsphere preparation process. Additionally, the stability study results confirmed that FMS6 is not only the ideal formulation but also stable, ensuring its suitability for practical applications.

Keywords: Box-behnken design, Water in oil emulsion cross-linking method, Berberine HCl, Microspheres

PAPER PUBLISHED
(AIP CONFERENCEPROCEEDING)

Guar Gum-g-Poly (Acrylamide): Microwave-Assisted Synthesis and Characterization

Gautam Kumar[1,2,a)], Narendra Kumar Pandey[1,b)], Suraj Pal Verma[3,c)], Gazzal Mehta[2,d)], Jitender Singh[2,e)]

[1]School of Pharmaceutical Sciences, Lovely Professional University, Jalandhar (Punjab), India-144411
[2]Lord Shiva College of Pharmacy, Sirsa, Haryana, India-125055
[3]School of Pharmaceutical Sciences, Delhi Pharmaceutical Sciences and Research University, Delhi, India-110017

a)gksuthar81@gmail.com
b)Corresponding author: herenarendra4u@gmail.com
c)surajpal_1982@yahoo.co.in
d)goodday.guddu@gmail.com
e)saggujittu@yahoo.com

Abstract. The microwave-assisted graft-copolymerization of acrylamide on guar gum was optimized using the 3-Factor, 3-Level Box Behnken experimental design. Experiments were used to assess the effects of microwave power, microwave exposure period, and concentration of initiator, guar gum, and monomer on percent yield and grafting efficiency. The effect of the independent variables on the dependent variables was examined using Design Expert version 7 software. The concentration of guar gum (g) (a), the amount of monomer (g) (b), and the time (in minutes) (c) were the independent variables while Percentage yield (r^1), percentage grafting (r^2), and percentage grafting efficiency (r^3) were used as dependent variables. Microwave power of 100 W, microwave exposure period of 2.4 min, ammonium persulfate concentration of 0.2 g, guar gum concentration of 0.59 g, and monomer concentration of 10.74 g (w/v) were the best values evaluated. In 2.4 minutes, the maximum percent yield and grafting efficiency were 97.311 percent and 101.234 percent respectively. Fourier transforms infrared spectroscopy (FTIR), differential scanning calorimetry (DSC), X- ray diffraction (XRD), and scanning electron microscopy(SEM)were used to characterize a representative MW grafted copolymer.

Keywords: Microwave-assisted synthesis, Box Behnken experimental design, Guar Gum, Acrylamide.

PAPER PUBLISHED
(AIP CONFERENCE PROCEEDING)

Gum Linum Usitatissimum-g-poly (acrylamide): Microwave-Assisted Synthesis, Characterization and Release Behaviour

Anju Bala[1,a], Gautam Kumar[1,2, b], Narendra Kumar Pandey[2,c], Sonali Sughandita Sahoo[2,d], Gazzal Mehta[1,e], Jitender Singh[1,f]

[1]*Lord Shiva College of Pharmacy, Sirsa, Haryana, India-125055*
[2]*School of Pharmaceutical Sciences, Lovely Professional University, Phagwara, Punjab, India-144411*

[a] anjunadha@1994gmail.com
[b] Corresponding author:gksuthar81@gmail.com
[c]:herenarendra4u@gmail.com
[d]sonalilagna92@gmail.com
e) goodday.guddu@gmail.com
[f]saggujittu@yahoo.com

Abstract. Microwave grafting of Linum usitatissimum gum on poly(acrylamide) was performed using a three-level four-factor central composite experimental design. Gum linum usitatissimum-g-poly (acrylamide) was characterized by Fourier transform infrared spectroscopy, differential scanning calorimetry, X-ray diffraction, and scanning electron microscopy. Microwave power, microwave exposure time, and ammonium persulfate concentration had a significant synergistic effect on grafting efficiency, while Linum usitatissimum gum concentration had no significant effect. The optimal calculated parameters were microwave power-80%, microwave exposure time-70s, concentration of ammonium persulfate-0.4g and concentration of gum linum usitatissimum-1g, acrylamide 7.5g. The maximum grafting efficiency was 90.7 percent. Comparative in vitro release evaluation of lornoxicam from gum linum usitatissimum-g-polyacrylamide and gum linum usitatissimum-g-polyacrylamide matrix tablets revealed sustained drug release from gum linum usitatissimum-g-polyacrylamide. It was observed that as the percentage of natural polymer increased, the release rate decreased, although the drug release pattern was mainly dependent on the type of polymer. A dissolution study demonstrated that Linum usitatissimum seed mucilage can be used as a matrix-forming material for the production of Lornoxicam 24-hour sustained-release matrix tablets.

Keywords: Microwave-assisted synthesis, Central composite design, Lornoxicam, Grafted *Linum usitatissimum*, HPMC K100M, Ungrafted *Linum usitatissimum*, acrylamide.

PATENT PUBLISHED

(12) PATENT APPLICATION PUBLICATION

(19) INDIA

(22) Date of filing of Application :30/07/2020

(21) Application No.202011032619 A

(43) Publication Date : 09/10/2020

(54) Title of the invention : A NOVEL FORMULATION OF BERBERINE HCL FOR COLON SPECIFIC DELIVERY

(51) International classification	:A61K0031437500, A61K0009280000, A61K0009000000, A61K0009200000, A61K0009500000	(71)Name of Applicant : 1)Lovely professional University Address of Applicant :Lovely Professional University Jalandhar Delhi GT road Phawgara Punjab India (72)Name of Inventor : 1)Surajpal Verma 2)Gautam Kumar 3)Pankaj Wadhwa
(31) Priority Document No	:NA	
(32) Priority Date	:NA	
(33) Name of priority country	:NA	
(86) International Application No Filing Date	:NA :NA	
(87) International Publication No	: NA	
(61) Patent of Addition to Application Number Filing Date	:NA :NA	
(62) Divisional to Application Number Filing Date	:NA :NA	

(57) Abstract :

The purpose of the present investigation is to prepare formulation containing grafted copolymer and coating of eudragit for the delivery of Berberine HCl in the colon. In this delivery system, pH sensitive eudragit coating of solid dosage form of drug Berberine HCL will be carried out ito prevent the drug from first pass metabolism and degradation in upper part of the GIT. The said formulation is to treat IBD by colon specific delivery, so that maximum concentration of the Berberine HCl reaches to the colon and increases the residence time of the drug there.

No. of Pages : 23 No. of Claims : 3